Professur für Hydrologie

der Albert-Ludwigs-Universität Freiburg i. Br.

Anne Pirk

Long-term data set analysis of stable isotopic composition in German rivers

Referentin: PD Dr. Christine Stumpp

Korreferent: Prof. Dr. Markus Weiler

Masterarbeit unter Leitung von PD Dr. Christine Stumpp

Freiburg i. Br., September 2015

Table of contents

List of figures

List of tables

List of figures in appendix

List of tables in appendix

Acknowledgements

First of all, I would like to express my gratitude to my supervisor Dr. Christine Stumpp, who provided me the opportunity to join her team, for her continuous support during my thesis work. I am thankful for her insightful comments and suggestions and in particular for her encouragements.

Furthermore, I would like to thank my second supervisor Prof. Dr. Markus Weiler for the useful comments and remarks.

Many thanks go to the BfG and the Helmholtz Zentrum München by which the sampling of the data was conducted and also to the FOEN Switzerland, which provided additional data for this thesis.

I appreciate the feedback I got from Willibald Stichler, Dr. Jim Hendry, Prof. Dr. Piotr Maloszewski and many others.

I would also like to thank all members of the IGOE, who warmly welcomed me at the institute, for the friendly atmosphere.

I am very thankful to my friend Christian who probably had the most tedious work of correcting the language of my thesis. Without his encouragements and patience, it would have been tough for me to finish this thesis.

Kurzfassung

Für eine nachhaltige Nutzung von Wasserressourcen bedarf es eines umfassenden Verständnisses von hydrologischen Prozessen in Einzugsgebieten. Zur Untersuchung dieser Prozesse können die stabilen Wasserisotope Sauerstoff-18 (^{18}O) und Deuterium (^{2}H) als natürliche Tracer im Wasserkreislauf genutzt werden. Bisher gibt es jedoch wenige Isotopenstudien in großskaligen Einzugsgebieten und nur selten sind Isotopengehalte über längere Zeiträume beobachtet worden. Die Isotopengehalte der neun größten Flüsse in Deutschland wurden über 12 bzw. 26 Jahre gemessen. Diese Arbeit gibt einen Überblick über die räumliche und zeitliche Variabilität der Isotopengehalte im Flusswasser in Deutschland. Die räumlichen und zeitlichen Muster, die im regionalen Niederschlag beobachtet wurden (Stumpp et al., 2014), lassen sich in den Flüssen allgemein wiedererkennen. Es zeigte sich, dass die Jahresgänge der Isotope stark von den Abflussregimen der Flüsse abhängig sind. Des Weiteren wurden in zwei der neun Flüsse statistisch signifikante Langzeittrends erkannt, wobei sich allerdings keine konkreten Rückschlüsse auf die bestimmenden Faktoren machen lassen. Die zeitlichen Variationen in den Isotopengehalten ermöglichen es, den Anteil an direkten Abflusskomponenten im Flusswasser und deren Verweilzeiten zu ermitteln. Auf der Grundlage von Lumped-Parameter Modellen wurden für die direkten Abflusskomponenten in den Einzugsgebieten Verweilzeiten von 1 bis 5 Monaten abgeschätzt. Die Modelle ergaben zudem, dass die Flüsse zu 60 bis 80 % aus Grundwasser gespeist werden. Abweichungen zwischen den Isotopengehalten im Flusswasser und im Niederschlag wurden in komplexeren Einzugsgebieten festgestellt. Diese Abweichungen können auf Prozesse und Einflüsse auf Einzugsgebietsebene zurückgeführt werden, wie z. B. auf Verdunstung, Speicherung und Stauung des Abflusses. Für komplexere Einzugsgebiete konnten mit einfachen Lumped-Parameter Modell keine zufriedenstellenden Ergebnisse erreicht werden. Hierfür werden flexiblere und differenziertere Modelle benötigt.

Stichworte: Stabile Isotope, Langzeitdaten, Trendanalyse, Verweilzeiten,
große Flusseinzugsgebiete, Deutschland

Abstract

A sustainable management of water resources requires a full understanding of catchment processes. The stable isotopes oxygen-18 (^{18}O) and deuterium (^{2}H) are commonly used to investigate hydrological processes in catchments. However, only a few isotope studies have been conducted on a large scale and rarely over long time periods. The stable isotopic composition of river water has been measured in nine large river catchments in Germany for the last 12 years and 26 years, respectively. This thesis provides a broad overview about the temporal and spatial variability of the isotopic composition in German rivers. The spatial and temporal patterns which have been observed in German precipitation (Stumpp et al., 2014) are generally reflected in the rivers. The isotopic seasonalities appear to be linked to the discharge regime of the rivers. Statistically significant long-term trends in the isotopic composition could be identified for two out of the nine rivers whereby the determining factors are unclear. Temporal variations in the isotopic composition enable to quantify the contribution of direct flow components and to estimate their timescales. For the investigated rivers, mean transit times of fast flow components were estimated to be between 1 and 5 months using lumped parameter models. Groundwater contributions to discharge of 60 to 80 % were assumed. Deviations from isotopic compositions in local precipitation were observed in catchments with complex flow systems. These deviations can be ascribed to catchment processes and influences like evaporation, damming and storage. In complex catchments, the mean transit time of fast runoff components could not be adequately estimated with simple lumped parameter models, suggesting that more sophisticated and flexible models are required.

Keywords: stable isotopes, long-term data, trend analysis, mean transit times, large river catchments, Germany

1 Introduction

Human use of water is essentially dependent on river water as the majority of the global population lives close to large rivers. It uses them for transportation, irrigation, water supply or power generation (Gibson et al., 2002). The natural state of almost all rivers has been highly modified for the last decades. Discharge regimes are strongly altered through dams and an extensive straightening of rivers. In combination with other human impacts such as intense agriculture or industrial water use, this leads to issues regarding water quantity and quality. In Central Europe, for instance, floods frequently cause considerable damages and some rivers are polluted by fertilizers and pesticides from agriculture. Therefore, it is important to assess the hydrologic vulnerability of rivers. This becomes particularly important as we still have little knowledge regarding the impact of climate change on rivers. It is necessary to fully understand catchment processes for a sustainable water resource management. In order to assess the vulnerability of a river, it is essential to quantify flow components and estimate their timescales. Stable water isotopes are commonly used to investigate hydrological processes within catchments. The stable water isotopes oxygen-18 (^{18}O) and deuterium (^{2}H) are ideal natural tracers since they are constituents of the water molecule itself. Isotopic composition data for precipitation and river water provide unique insight into processes from precipitation to discharge. Furthermore, isotopic data enable to estimate timescales of runoff processes, which give information about storage and flow paths. In order to understand how these processes are affected by climatic changes, long-term data sets are needed.

1.1 Current state of research

Stable isotopes are ideal natural tracers of the hydrological cycle. They have been used in hydrological science for decades and developed to a well-established tool. Initially, the research focus laid on the analysis of isotopic composition of atmospheric waters. This resulted in an extensive understanding of the fractionation processes of water isotopes. Although isotopes have been used in catchment studies since the 1960s, in the beginning it remained limited to a few studies (IAEA, 2012). The big advantage of analysing river water instead of precipitation is that river water reflects the isotopic composition in a catchment better than precipitation since in river water precipitation from the whole catchment is accumulated, whereby precipitation samples are only gathered at single locations in the catchment (Kendall and Coplen, 2001). Additionally, river water usually consists of at least two components: precipitation and groundwater. This enables to trace runoff processes from precipitation to discharge as well as to estimate the contribution of

groundwater to the river water. The isotopic composition of river water is influenced by many different factors such as the specific variability of precipitation, the contribution of other flow sources and evaporation from the river. Combined with isotope measurements of the contributing flow sources, it provides insight into various hydrological processes in catchments. With relatively little monitoring effort, one can gain broad knowledge about the hydrological system.

1.1.1 Isotope studies in large river catchments (> 1,000 km^2)

Researchers expect that the use of isotopes in large catchment studies has a high potential (Gibson et al., 2002; Vitvar et al., 2007). On the contrary, the great complexity in large catchments is also one of the main challenges in this field of research. In complex systems, the interpretation of isotopic signals can be difficult since many different processes overlap. So far, most isotope-based catchment studies have been executed on a small scale in well-instrumented catchments with an area less than 100 km^2 (Buttle, 1998). Reliable methods to analyse runoff processes on a small scale have been developed. In contrast, the application of isotopes to trace the hydrological cycle of large catchments seemed like a scientific frontier and gained attention only in recent years (Gibson et al., 2002). However, a few studies exist in which stable isotopes have been used to investigate large river catchments (e.g. Frederickson and Criss, 1999 *(Meramec River, USA)*; Martinelli et al., 1996 *(Amazon River, South America)*; Rank et al., 1998 *(Danube River, Europe)*; Yi et al., 2010 *(Mackenzie River, Canada)*). Initially, it needs to be figured out to what extent methods applied on a small scale can be transferred to large catchments. There is also a lack of long-term observations as a broad monitoring of isotopic composition in river water has been considered to be valuable only recently.

1.1.2 Spatial distribution of stable isotopes in river water

Spatial patterns of isotopic compositions in precipitation have been first observed in the 1950s (Dansgaard, 1954; Friedman, 1953). In the following decades, these spatial patterns have been extensively investigated. As isotope data of precipitation is collected and shared through open access by the International Atomic Energy Agency (IAEA) within the GNIP (https://nucleus. iaea.org/wiser/), many studies on a local, continental and global scale exist (e.g. Bowen et al., 2005; Dutton et al., 2005; Liu et al., 2010; Rozanski et al., 1993; Schotterer et al., 2010; Schürch et al., 2003; Stumpp et al., 2014). All these studies have demonstrated that the isotopic composition in precipitation is mainly dependent on the local temperature, continentality, latitude, longitude and altitude. These effects are further discussed in chapter 2. They are well understood, so that the isotopic composition of precipitation is reproducible even on a global scale with models based on topographic and climatic data (Terzer et al., 2013). In Germany, the monitoring network for isotopes in precipitation is dense, with 28 sites for which isotopic compositions have been

recorded for up to 36 years (Stumpp et al., 2014). Most of these stations are part of the Global Network for Isotopes in Precipitation (GNIP). In a recently published paper, Stumpp et al. (2014) have provided an overview about the spatial variability of the isotopic composition in German precipitation. The results indicate that in Germany, long-term averages of $\delta^{18}O$ and $\delta^{2}H$ are mainly related to continentality, latitude, altitude and mean temperature of the station, whereas longitude has a minor effect.

There have been a few studies which analyse the spatial distribution of isotopes in river water on a continental and regional scale. Kendall and Coplen (2001), for instance, have created maps showing the spatial distribution of stable isotopes in surface water across the USA. Based on the maps by Kendall and Coplen (2001), Dutton et al. (2005) have compared the isotopic signature of US precipitation and river water. They have found that the isotopic composition in precipitation is well reflected in river water but they could also localise regions where the isotopic composition in the rivers substantially deviates from the precipitation, which are worth further investigations. Similar studies have been done for surface water in Ireland and Japan (Diefendorf and Patterson, 2005; Mizota and Kusakabe, 1994, M. Katsuyama 2015). In all these studies, the isotopic compositions in river water are closely related to that of the local precipitation and show a good correlation with climatic parameters. Furthermore, it has been shown that the spatial distribution of isotopes in river water closely matches the topography. The isotopic compositions of rivers in Central Europe have been surveyed only in single catchments, yet (Königer et al., 2009 *(Weser catchment)*; Rank et al., 1998 *(Danube catchment)*; Schotterer et al., 2010 *(several catchments in Switzerland)*; Uhlenbrook et al., 2002 *(Brugga catchment)*). However, a comprehensive study about the spatial distribution of isotopes in German rivers is lacking. So far, we do not know whether rivers in Germany are good proxies for the isotopic composition in precipitation.

1.1.3 Environmental and geographical controls

As stated, the isotopic composition of river water is determined by the isotopic composition of the precipitation in the catchment. The isotopic composition in precipitation is, in turn, mainly controlled by the environmental factors altitude, latitude, longitude and temperature (Clark and Fritz, 1997; Dansgaard, 1964). Thus, it can be assumed that river water fed from precipitation is subject to the same controls, which has been confirmed in several studies on different scales (*on regional scale* (e.g. Katsuyama et al., 2015; Winston and Criss, 2003), *on continental scale* (e.g. Dutton et al., 2005; Kendall and Coplen, 2001)). Several processes and conditions in catchments lead to modifications of the isotopic input signal (in precipitation), e.g. groundwater inflow, confluence with tributaries, delayed snow and glacier melt water input, evaporation or

anthropogenic influences such as reservoirs or irrigation (Dutton et al., 2005; Rank et al., 2012). It has been often observed that the isotopic composition of river water deviates considerably from that of the local precipitation due to such influences (Dutton et al., 2005; Gremillion and Wanielista, 2000; Martinelli et al., 2004; Schürch et al., 2003; Simpson and Herczeg, 1991). Dutton et al. (2005) have shown that the river water of some regions in the USA is on average depleted in ^{18}O compared to the precipitation. These rivers are fed by snowmelt driven discharges, which are typically depleted in heavy isotopes. Yi et al. (2010) have found a negative correlation between $\delta^{18}O$ and discharge in a three-year survey in the Mackenzie River catchment. The authors ascribe this to the snowmelt driven discharge regime in the Mackenzie River. Dutton et al. (2005) have also found that the river water is enriched by evaporation in some more arid regions of the USA. Such evaporation effects have been observed by Gremillion and Wanielista (2000) and Simpson and Herczeg (1991), too. On the catchment scale, it has been also shown that stable isotope values increase downstream with lower values in the headwater region and higher values in the lower catchment (Lu et al., 2012; Rank et al., 1998; Winston and Criss, 2003). This is mainly due to the altitude effect (Rank et al., 1998) or an enhancing evaporation along the river course (Lu et al., 2012), whereas the evaporation effect is more relevant for arid and semi-arid zones than for humid regions (Gibson et al., 2002).

1.1.4 Temporal variations

The isotopic composition of precipitation is not static. As it has been shown in several studies, it is characterized by seasonal variations caused by climatic factors (e.g. Jacob and Sonntag, 1991; Peng et al., 2004; Rozanski et al., 1992, 1993). During the transport of water through the catchment, the isotope signal observed in precipitation can be substantially modified. The isotopic variations in river discharge are generally damped due to catchment buffering and a high contribution of groundwater, which has a relatively stable isotope signal (Halder et al., 2015). Seasonal variations may be completely eliminated in catchments where the transit times are long or the contribution of groundwater in the discharge is high. However, seasonal variations in the isotopic composition of river water have been observed in a number of studies (e.g. Halder et al., 2015; Lu et al., 2012; Rank et al., 2014; Speed et al., 2011). In the recently published study of Halder et al. (2015), the seasonal variations of isotopic composition gathered at more than 200 river water sampling sites have been analysed. They showed that the discharge regime of the river has a substantial influence on the seasonal patterns of the isotopic composition. Rivers with similar discharge regimes are also similar in the seasonal variations of the isotopic composition.

It has also been observed, that the isotopic composition of precipitation underlies long-term changes (on a decadal scale) (Kaiser et al., 2002; Klaus et al., 2015; Lykoudis and Argiriou, 2011; Rozanski and Gonfiantini, 1990; Stumpp et al., 2014). Lykoudis and Argiriou (2011) have investigated isotopic composition trends in precipitation sampled at nine sites in Central Europe and the Eastern Mediterranean area. At some stations, they have identified significant trends in the time series. Time series of isotopic composition in precipitation gathered at 17 meteorological stations in Germany have been also examined for long-term trends (Klaus et al., 2015). Significant trends have been detected for three stations whereas two of these stations show a positive and one station a negative trend. Interestingly, the three stations are all located at low elevations. Stumpp et al. (2014) suggest that temperature change is an important factor controlling the long-term behaviour of isotopic composition in German precipitation. However, there is evidence that other rather local factors also play an important role.

If long-term trends can be observed in precipitation, isotopic compositions in river water may also show long-term changes. This has been rarely investigated, yet. Only a few studies have been published in which long-term time series of isotopes in rivers have been analysed (Panarello and Dapeña, 2009 *(Parana River, South America, 10 yr)*; Rank et al., 2014 *(Danube River, Europe, > 45 yr)*; Schotterer et al., 2010 *(several Swiss rivers, Europe, 18 yr)*). The presumably longest time series of isotope data gathered in a large river catchment exists for the Danube (catchment area ca. 103,000 km^2) (Rank et al., 2014). The isotopic composition in the Danube has been measured for stable water isotopes at a station located in Vienna since 1968 (Rank et al., 2014). The data show a remarkable increase of $\delta^{18}O$ in the 1980s, as it has been also observed in precipitation in Central Europe (Rozanski et al., 1992). Similar trends have been found in other Austrian rivers (Rank et al., 2012). Rank et al. (2014) explain the increase of $\delta^{18}O$ with rising temperatures caused by the climate change.

1.1.5 Mean transit time modelling

As the number of isotope-based catchment studies on a large scale increases, a growing interest in estimating the mean transit time of large catchments by using stable isotopes can also be seen (McGuire and McDonnell, 2006). The transit time is the time a water molecule needs from entering the catchment until leaving it through the catchment outlet (Yurtsever, 1995). The catchment transit time is a strong indicator for hydrological processes and the catchment's response to impacts like water extractions, contaminations or changes in land use (Vitvar et al., 2005). As stated above, isotopic compositions in river water and precipitation are characterized by seasonal variations. In a direct comparison, the seasonal variations in precipitation are reflected

in river water. They are, however, damped and time shifted. These seasonal variations can be interpreted to estimate transit times of fast runoff components. The transit time of groundwater is considerably longer with the result that variations of stable isotopes are nearly averaged out in groundwater. Thus, other tracers must be used for transit time estimation of groundwater - most commonly tritium (^3H) (e.g. Königer et al., 2005; Maloszewski et al., 1992; Michel, 1992).

The determination of mean transit times is usually done by modelling. One common approach is the use of lumped parameter models, which simulate the integrated tracer transport through a system (Maloszewski and Zuber, 1982; McGuire and McDonnell, 2006). The advantage of lumped parameter models is that they do not require a detailed characterisation of the hydrological system (McGuire and McDonnell, 2006). Therefore, they yield reasonable results even in catchments where data availability is limited. There are a few other approaches to model the mean transit time in a catchment such as the spectral analysis or the sine-wave approach. These methods are not further considered in this thesis but a detailed review is provided by McGuire and McDonnell (2006).

On the basis of stable isotope data, mean transit times have been estimated for large river catchments around the world (e.g. Burgman et al., 1987; Frederickson and Criss, 1999; Königer et al., 2009; Ogrinc et al., 2011; Rank and Papesch, 2010; Rank et al., 1998). In Central Europe, the transit times of the Danube and the Weser catchment have been previously investigated (Königer et al., 2009; Rank et al., 1998). Königer et al. (2009) have estimated transit times for fast runoff components in the Weser catchment by applying lumped parameter models. Their simulations suggest transit times for direct runoff between 1 and 3.5 months. Rank et al. (1998) have used a rather simple approach to estimate transit times of fast runoff components. They have graphically compared long-term trends (seasonality was removed) of $\delta^{18}O$ in precipitation and the Danube river water sampled at Vienna. They have estimated the mean transit time of fast runoff components to be around 1 year. In a later study, Rank and Papesch (2010) have adapted this approach to determine transit times of base flow. By calculating ten-year moving averages, they have removed not only seasonal but also short-term variations from $\delta^{18}O$ time series. They have assumed that these smoother time series mainly represent base flow in the catchment. The comparison of the two trend curves leads to a transit time of approximately 3 years.

1.2 Objectives

Stable isotopic compositions of river water from nine large catchments in Germany have been measured at seven sites for the last 12 years and at another two sites for the last 26 years. Additionally, stable isotopic composition of precipitation from 28 sites across Germany are

available covering the last two to three decades. The long-term data will be used to investigate the spatial and temporal variability of isotopic composition in river water. This thesis is furthermore aimed to quantify the contribution of direct flow components and their timescales as well as to identify dominating catchment processes within the nine catchments and their environmental controls. The specific objectives of this thesis are to

(a) provide an overview of the temporal and spatial variability of isotopic compositions in river water;

(b) investigate which geographical and environmental parameters mainly influence the isotopic composition of river water;

(c) determine whether there are long-term trends in the isotopic time series of river water;

(d) compare isotopic compositions of river water to that of regional precipitation;

(e) estimate mean transit times of fast runoff components and their contribution to river water.

The objectives will be obtained by using statistical analyses and mathematical modelling. The results shall give a basic notion to the stable isotopic nature of the major rivers in Germany. This will be valuable for future research in isotope hydrology and catchment studies, in particular in Central Europe and other regions with similar climatic conditions. The results may help to better understand the relation between isotopic compositions in river water and precipitation including the controlling factors. This in turn may gain expertise to what extent methods developed for smaller scales can be adopted and how stable isotopes can be used as proxies for anthropogenic influences and climatic changes. With the long time-series available, it is hoped to enhance understanding in long-term changes of isotopic composition and how these are related to environmental changes.

1.3 IAEA Coordinated Research Project

This thesis is integrated in a Coordinated Research Project (CRP) initiated by the IAEA (IAEA, 2014). The title of the project is *"Application and development of isotope techniques to evaluate human impacts on water balance and nutrient dynamics of large river basins"*. Motivated by the water quantity and quality issues stated above, the project is aimed to enhance expertise and skills in the use of environmental isotopes for tracing processes in large river catchments. Further, it is intended to improve existing analytical and sampling methods as well as to develop new methods. Research outcomes will contribute to the establishment of the IAEA's Global Network of Isotopes in Rivers. In 2002, the IAEA initiated the Global Network for Isotopes in Rivers (GNIR)

complementary to the Global Network for Isotopes in Precipitation (GNIP). These networks are aimed to establish long-term data collections of global isotopic signatures in precipitation and river water. The systematic survey of water isotopes in precipitation has a long tradition. As early as 1961, the IAEA and the World Meteorological Organization launched the GNIP. Owing to a well-working cooperation between numerous scientific institutions, it has become possible to maintain over 1,000 meteorological stations in more than 125 countries (IAEA, n.d. a). The GNIR works similar to the GNIP which is based on the voluntary partnership with scientific institutions worldwide (IAEA, n.d. b) and has been operating since 2007. Currently, around 750 sites in 35 countries are part of the GNIR network (IAEA, n.d. b). The sites are located in large river catchments over various climate zones. They cover approximately 20 % of the continental land surface and 30 % of the global river water in total (Gibson et al., 2005). Until now, around 21,000 stable water isotope records and 12,000 tritium records have been added to the database (IAEA, n.d. b). A number of pilot projects and coordinated research projects has been started in order to support the establishment of the GNIR by testing and evaluating methods and techniques. Moreover, they are aimed to improve expertise, address open research questions and provide scientific exchange in this field of research.

2 Theoretical Background

2.1 Stable isotopes in water

In nature, most of the water molecules consist of the oxygen and hydrogen isotopes oxygen-16 (^{16}O) and protium (^{1}H). The stable isotopes oxygen-18 (^{18}O), deuterium (^{2}H) are also natural constituents of the water molecule, but they are rare. The abundance of these rare isotopes is a characteristic fingerprint of water, which gives evidence to the origin of the water. Therefore, the stable isotopic composition of water can serve as a tracer for the hydrological cycle. Since the stable isotopes ^{18}O and ^{2}H are inherent components of water, they are ideal natural tracers, i.e. they have the same flow paths as water and do not need to be injected.

2.1.1 Notation

The abundance ratio of an isotope is defined as the ratio between the rare isotope N_i and the more abundant isotope N (Leibundgut et al., 2009).

$$R = \frac{N_i}{N} \tag{1}$$

Isotope ratios are expressed relatively to a certain standard. For water isotopes the Vienna Standard Mean Ocean Water (VSMOW) is used

$$R_{\frac{^{18}O}{^{16}O}} = \left(\frac{^{18}O}{^{16}O}\right)_{VSMOW} = 2005.2 \pm 0.45 \cdot 10^{-6} \tag{2}$$

$$R_{\frac{D}{H}} = \left(\frac{^{2}H}{^{1}H}\right)_{VSMOW} = 155.76 \pm 0.05 \cdot 10^{-6} \tag{3}$$

(Leibundgut et al., 2009).

The isotope ratio of a sample is related to the respective standard, which gives the δ-value. This common notation provides information whether a sample is enriched or depleted in heavy isotopes (Leibundgut et al., 2009). A negative δ-value indicates that the sample is depleted regarding to the standard, while a positive δ-value denotes an enrichment regarding the standard. In most cases, δ-values of fresh water samples are negative since sea water is relatively heavy.

$$\delta = \frac{R_{sample} - R_{standard}}{R_{standard}} \cdot 1000 \tag{4}$$

2.1.2 Meteoric water lines

It has been found that $\delta^{18}O$ and $\delta^{2}H$ observations of meteoric water reveal a clear linear correlation ($\delta^2 H = 8 \cdot \delta^{18} O + 10$) (Craig, 1961; Dansgaard, 1964) whereby the given relation describes the global average and is termed as Global Meteoric Water Line (GMWL). Depending on the local conditions of rainout and condensation, this linear relationship may deviate from the GMWL which results in Local Meteoric Water Lines (LMWLs) (Kresic and Stevanovic, 2009; Stumpp et al., 2014) . From the GMWL, another measure is derived: the deuterium excess, which is defined as $d = \delta^2 H - 8 \cdot \delta^{18} O$. On a global average, the d-excess is 10 ‰, but it varies locally since it is influenced by temperature, relative humidity and evaporation (Clark and Fritz, 1997). Therefore, it can be used as an indicator for climatic conditions and evaporation processes.

2.2 Fractionation processes in the hydrological cycle

Isotopic variations in water are caused by isotope fractionation that happens during physical and chemical processes (Leibundgut et al., 2009). Phase transitions between ice, water and vapour are relevant for stable water isotopes. The different masses of the isotopes result in different physical properties of the water molecules. Water molecules with heavier isotopes have, among other properties, higher melting and boiling points than water molecules with lighter isotopes (Leibundgut et al., 2009). Therefore, the isotope ratios in phases can change due to phase transitions such as evaporation or condensation. There are two types of fractionation processes: equilibrium fractionation and kinetic fractionation, which are in detail described in Clark and Fritz (1997) and Leibundgut et al. (2009).

2.2.1 Equilibrium fractionation

Isotope fractionation under chemical equilibrium is caused by the different bond strengths of light and heavy water molecules. In molecules, a bond between ^{18}O and H is more stable than between ^{16}O and H. Therefore, the vapour pressure of $H_2{}^{18}O$ is lower than of $H_2{}^{16}O$ (Clark and Fritz, 1997). During evaporation, for instance, the vapour phase gets enriched in ^{16}O due to the greater vapour pressure of ^{16}O. The remaining liquid water is consequently enriched in ^{18}O. Equilibrium fractionation is the same for ^{1}H and ^{2}H, only the magnitude of the fractionation is different (Clark and Fritz, 1997).

2.2.2 Kinetic fractionation

Often, fractionation occurs under non-equilibrium conditions, e.g. due to fast changes in temperature or when the product gets isolated from the reactants during the reaction (Clark and Fritz, 1997; Leibundgut et al., 2009). In this case, kinetic fractionation takes place, e.g. when water evaporates from a water body and water vapour is immediately transported further by wind.

2.3 Observed isotope effects

The fractionation processes described above lead to isotopic variations within the hydrological cycle. In isotope samples of precipitation and surface water, the following effects can be observed.

Temperature effect

The magnitude of isotopic fractionation is strongly dependent on temperature (Leibundgut et al., 2009). Fractionation during phase transitions between vapour and water is stronger at low temperatures. Thus, precipitation is more depleted at lower temperatures.

Altitude effect

Precipitation formed at higher altitudes is generally lighter than at lower altitudes. This can be explained by the temperature effect combined with higher humidity at high altitude (Leibundgut et al., 2009). Both, low temperature and high humidity lead to pronounced fractionation.

Amount effect

During rainfall events, heavier isotopes rain out initially and the remaining vapour becomes depleted (Dansgaard, 1964; Rozanski et al., 1993). Thus, precipitation gets increasingly depleted with rising precipitation amount.

Continental effect

It has been observed that precipitation gets more depleted with further distance from the coast (e.g. Rozanski et al., 1993). Air masses coming from the ocean get increasingly depleted with each rain fall event - similar to the amount effect.

Evaporation

When water evaporates, the water molecules with lighter isotopes initially become gaseous, which leads to an enrichment of the remaining liquid phase (Leibundgut et al., 2009).

3 Methods

3.1 Study sites and monitoring data

River water samples were collected at nine locations in Germany (see Figure 1 and Table 2) on a monthly basis. Sampling has been conducted by the German Federal Institute of Hydrology (BfG) since 1988 at the Mosel and the Rhine and since 2001 at the remaining sites. The time series extend to the end of the year 2013. Thus, data covering 26 and 12 years, respectively, are available. Complementary to isotopic compositions in river water, discharge data from gauges close to the isotope sampling sites are provided by the BfG (see Table 2). The data are given as monthly mean discharge and cover the same time periods as isotopic time series.

The corresponding catchments are the major catchments in Germany covering almost the entire area of the country. It should be noted that the catchments of the Main and the Neckar are sub-catchments of the Rhine-catchment, while the Mosel enters the Rhine shortly after the sampling site at the Rhine. The catchment areas range between 5,000 km^2 and 135,000 km^2, with the Ems as the smallest and the Elbe as the largest catchment (see Table 1). Catchments in the South of Germany have in general a higher mean elevation than catchments in the North. Southern Germany is characterized by highlands and mountains, whereas the terrain in Northern Germany is predominantly flat (see Figure A 1, appendix). All rivers except for the Danube enter the North Sea and Baltic Sea. The Danube flows further eastwards and enters the Black Sea. The climate in Germany is temperate and annual precipitation amounts range between 400 mm in lowlands and 3,200 mm in alpine regions (BMU, 2003).

Table 1: Areas and mean altitudes of the catchments and flow lengths of the river networks.

	Area (km^2)	Mean altitude (m a. s .l)	Flow length (km)
Danube	47,739	628	947
Elbe	135,000	281	2,046
Ems	5,051	70	198
Main	27,065	351	459
Mosel	28,000	342	429
Neckar	13,803	437	301
Oder	112,950	170	1,207
Rhine	109,954	574	2,010
Weser	38,154	223	1,140

In addition, long term isotope data of precipitation samples gathered at 28 precipitation stations in Germany are available (see Figure 2), which were published recently (Stumpp et al., 2014). At 16 of these stations, stable isotopic compositions have been measured since 1978 by several scientific organisations, which are part of the GNIP. Another 12 stations have been operated by the Germany's National Meteorological Service (DWD) since 1997. The amount of precipitation was recorded at the meteorological stations. Air temperature data and missing precipitation data were derived from the DWD. Climate data from 78 meteorological stations operated by the DWD are accessible for free online (http://www.dwd.de/cdc).

Table 2: Geographic locations of the river water sampling sites for isotopic composition and discharge.

Catchment	Sampling site	Parameter	Latitude (°)	Longitude (°)	Record periods
Danube	Hofkirchen	Q	48.676643	13.115178	10/2001 – 12/2013
	Vilshofen	$\delta^{18}O$, $\delta^{2}H$	48.641762	13.180312	
Elbe	Neu Darchau	Q	53.232298	10.888751	10/2001 – 12/2013
	Geesthacht	$\delta^{18}O$, $\delta^{2}H$	53.429427	10.335367	
Ems	Dalum	Q	52.595602	7.248462	10/2001 – 12/2013
	Geeste	$\delta^{18}O$, $\delta^{2}H$	52.598642	7.249473	
Main	Raunheim	Q	50.016150	8.448263	10/2001 – 12/2013
	Eddersheim	$\delta^{18}O$, $\delta^{2}H$	50.043381	8.474723	
Mosel	Cochem	Q	50.143342	7.168247	01/1988 – 12/2013
	Koblenz	$\delta^{18}O$, $\delta^{2}H$	50.368984	7.583490	
Neckar	Rockenau	Q	49.438249	9.005011	10/2001 – 12/2013
	Schwabenheim	$\delta^{18}O$, $\delta^{2}H$	49.443056	8.632472	
Oder	Hohensaaten	Q	52.870060	14.140858	10/2001 – 12/2013
	Schwedt	$\delta^{18}O$, $\delta^{2}H$	53.039219	14.311370	
Rhine	Kaub	Q	50.085428	7.764934	01/1988 – 12/2013
	Koblenz	$\delta^{18}O$, $\delta^{2}H$	50.351637	7.597159	
Weser	Intschede	Q	52.964180	9.125735	10/2001 – 12/2013
	Langwedel	$\delta^{18}O$, $\delta^{2}H$	52.968197	9.151965	

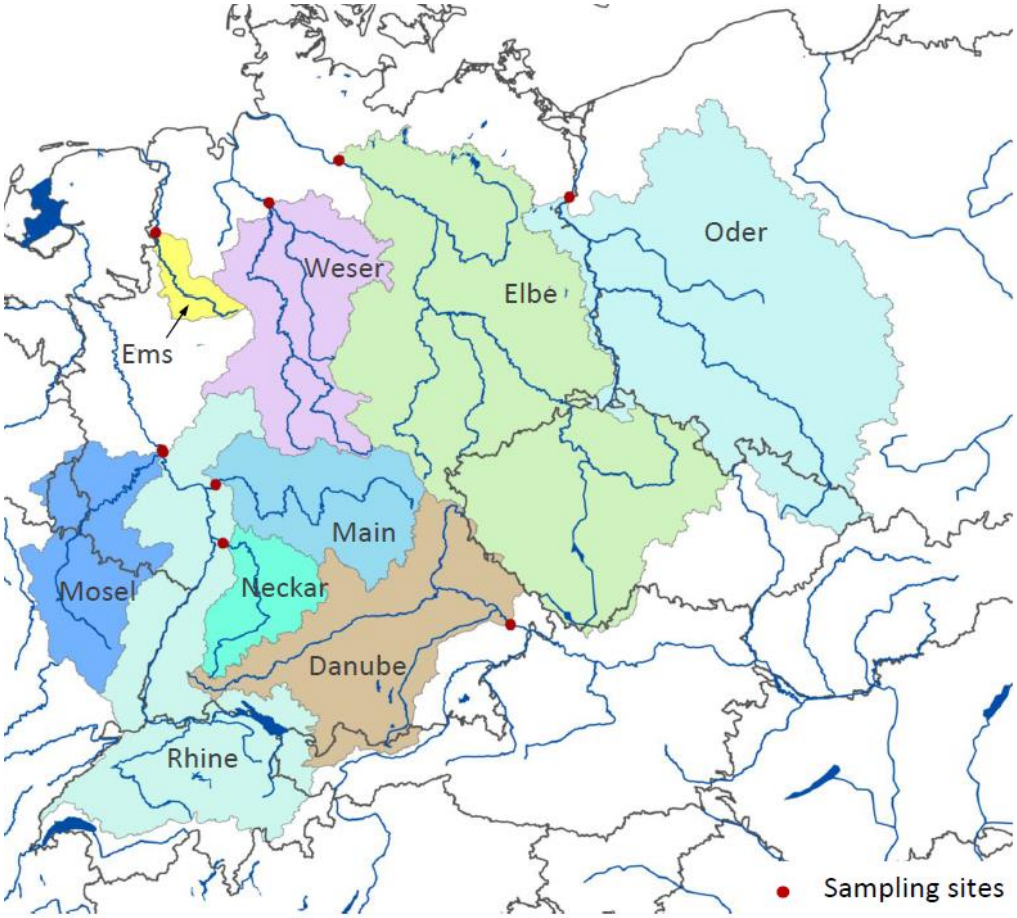

Figure 1: Map of the catchment areas and the river water sampling sites for isotopic composition.

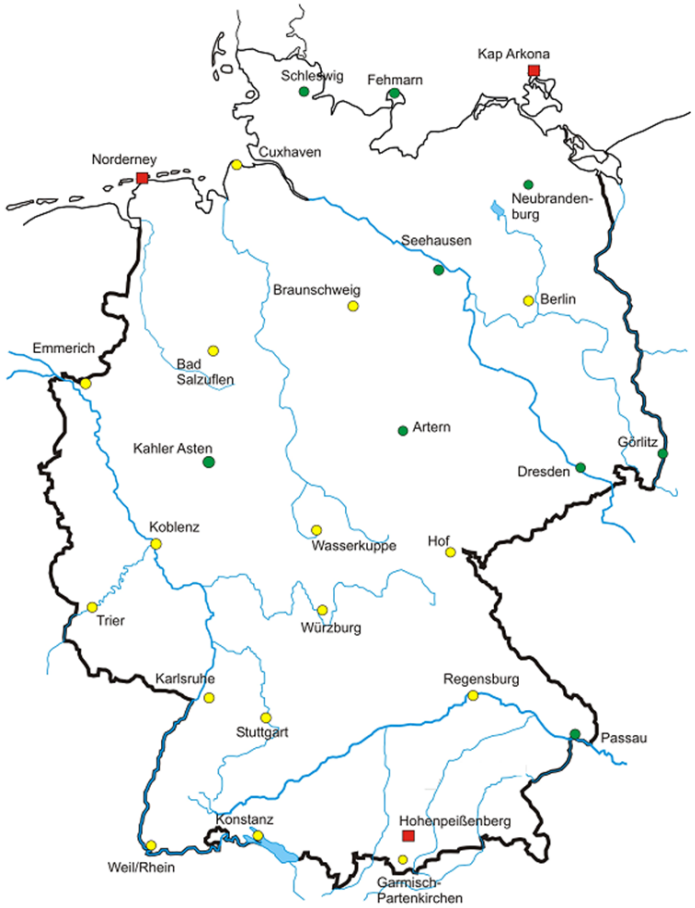

Figure 2: Map of the precipitation sampling sites in Germany (from Stumpp et al., 2014).

3.1.1 Measurement

Both, the precipitation and river water samples, are bulk samples. Therefore, they reflect the mean isotopic composition of the whole month. The isotope analyses of the river water and precipitation samples were conducted at the Helmholtz Zentrum München. Samples were analysed for ^{18}O and ^{2}H ratios without any pre-treatment. Up to September 2011, isotope ratios had been measured using dual-inlet mass spectrometry. From then on, the cavity ring-down spectrometer *Picarro Isotopic Water Analyzer L2120-i* has been used for isotope analyses. The precision of the dual-inlet mass spectrometry is ±0.15‰ for $\delta\ ^{18}O$ and ±1‰ for $\delta^{2}H$. Measurements of the cavity ring-down spectrometer have a precision of ±0.1 ‰ for $\delta^{18}O$ and ±0.5 ‰ for $\delta^{2}H$.

3.1.2 Additional data for the Rhine catchment

In the Rhine catchment, the isotopic compositions of river water and precipitation have been measured at further locations. The Swiss Federal Office for the Environment (FOEN) provided long-term isotope data of five river water and one precipitation sampling sites. The stations are part of the Swiss National Network for the Observation of Isotopes in the Water Cycle (NISOT). The river water sampling sites are located along the Rhine and the Aare, a main tributary of the Rhine (see Figure A 2, appendix). The meteorological station is located in Bern. For all stations, data is available for the time period from 1997 to 2014. At some stations earlier measurements exist. Isotope values are either derived from bulk samples or from a mixture of two grab samples, one taken in the beginning of the month and the other one in the end of the month (Schürch et al., 2003).

3.1.3 Data preparation

All data were checked for consistency and plausibility. Missing values in the data sets were replaced by long-term monthly averages. For the analyses, the average precipitation isotope signal for each catchment is required. For this purpose, the data of the meteorological stations in the proximity of each catchment, preferably within the catchment, were averaged (see Table 3).

Table 3: Meteorological stations used for average precipitation signal.

Catchment	Meteorological stations			
Danube	Regensburg	Hohenpeißenberg	Garmisch	
Elbe	Berlin	Dresden	Artern	Hof
Ems	Bad Salzuflen	Emmerich		
Main	Würzburg			
Mosel	Trier	Koblenz		
Nekar	Stuttgart			
Oder	Görlitz			
Rhine	Weil	Karlsruhe	Koblenz	Bern
Weser	Braunschweig	Wasserkuppe	Bad Salzuflen	

3.2 Spatial analysis

Weighted long-term averages were computed for isotopic time series of precipitation and river water. Isotope values of precipitation were weighted by the cumulated monthly precipitation amount. Isotope values of river water were weighted by the average monthly discharge as follows

$$\bar{\delta} = \frac{\sum_{i=1}^{N} \delta_i \cdot W_i}{\sum_{i=1}^{N} W_i} \tag{5}$$

where W is the weight, i.e. precipitation or discharge amount, respectively.

Linear regression models are used to estimate the linear relationship between $\delta^{18}O$ and $\delta^{2}H$ observations in river water. In terms of river water, this linear relationship is referred to as River Water Line (RWL).

3.3 Environmental and geographical controls

The geographical parameters catchment area, mean catchment altitude, latitude and longitude as well as the flow length of the river network were determined using the GIS software ArcGIS 10.3. Analyses are based on publicly accessible geodata. Geodata containing catchment borders, river network and lakes within Europe are provided from the European Environment Agency (European Environment Agency, 2008, 2009). Global digital elevation maps with a spatial resolution of 7.5 arc-seconds are taken from the U.S. Geological Survey and the National Geospatial-Intelligence Agency USA (http://topotools.cr.usgs.gov/gmted_viewer/).

Pearson's correlation coefficient

In order to identify similarities between sample sites and variables, Pearson's correlation coefficient (Pearson's r) was determined. Pearson's r identifies linear associations and measures the strength and direction of it. Pearson's r is defined as

$$r = \frac{1}{n-1}\sum_{i=1}^{n}\left(\frac{x_i - \bar{x}}{s_x}\right)\left(\frac{y_i - \bar{y}}{s_y}\right) \tag{6}$$

where n is the number of observations, x_i are the data points, $\bar{x}$ is the mean and s_x is the standard deviation (Helsel and Hirsch, 2002).

Values close to 1 and -1 indicate a strong relation between the variables, whereby a Pearson's r of 0 indicates no correlation. Statistical significance of Pearson's r was tested using a hypothesis test. Null hypothesis is that r = 0, i.e. that there is no relation between the variables.

The test statistic t_r is calculated as follows

$$t_r = \frac{r\sqrt{n-2}}{\sqrt{1-r^2}} \tag{7}$$

where n is the number of observations. Decision is based on the t-distribution (Helsel and Hirsch, 2002). Correlation coefficients were calculated using the statistical software R (R Core Team, 2014). This also applies to the following statistical analyses. In Table 4, the specific R functions and packages are listed.

3.4 Time series analyses

3.4.1 Smoothing and normalisation

The time series were smoothed and normalised to make long-term trends visible. This was done according to the procedure proposed by Rozanski et al. (1992). The seasonal variations were removed by computing 12-month moving averages, which are the averages of a moving period of 12 months. Moving averages are centred, i.e. the 12-month moving average at the time t is calculated from the five previous data points, the data point at time t and the six subsequent data points. The moving average of a data point at the time t is defined as

$$MA(x_t) = \begin{cases} \frac{1}{n}\left(\sum_{i=-m+1}^{m} x_{t+i}\right) & if\ n\ is\ even \\ \\ \frac{1}{n}\left(\sum_{i=-m}^{m} x_{t+i}\right) & if\ n\ is\ uneven \end{cases} \tag{8}$$

with
$$m = \begin{cases} \frac{n}{2} & if\ n\ is\ even \\ \frac{n-1}{2} & if\ n\ is\ uneven \end{cases} \quad (9)$$

where *n* is the number of observations.

The normalisation was done by subtracting the resulting moving averages from the long-term average of each time series. Then, the resulting data were smoothed again by computing 12-month moving averages.

3.4.2 Trend-Tests

In order to identify long-term trends in the time series, the Mann-Kendall statistical test was used (Kendall, 1975; Mann, 1945). The Mann-Kendall test is a commonly applied trend test in hydrological science (Yue et al., 2002). The null hypothesis H_0 of the test is that the data values are independent and identically distributed. The alternative hypothesis H_1 is that the data feature a monotonic trend.

The Mann-Kendall statistic *S* is defined as follows

$$S = \sum_{i=1}^{n-1} \sum_{j=i+1}^{n} sgn(x_j - x_i) \quad (10)$$

where x_j are the consecutive data points, *n* is the length of the time series and

$$sgn(x_j - x_i) = \begin{cases} 1 & if\ x_j - x_i > 0 \\ 0 & if\ x_j - x_i = 0 \\ -1 & if\ x_j - x_i < 0 \end{cases} \quad (11)$$

It is assumed that the statistic *S* is nearly normally distributed when n is greater or equal than 8 with mean *(E)* and variance *(V)* as follows:

$$E(S) = 0 \quad (12)$$

$$V(S) = \left(\frac{n(n-1)(2n+5) - \sum_{m=1}^{n} t_m m(m-1)(2m+5)}{18} \right) \quad (13)$$

where t_m is the number of ties with the extent *m*. The standardised test statistic *Z* is calculated by the following equation

$$Z = \begin{cases} \dfrac{S-1}{\sqrt{V(S)}} & S > 0 \\ 0 & S = 0 \\ \dfrac{S+1}{\sqrt{V(S)}} & S < 0 \end{cases} \quad (14)$$

The standardised statistic is normally distributed, i.e. it has a mean value of 0 and variance value of 1. A positive *Z*-value implies that observations increase and a negative value that observations decrease. *Z* is tested for its statistical significance whereby the decision is based on the standard normal distribution (Helsel and Hirsch, 2002). Since it is a nonparametric test, it is also applicable to non-normal distributed data. In addition, this rank-based test is not sensitive to outliers (Helsel and Hirsch, 2002). However, the Mann-Kendall test requires non-autocorrelated data. It has been shown that the result of Mann-Kendall test is biased when it is applied to autocorrelated data (Zwiers and von Storch, 1995). Autocorrelation is present when data points in a time series are systematically correlated with other data points in the same time series but at different points of time. Hydrological time series which show seasonal or daily patterns are in most cases significantly autocorrelated (Yue et al., 2002).

Trend-free pre-whitening

Therefore, Zwiers and von Storch (1995) proposed a method, in which the first order autocorrelation is removed from the data and the Mann-Kendall test is applied to the adjusted data. Yue et al. (2002) developed an advancement of this pre-whitening method, called trend-free pre-whitening (TFPW) method. The authors found out that the removal of autocorrelation reduces the magnitude of an existing trend. Thus, some significant trends might not be detected in subsequent trend tests. They suggest to subtract the trend form the time series initially, remove the autocorrelation and reunite both afterwards. The trend of the time series will be only roughly estimated using the approach of Sen (1968).

Sen-Theil Slope

To quantify trends, the slope and direction is computed using the approach of Sen (1968). In this approach, the slope between all possible data pairs is calculated. The Sen-slope is the median of all these pairwise slopes.

3.5 Spatiotemporal analysis

Cluster analysis

Hierarchical cluster analysis was conducted to identify similarities between the sample sites. In this method, objects are grouped into clusters based on their similarity to each other. First, each object is assigned to its own cluster and then, the two most similar clusters are joined.

This procedure is continued until all clusters are joined to one single cluster. Clustering is done according to the complete-linkage method. Pearson's r is used as measure of similarity. The result of a cluster analysis is visualised in a dendrogram which is a graph that is structured like a tree.

Table 4: R-functions and packages used for statistical analyses (Packages from Bronaugh and Werner, 2013; R Core Team and contributors worldwide, 2015).

Analysis	R function	Package
Autocorrelation	acf( )	stats
Cluster analysis	hclust( )	stats
Linear regression	lm( )	stats
Moving averages	filter( )	stats
Pearson's r	cor.test( )	stats
Sen-slope	zyp.sen( )	zyp
TFPW; Mann-Kendall test	zyp.trend.vector( )	zyp

3.6 Mean transit time modelling

A common approach to estimate the mean transit time of a catchment is the use of lumped parameter models, which have been introduced by Maloszewski and Zuber (1982). Lumped parameter models use the temporal variations of the input tracer signal ($C_{in}(t)$) to estimate the output tracer concentration ($C_{out}(t)$) (Leibundgut et al., 2009; Maloszewski and Zuber, 1996). The predicted output concentrations are then compared to the observed output concentrations. In the case of stable isotopes, the relation between $C_{in}(t)$ and $C_{out}(t)$ is described by the convolution integral

$$C(t) = \int_0^\infty C_{in}(t - t')\, g(t')\, dt' \tag{15}$$

where t' is the transit time and $g(t')$ is the transit time distribution (Maloszewski and Zuber, 2002). Two general assumptions of lumped-parameter models are that the hydrological system is at steady-state conditions and that it is possible to determine representative input tracer concentrations (McGuire and McDonnell, 2006).

Lumped parameter models are based on different transit time distributions (TTD) (Leibundgut et al., 2009). As the flow paths through a catchment are diverse, distances to the catchment outlet strongly vary, with the result that a water sample gathered at the catchment outlet contains water with different transit times. The distribution of the transit times is dependent on the catchment properties. In order to choose the appropriate model, the TTD must be assumed based on the knowledge about the catchment (Leibundgut et al., 2009). Frequently used kinds of models are the piston flow model, the exponential model, the combined

exponential piston flow model and the dispersion model (Leibundgut et al., 2009). The exponential model was chosen as model type since literature describes it as the most reliable model for catchment studies (McGuire 2006, McGuire 2005). It is also the simplest model with only one fitting parameter. Models with larger number of parameters may produce better model results as they are more flexible (McGuire 2005), but with each additional parameter the model complexity increases and it gets more and more difficult to deal with parameter interdependencies.

Exponential model

In exponential models, transit times are exponentially distributed and range from zero to infinity (Maloszewski and Zuber, 2002). The exponential TTD is defined as

$$g(t') = \frac{1}{t_t}\exp\left(-\frac{t'}{t_t}\right) \tag{16}$$

where t_t is the mean transit time of a tracer. Using the exponential model, only one parameter is unknown and needs to be fitted, the mean transit time of the tracer *(t_t)*. The transit time of the tracer is identical with the transit time of the water since stable isotopes behave conservative (Maloszewski and Zuber, 1996). Additionally, it is possible to include a constant flow component *(β)*. In the case of river water, the constant flow component is the groundwater influx. The tracer concentration *(C_β)* of the constant flow component is assumed to be the long-term average concentration of the surface water. The relative contribution of groundwater on river water is unknown and needs to be fitted, too.

3.6.1 Model calibration

In the process of model calibration, parameter values are adjusted to fit the model predictions to the observed values (Maloszewski and Zuber, 2002), i.e. in this case the observed $\delta^{18}O$ values in the rivers. The goodness of fit is measured by the Root Mean Square Error (RMSE), which is the square root of the mean squared difference between the model predictions *(P)* and observations *(O)*. Low RMSE values close to zero stand for a good model fit.

$$RMSE = \sqrt{\frac{\sum_{i=1}^{n}(P_i - O_i)^2}{n}} \tag{17}$$

The model performance is quantified by the Nash-Sutcliffe efficiency (NSE) (Nash and Sutcliffe, 1970) which is defined as follows

$$NSE = 1 - \frac{\sum_{i=1}^{n}(O_i - P_i)^2}{\sum_{i=1}^{n}(O_i - \bar{O})^2} \tag{18}$$

Values of the NSE range between minus infinite and 1. A NSE value of 1 indicates a perfect model performance, while a NSE value of zero indicates that the model performs, on average,

only as good as a straight line through the average of all observations. Thus, values above zero and close to 1 stand for a good model performance.

The aim of the calibration process is to find the optimal parameter values for t_t and β providing the best goodness-of-fit and model performance. This can either be done automatically or manually by a trial and error procedure. When using the software Flow PC *(Manual and Documentation:* Maloszewski and Zuber, 2002), fitting is conducted manually. As only two parameters need to be varied the effort is still reasonable and interdependencies between parameters are assessable. Approximately two-thirds of the time series were used for model calibration. The models were calibrated based on observation data from 10/2001 to 12/2009 for short time series and from 01/1988 to 12/2005 for long time series, respectively.

3.6.2 Model validation

In order to test whether the estimated model is an accurate representation of the real system, the model is validated. In model validation, predictions derived from calibrated models are compared to observations which were not used for model calibration before. As models are calibrated on the first two-thirds of the time series, the last third is used for model validation. If model predictions agree with new observations, it can be assumed that the model accurately describes the real system. It must be noted, that the validation process is rather qualitative and dependent on the evaluation of the modeller (Maloszewski and Zuber, 2002).

4 Results

4.1 River hydrology

Long-term mean discharges (records from 2002 to 2010) of the rivers are diverse, ranging between 46 m^3/s in the Ems at Dalum and 1,700 m^3/s in the Rhine at Kaub (see Table 5). The discharge regimes of the rivers are shown in Figure 3 (for value variations see Figure A 3 in the appendix). Rivers in Northern and Central Germany are characterised by pluvial discharge regimes, i.e. the amount of discharge is mainly controlled by rainwater input. Discharge maxima occur in winter and discharge minima in late summer. The Upper Danube (up to Hofkirchen) is influenced by rainwater and water originating from snow melt, which is termed as pluvio-nival discharge regime. Due to the influence of snow melt water, discharge maximum is shifted to spring. The discharge regime of the Middle Rhine at Koblenz is even more complex. In the headwater region, located in the Swiss alps, the Rhine has a runoff regime which is dominated by melt water from glaciers and snow (Bormann, 2010). In Germany, the runoff regime changes to pluvio-nival since large rainwater dominated tributaries (e.g. Neckar and Main) enter the Rhine (Bormann, 2010).

Table 5: Long-term mean discharge of the rivers.

River	Gauge	Long-term mean discharge [m^3/s]
Danube[a]	Hofkirchen	636
Elbe[a]	Neu Darchau	758
Ems[a]	Dalum	46
Main[a]	Raunheim	223
Mosel[b]	Cochem	321
Neckar[a]	Rockenau	140
Oder[a]	Hohensaaten	529
Rhine[b]	Kaub	1,700
Weser[a]	Intschede	317

[a] Records from 01/2002 to 12/2013; [b] Records from 01/1988 to 12/2013

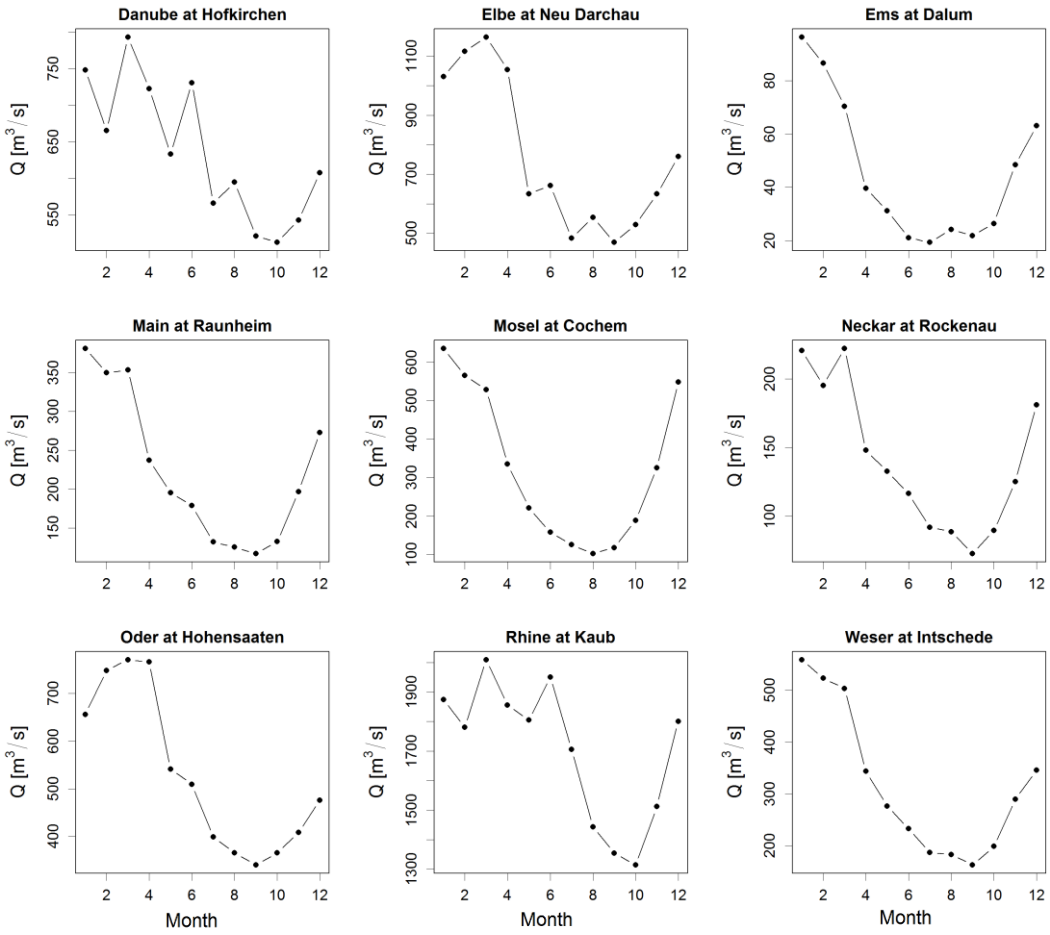

Figure 3: Discharge regimes based on monthly mean discharge. Data from 2002 to 2013 were used, except for the Mosel and the Rhine for which data from 1988 to 2013 were used. Calendar year is used.

4.2 Spatial analysis

4.2.1 Long-term averages

For the nine rivers, unweighted and discharge weighted long-term averages of $\delta^{18}O$, $\delta^{2}H$ and d-excess were calculated (see Table 6). Discharge weighted averages of $\delta^{18}O$ and $\delta^{2}H$ are in general lower than unweighted averages (except for ^{2}H in the Rhine), while weighted averages of d-excess are higher than unweighted averages. Since all rivers have higher discharges in winter and spring, the winter and spring discharges are underestimated in unweighted averages. In weighted averages, the higher contribution of light winter and spring discharge is taken into account. Therefore, weighted long-term averages better represent the average isotopic composition in the rivers and will be used in the following analyses. Long-term averages show that the Danube and the Rhine have on average the lowest $\delta^{18}O$ and $\delta^{2}H$ values (< -9 ‰). Both catchments are located in the South of Germany. The Ems, the Mosel and the Weser have relatively high $\delta^{18}O$ and $\delta^{2}H$ values (> -7 ‰). These catchments are located in the Northwest of Germany. Long-term averages of $\delta^{18}O$ in river water show a clear linear relation to long-term averages of the mean catchment precipitation (R^2 = 0.74) (see Figure A 4 and

Table A 1, appendix). However, this cannot be observed for long-term averages of d-excess ($R^2 = 0.09$) and values are also not linked to geographic locations of the catchments.

Table 6: Long-term averages of isotopic composition in river water.

	Long-term averages unweighted			Long-term averages weighted		
	$\delta^{18}O$ (‰)	**$\delta^{2}H$ (‰)**	**d (‰)**	**$\delta^{18}O$ (‰)**	**$\delta^{2}H$ (‰)**	**d (‰)**
Danube[a]	-9.69	-69.89	7.64	-9.73	-70.14	7.69
Elbe[a]	-8.23	-59.51	6.31	-8.43	-60.60	6.87
Ems[a]	-6.87	-47.52	7.41	-7.09	-48.85	7.85
Main[a]	-8.35	-59.50	7.32	-8.57	-60.76	7.77
Mosel[b]	-7.37	-51.12	7.84	-7.70	-52.94	8.69
Neckar[a]	-8.55	-60.70	7.68	-8.74	-62.00	7.96
Oder[a]	-8.48	-61.17	6.68	-8.64	-62.23	6.89
Rhine[b]	-9.08	-66.76	5.90	-9.08	-66.67	5.95
Weser[a]	-7.69	-54.21	7.31	-7.78	-54.75	7.50

[a] Records from 01/2002 to 12/2013; [b] Records from 01/1988 to 12/2013

4.2.2 River water line

Overall, the values of $\delta^{18}O$ and $\delta^{2}H$ observed at the nine river sampling sites range from -10.8 to -5.6 % and from -79 to -40 %, respectively (see Table 7). When $\delta^{18}O$ and $\delta^{2}H$ are plotted in a dual-isotope plot, the linear relationship between both variables is obvious (not shown). This relationship is termed as River Water Line (RWL). In Table 7, the intercepts, slopes and coefficients of determinations (R^2) of the RWLs for the nine rivers are listed. Compared to the LMWL of Germany, $\delta\,^{2}H = 7.72\,\delta^{18}O + 4.90$ (Stumpp et al., 2014), slopes of the RWLs are generally smaller (between 5.4 and 6.7). The intercepts, in contrast, have lower and higher values than the LMWL. The fits of linear regressions are given by the coefficient of determination (R^2) which range between 0.68 and 0.86.

Table 7: River water lines and value ranges of $\delta^{18}O$ and $\delta^{2}H$.

	Intercept (‰)	Slope	R^2	Range $\delta^{18}O$ (‰)	Range $\delta^{2}H$ (‰)
Danube[a]	-4.77	6.72	0.77	-10.77 to -8.29	-78.45 to -58.90
Elbe[a]	-12.59	5.70	0.83	-9.46 to -7.17	-67.59 to -52.80
Ems[a]	-7.89	5.77	0.70	-7.97 to -5.62	-54.90 to -40.40
Main[a]	-7.29	6.25	0.85	-9.97 to -7.13	-70.90 to -52.40
Mosel[b]	-7.77	5.88	0.80	-9.07 to -5.99	-63.60 to -40.85
Neckar[a]	-3.92	6.64	0.86	-9.86 to -6.95	-70.82 to -50.32
Oder[a]	-9.63	6.08	0.82	-10.31 to -6.10	-74.15 to -45.66
Rhine[b]	-13.27	5.89	0.83	-10.66 to -7.32	-77.90 to -56.00
Weser[a]	-12.57	5.41	0.68	-8.91 to -6.28	-62.67 to -46.90

[a] Records from 10/2002 – 12/2013; [b] Records from 01/1988 – 12/2013

4.3 Environmental and geographical controls

It was tested to what extent $\delta^{18}O$ and d-excess values are influenced by geographical parameters. For that, linear regression models between long-term weighted $\delta^{18}O$ and d-excess averages and geographical parameters of the catchments were established. Correlations with the following geographical parameters were tested: mean catchment altitude, latitude, longitude, flow length of the river system and catchment area.

4.3.1 Geographical parameters

In the figures below, only significant correlations are shown. Weighted long-term averages of $\delta^{18}O$ in the rivers clearly correlate with mean catchment altitude and latitude (see Figure 4.a and b). Catchments with high altitudes have obviously lower $\delta^{18}O$ averages than catchments in lowland. The altitude effect for the rivers is estimated to be 0.36 ‰ per 100 m. Catchments located in the South have on average lower $\delta^{18}O$ values than catchments in the North. In general, long-term $\delta^{18}O$ averages in river water follow a northwest-southeast gradient. The relation to altitude is more distinct ($R^2 = 0.69$, r = 0.83) than to latitude ($R^2 = 0.46$, r = 0.68). Long-term averages of d-excess correlate significantly with flow length and catchment area (see Figure 4.c and d). The correlation coefficients are negative, i.e. d-excess values decrease with increasing flow length and catchment area. The fit of the regression model between d-excess and flow length is slightly better than between d-excess and catchment area.

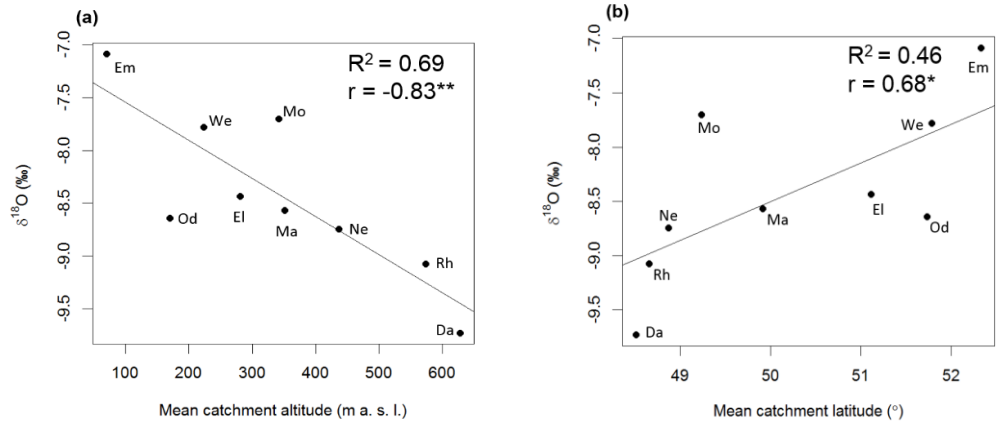

Figure 4: Correlations between weighted $\delta^{18}O$ long-term averages and mean catchment (a) altitude and (b) latitude and between weighted d-excess long-term averages and (c) flow length and (d) catchment area. Records from 2002 to 2013.

***Significant on a significance level of 0.05** ****Significant on a significance level of 0.01**

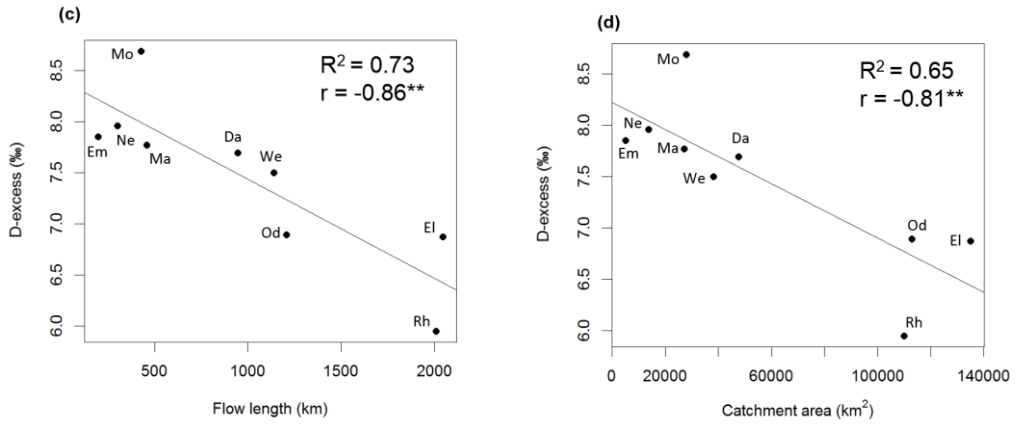

Figure 4: Continued

4.3.2 Discharge

It was also tested how the amount of discharge affects the $\delta^{18}O$ and d-excess values. Monthly $\delta^{18}O$ and d-excess values were plotted against mean monthly discharge. Similar as for geographical parameters, linear regression models and correlation coefficients were calculated. Between $\delta^{18}O$ and discharge, correlations are generally negative, i.e. $\delta^{18}O$ values are lower with increasing discharge (see Figure 5). The correlation coefficients are statistically significant for all rivers except for the Rhine. They range between r = -0.3 and r = -0.7. Although linear regression models do not fit well ($R^2 \leq 0.51$), the relation between $\delta^{18}O$ and discharge is obvious. For some rivers, it seems that the dependence between both variables is rather exponential than linear (e.g. Mosel and Ems), which could explain the poor fit of the linear regression models.

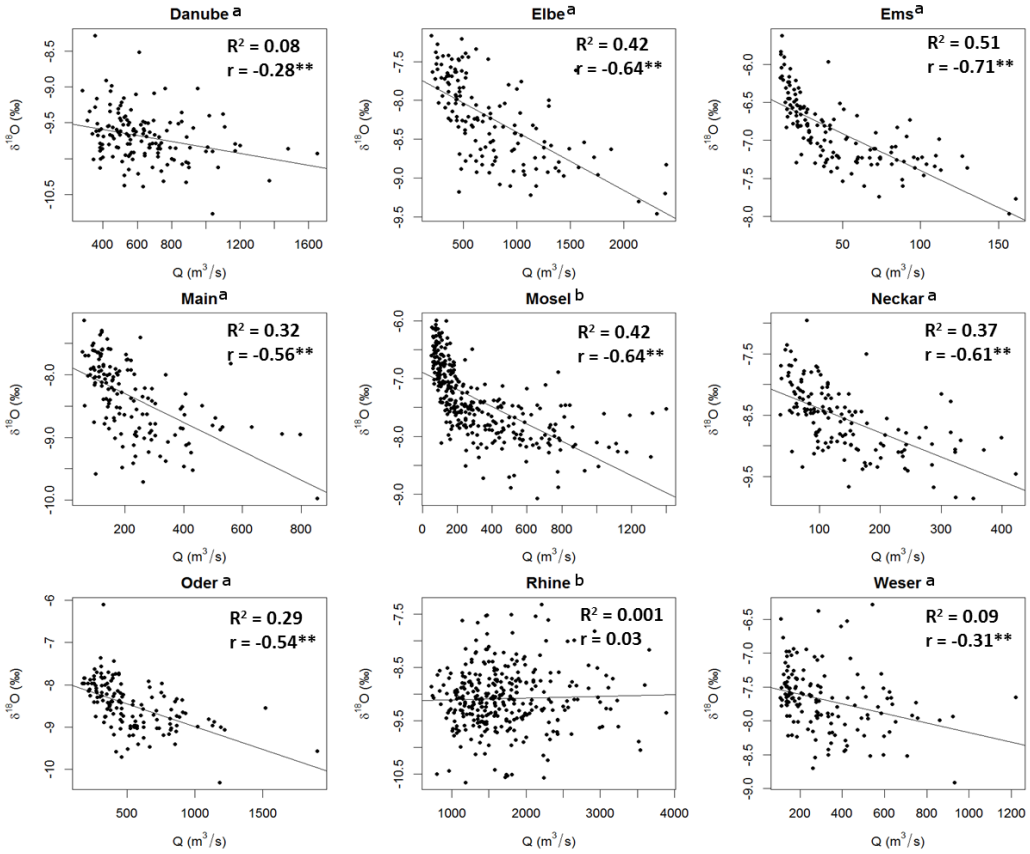

Figure 5: Dependence between $\delta^{18}O$ and discharge separately for each river.
[a] Monthly records from 2002 to 2013 [b] Monthly records from 1988 to 2013

Figure 6 shows the d-excess observations plotted against the discharge observations. Correlations between d-excess and discharge are rather weak. The correlations coefficients are positive in all cases but only for six rivers statistically significant. In the Rhine, the Danube and the Weser d-excess values do not significantly correlate with discharge. The fit of the linear regression models are poor for all rivers. Here, relations also appear to be not linear but exponential. Nevertheless, a tendency that d-excess values are lower at low water conditions can be seen in some rivers (Elbe, Ems, Main and Mosel).

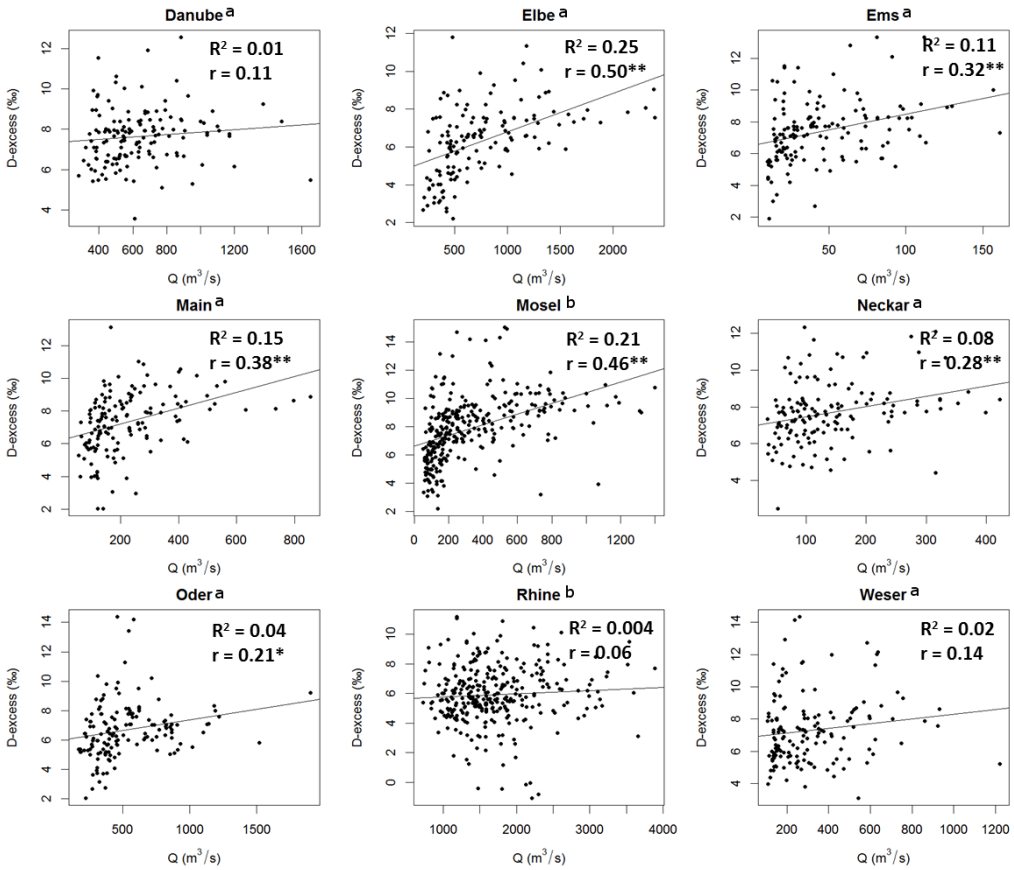

Figure 6: Dependence between d-excess and discharge separately for each river.
[a] Monthly records from 2002 to 2013 [b] Monthly records from 1988 to 2013

4.4 Seasonality

4.4.1 Oxygen-18

In Figure 7, time series of $\delta^{18}O$ in the Ems river water and in precipitation at the station Bad Salzuflen are shown as an example. In both time series, periodic variations are obvious whereas the amplitudes of $\delta^{18}O$ variations in precipitation are larger than in river water. The precipitation signal is also noisier than the river signal. The $\delta^{18}O$ time series (precipitation and river water) of the Rhine catchment are additionally shown in Figure 8. The time series of the Ems reveals a clear seasonal signal. In every year, $\delta^{18}O$ values are higher in summer and lower in winter. Similar signals can be observed for the majority of the rivers. In contrast, this regular seasonal signal is not observed in the time series of the Rhine river water, although the local precipitation shows a typical $\delta^{18}O$ seasonality. In the Rhine river water, the variability of the isotopic composition is irregular without pronounced minima and maxima over the years and there is no consistent pattern, which is repeated every year.

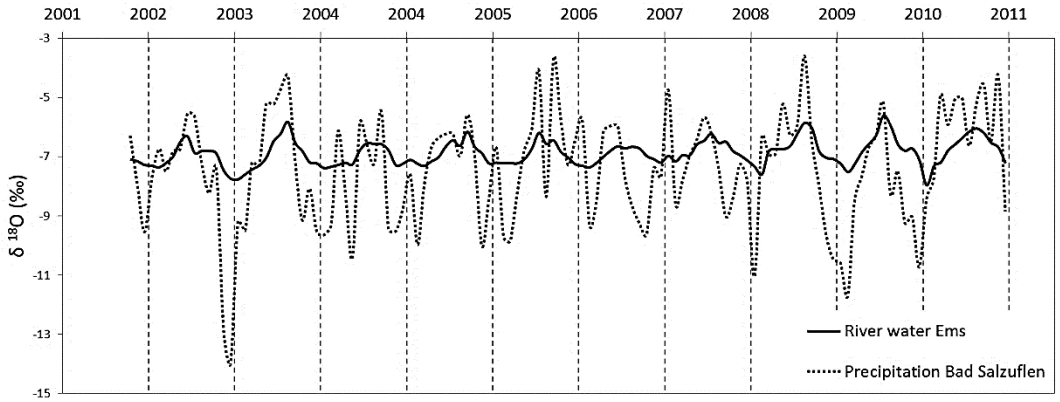

Figure 7: Time series of $\delta^{18}O$ in the Ems river water and precipitation at the station Bad Salzuflen.

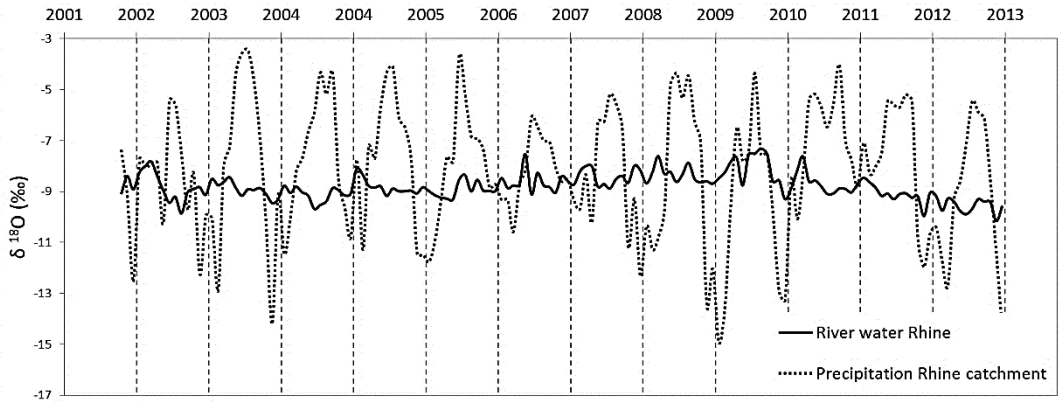

Figure 8: Time series of $\delta^{18}O$ in the Rhine river water and mean catchment precipitation.

The mean annual variations of $\delta^{18}O$ in the rivers are shown in Figure 9. In most rivers, seasonal signals are characterised by high $\delta^{18}O$ values in late summer (July to September) and low values in winter. Only the Rhine does not reveal a distinct seasonal signal. In the Mosel and the Weser the seasonal signals are also slightly indistinct, showing higher variations over the years than the other rivers. However, tendencies are still obvious in the Mosel and in the Weser and they correspond to the seasonal signal observed in the other rivers. In the Rhine, $\delta^{18}O$ values are almost constant throughout the year but slightly lower in summer (around June). The seasonal signals in all rivers (except for the Rhine) are similar to $\delta^{18}O$ seasonalities observed in the local precipitation (see Figure 10). In comparison, the river water signal is only damped and time shifted by 1 or 2 months. The damping of the signals is varyingly strong. The amplitudes of variations observed in the Weser, the Danube and the Rhine are relatively small (< 1 ‰, based on mean monthly values) compared to the remaining rivers (see Table A 2, appendix). Here, the seasonal variations are almost eliminated in river water. Amplitudes of the other rivers range between 1.1 and 1.4 ‰.

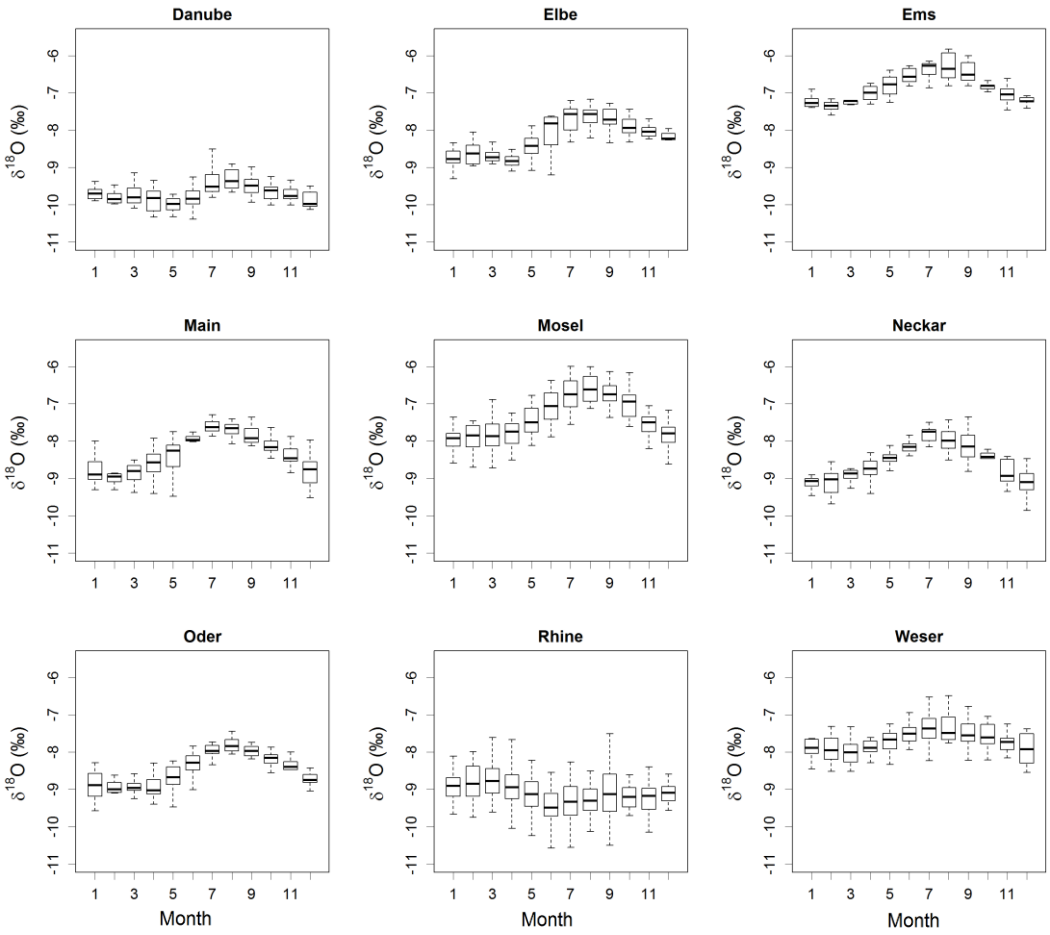

Figure 9: Mean annual variations of $\delta^{18}O$ in river water. The medians of the values are displayed as bold lines. The rectangles extent from the lower to the upper quartiles and the whiskers show the minimum and maximum values. Calculations are based on data from 2002 to 2013, except for the Mosel and the Rhine, where data from 1988 to 2013 were used. Calendar year is used.

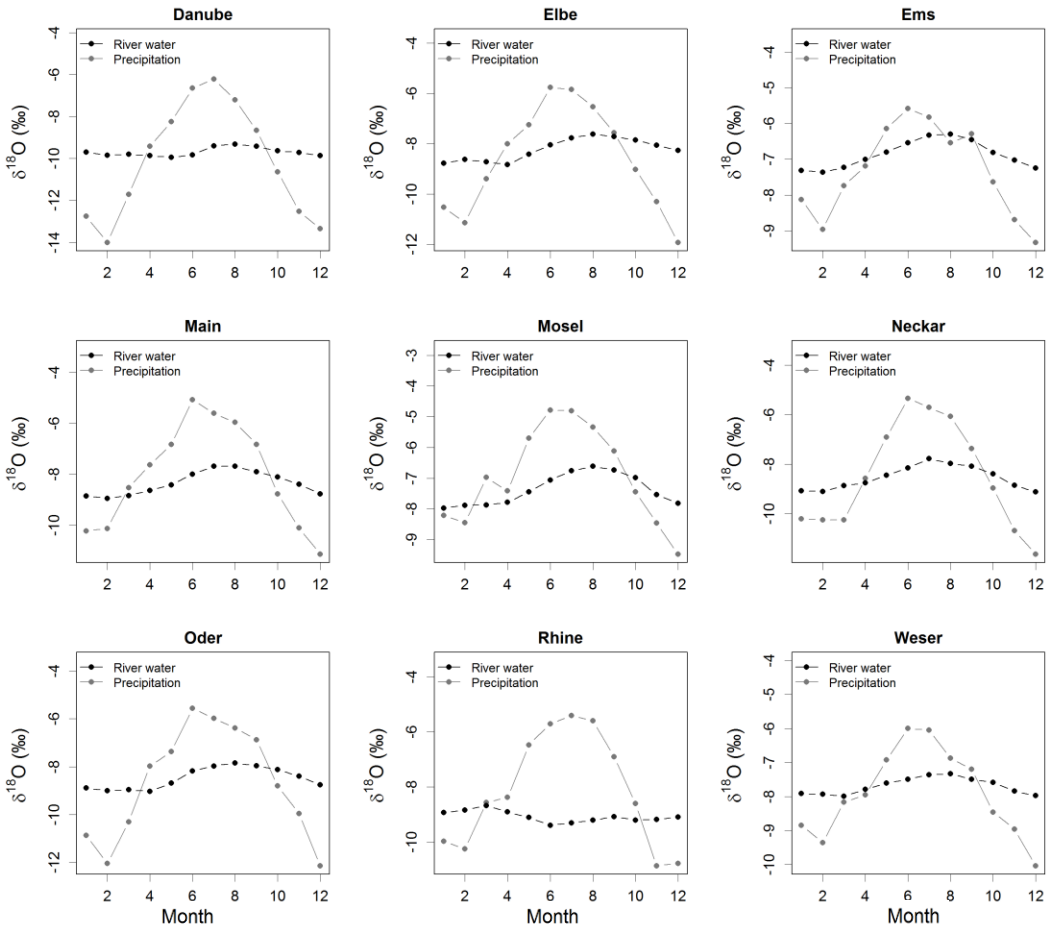

Figure 10: Mean annual variations of $\delta^{18}O$ in river water and mean catchment precipitation. Derived from data from 2002 to 2013, except for the Mosel and the Rhine for which data from 1988 to 2013 were used. Calendar year is used.

4.4.2 D-excess

The seasonal signals of d-excess in the rivers are in general less distinct than the seasonalities of $\delta^{18}O$ (see Figure 11). They are, however, in all rivers characterised by low d-excess values in summer and high values in winter, except for the Rhine, the Danube and the Weser. These rivers have the lowest d-excess values in July and August and the highest in January and February. In the Neckar, the d-excess is also low in May. The d-excess values in the Rhine, the Danube and the Weser do not reveal clear seasonal signals. In the Rhine and the Weser, the seasonal signals are indistinct with strongly varying mean monthly values. In contrast, the mean monthly values in the Danube do not vary much over the years but the seasonal variations are so much damped that the d-excess is nearly constant throughout the year. The seasonal signals of d-excess in the rivers compared to precipitation are shown in Figure 12. The d-excess seasonality in precipitation is in general characterised by low values from January to July whereby highest d-excess values occur from September to November. It cannot be clearly observed that the d-excess of precipitation is reflected in the river water.

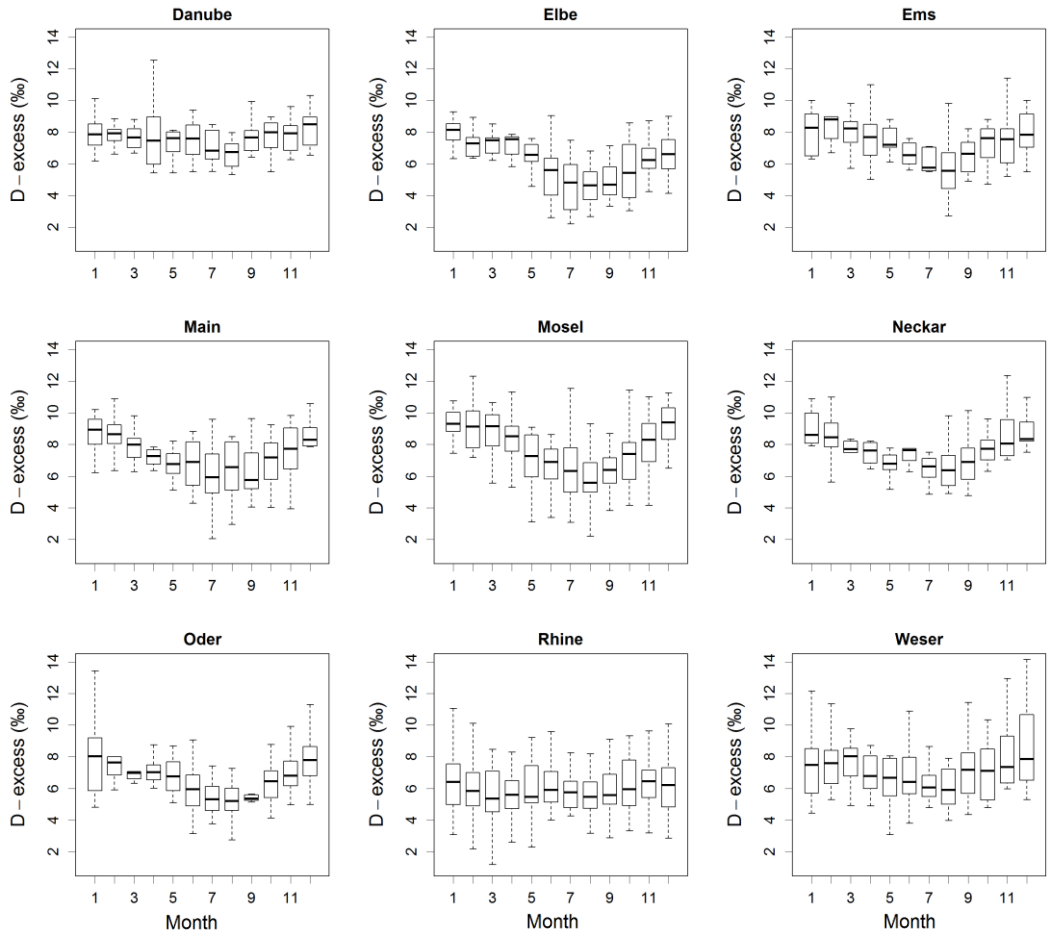

Figure 11: Mean annual variations of d-excess in river water. The medians of the values are displayed as bold lines. The rectangles extent from the lower to the upper quartiles and the whiskers show the minimum and maximum values. Calculations are based on data from 2002 to 2013, except for the Mosel and the Rhine, where data from 1988 to 2013 were used. Calendar year is used.

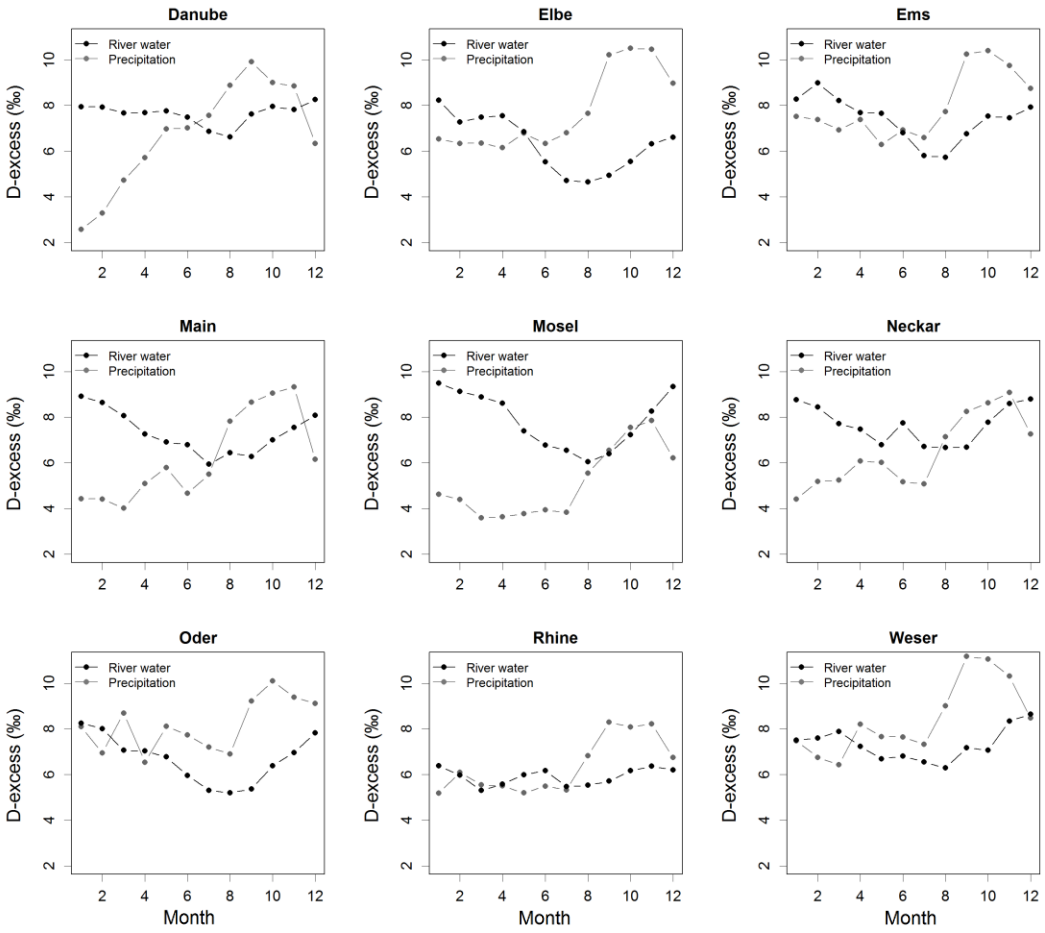

Figure 12: Mean annual variations of d-excess in river water and mean catchment precipitation. Derived from data from 2002 to 2013, except for the Mosel and the Rhine for which data from 1988 to 2013 were used. Calendar year is used.

4.5 Trend analysis

4.5.1 Oxygen-18

The long time series allow to explore the temporal behaviour of $\delta^{18}O$ in river water and precipitation. The smoothed and normalised time series are shown in Figure 13. For the Rhine and the Mosel, long-term trends are plotted from 1988 to 2013 and for the other rivers from 2002 to 2013. As a result of the smoothing procedure, there is no data for the first 11 months and the last 12 months of the original time series. Therefore, the smoothed time series are shorter than the original time series. The river water time series are plotted as solid lines and the precipitation time series as dashed lines. From visual assessment, positive long-term trends could be conjectured in the Danube, the Ems, the Oder and the Rhine time series. The Weser time series shows a negative trend. For the other rivers, no tendencies over time are recognisable.

Comparison to long-term trends in precipitation

Compared to the precipitation trend curves, the temporal variations of the river water trend curves are lower but similarities between both trend curves are still recognisable. In some rivers, the temporal development of the precipitation curve is clearly reflected in the river water curve but with a certain time shift. However, this is obviously observable only for the Elbe, the Main, the Neckar and the Oder (see Figure 13.b, e, g and h). In the other rivers, the river water trend curve corresponds only partly with the precipitation trend curve. The river water trend curve of the Rhine (see Figure 13.f) shows similar long-term trends as the precipitation in the first part of the observation period (~ 1988 to 2006). From 2006 on, temporal development of $\delta^{18}O$ in river water is not related to precipitation. Interestingly, similar phenomena can be observed in the Danube (see Figure 13.a). In both rivers, the precipitation trend curves have distinct minima in the year 2010, which are not reflected in the river water trend curve. Long-term development of $\delta^{18}O$ in the Weser river water also deviates from the one in precipitation (see Figure 13.i), but here in the first half of the time series. In the second half, river water trend is similar to the precipitation trend. For the Mosel and the Ems, it is hard to identify any similarities between precipitation and river water trend curves (see Figure 13.c and d). In the Ems, this is mainly due to the strong damping through which the temporal variations are almost vanished.

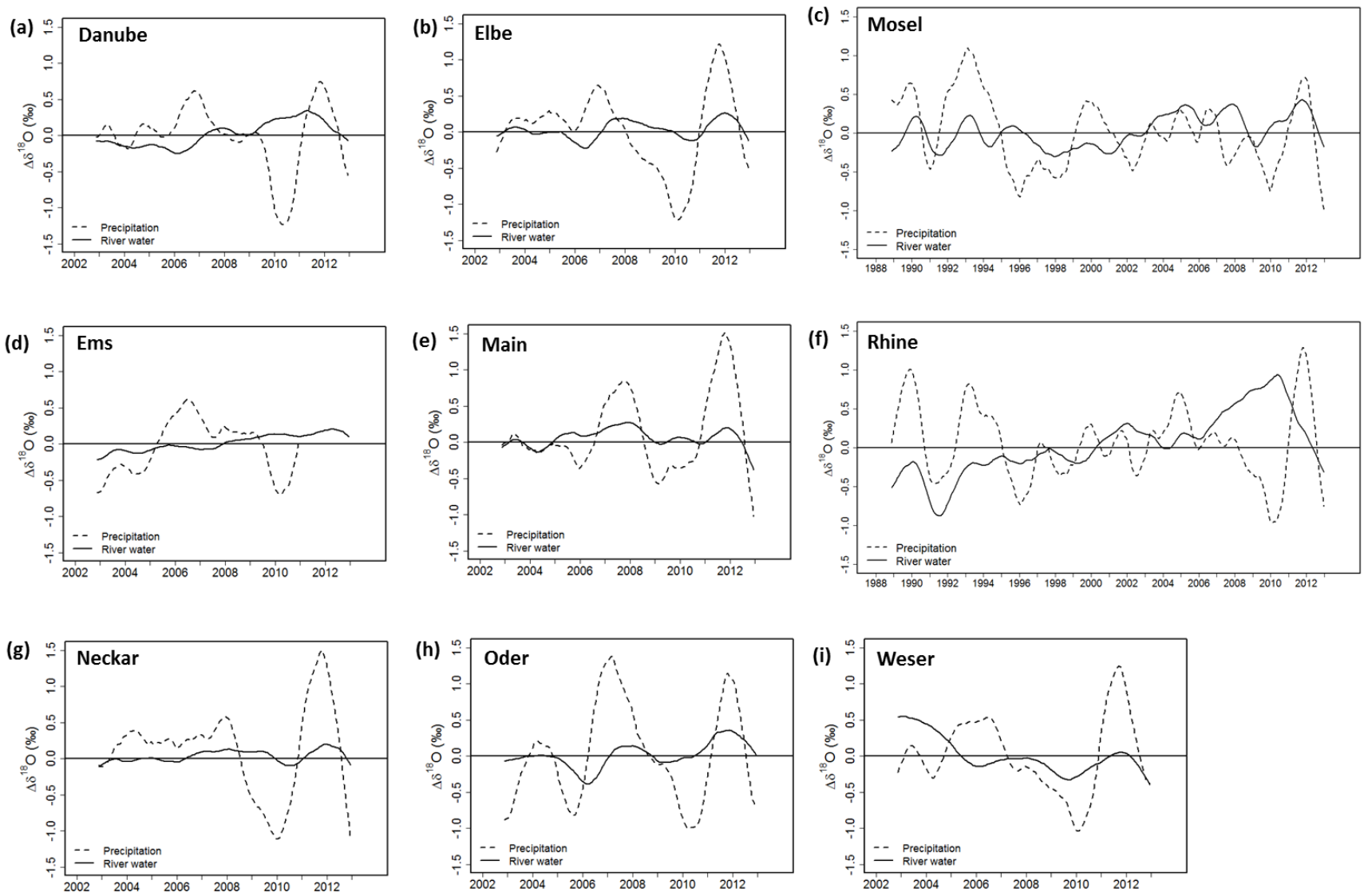

Figure 13: Long-term trends of $\delta^{18}O$ in river water and mean catchment precipitation. Time series were smoothed and normalised following the procedure of Rozanski et al. (1992).

Mann-Kendall trend test

The Mann-Kendall test is applied to statistically assess whether time series of $\delta^{18}O$ exhibit a monotonic trend. It is expected that the $\delta^{18}O$ time series (original, not smoothed and normalised) are autocorrelated since most of the rivers show clear seasonal signals. In correlograms, the autocorrelations of $\delta^{18}O$ time series are visualised (see Figure A 7, appendix). They demonstrate that the time series of all rivers are significantly autocorrelated with highest positive autocorrelation at lag 12. Some of them also show high negative autocorrelations at lag 6. Thus, first order autocorrelation in time series was removed from time series using TFPW method (Yue et al., 2002) to gain reasonable results from the Mann-Kendall trend test. However, in some time series higher order autocorrelations are still present (see Figure A 8, appendix).

The Mann-Kendall trend test is applied to adjusted data. Significant trends were found for the Rhine and the Weser time series (see Figure 14) with p-values < 0.01, whereas the trend in the Rhine is positive and negative in the Weser. For the Danube time series, a positive trend was detected with a p-value of 0.09, indicating at least a tendency. The previous visual assessment, conjecturing long-term trends in the Danube, the Ems, the Oder, the Weser and the Rhine time series, could be confirmed statistically only for the Rhine, the Weser and partly for the Danube time series. Although most of them are not significant, six out of nine rivers show a positive trend.

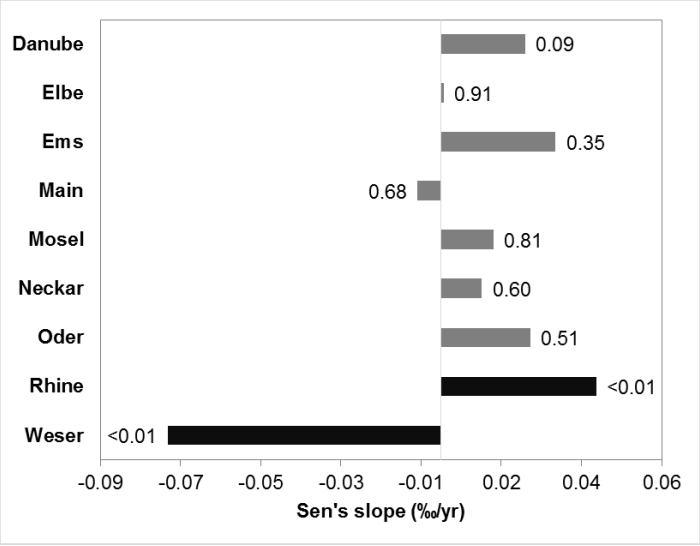

Figure 14: Sen-slopes (bars) and Mann-Kendall p-values (labels) of $\delta^{18}O$ time series. Black bars indicate significant trends. Significance level of 0.01.

4.5.2 D-excess

The d-excess time series of the rivers were also smoothed and normalised, just as it was done for $\delta^{18}O$ time series. The d-excess is from special interest since it is a strong indicator for evaporation. Lower d-excess values indicate a higher influence of surface evaporation. Below, smoothed and normalised d-excess time series of the rivers are shown. Short time series covering 12 years are plotted separately (see Figure 15) from long time series covering 25 years (see Figure 16). The short time series reveal that the temporal behaviour of the d-excess is similar for the seven rivers. Compared to the long-term averages, d-excess values are higher at about the year 2008 and lower during the periods from 2002 to 2007 and 2009 to 2011. The same can be observed for the Mosel but not for the Rhine (see Figure 16). The d-excess of the Rhine, in contrast, is decreasing in the period from 2007 to 2010. Interestingly, all nine rivers, including the Rhine, show a constant increase in d-excess starting in summer 2010. This general trend, observed for all rivers except for the Rhine, with high d-excess values at about the years 2008 and 2009, can also be observed in precipitation data, which is plotted in dashed lines. Only the d-excess trend of the Rhine shows considerable deviations from the precipitation. Yet, these deviations are only temporary.

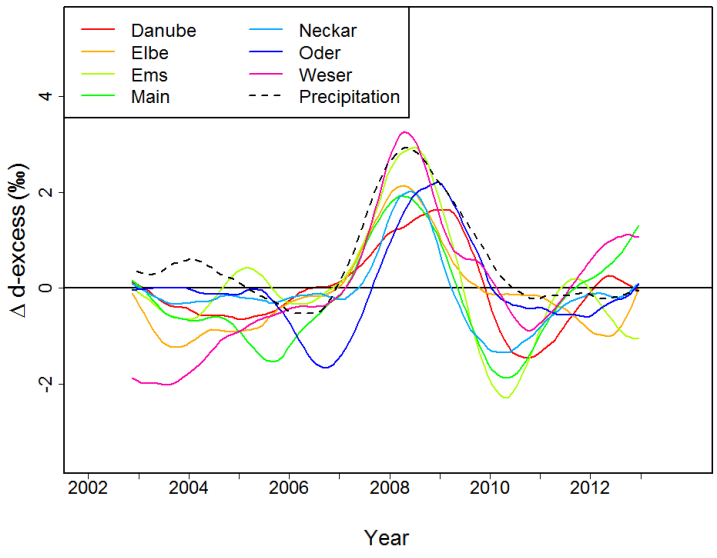

Figure 15: Long-term trends of d-excess in the rivers compared to the long-term trend in German precipitation (average derived from 28 meteorological stations). Only short time series from 2002 to 2013.

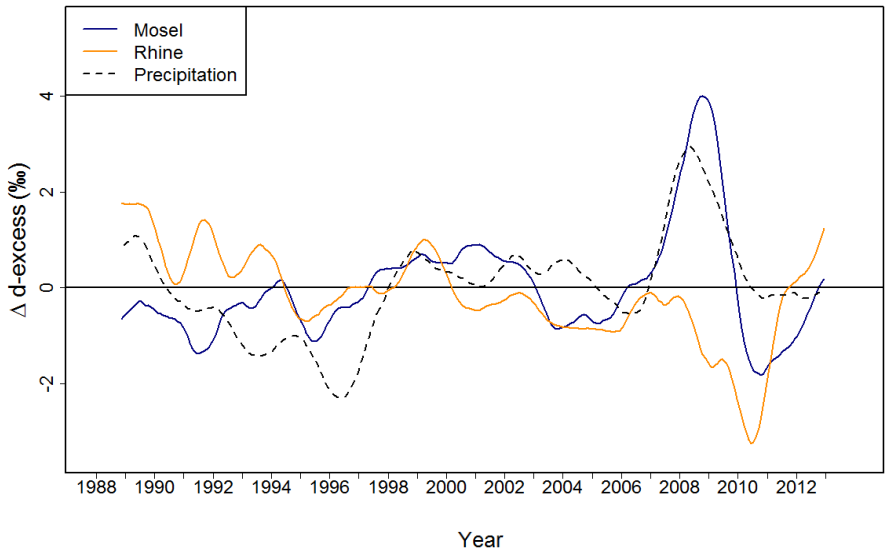

Figure 16: Long-term trends of d-excess in the rivers compared to the long-term trend in German precipitation (average derived from 28 meteorological stations). Only long time series from 1988 to 2013.

4.6 Spatiotemporal analysis

4.6.1 Original time series

Similarities between the $\delta^{18}O$ time series of the nine rivers were investigated using correlation and cluster analysis. Pearson's r was calculated between each pair of rivers based on the original time series. In Table 8, correlation coefficients among the $\delta^{18}O$ time series of the nine rivers are listed. The isotopic compositions of rivers in Northern and Central Germany (Elbe, Ems, Main, Mosel, Neckar and Oder) strongly correlate with each other ($r > 0.6$), red marks in Table 8. The isotopic compositions of the Danube and the Weser correlate slightly with the rivers mentioned above and show only little similarities with each other. The $\delta^{18}O$ time series of the Rhine significantly correlates with the $\delta^{18}O$ time series of the Danube, but with none of the other rivers.

Table 8: Correlation matrix showing similarities between original $\delta^{18}O$ time series of the sampling sites. Pearson's r were calculated for the period from 2002 to 2013. Red colours stand for high correlation coefficients close to 1 and green colours for low or negative correlation coefficients close to 0.

	Danube	Elbe	Ems	Main	Mosel	Neckar	Oder	Rhine	Weser
Danube	-								
Elbe	0.53*	-							
Ems	0.57*	0.65*	-						
Main	0.59*	0.74*	0.79*	-					
Mosel	0.57*	0.75*	0.77*	0.88*	-				
Neckar	0.53*	0.63*	0.79*	0.81*	0.79*	-			
Oder	0.59*	0.76*	0.70*	0.72*	0.77*	0.69*	-		
Rhine	0.32*	-0.07	0.03	0.14	0.02	0.04	-0.05	-	
Weser	0.27*	0.52*	0.43*	0.58*	0.57*	0.48*	0.51*	-0.04	-

*significant on a significance level of 0.01

Cluster analysis

The result of the cluster analysis is shown in Figure 17, where the rivers are grouped according to their similarities in $\delta^{18}O$ variations. Initially, rivers in the West of Germany (Ems, Neckar, Main and Mosel) are formed to one group and rivers in the Northeast of Germany (Elbe and Oder) are also clustered to one group. Both groups are then joined to one large group. The Danube, the Weser and the Rhine are joined to that group in the mentioned order. It can be stated that most of the rivers in Germany show similar $\delta^{18}O$ signals. Only the $\delta^{18}O$ time series of the rivers Danube, Weser and Rhine are different, whereby the signal of the Danube deviates only slightly from the other rivers. In contrast, the $\delta^{18}O$ signal of the Rhine shows hardly any similarities with other rivers. A slight correlation exists just between the Rhine and the Danube.

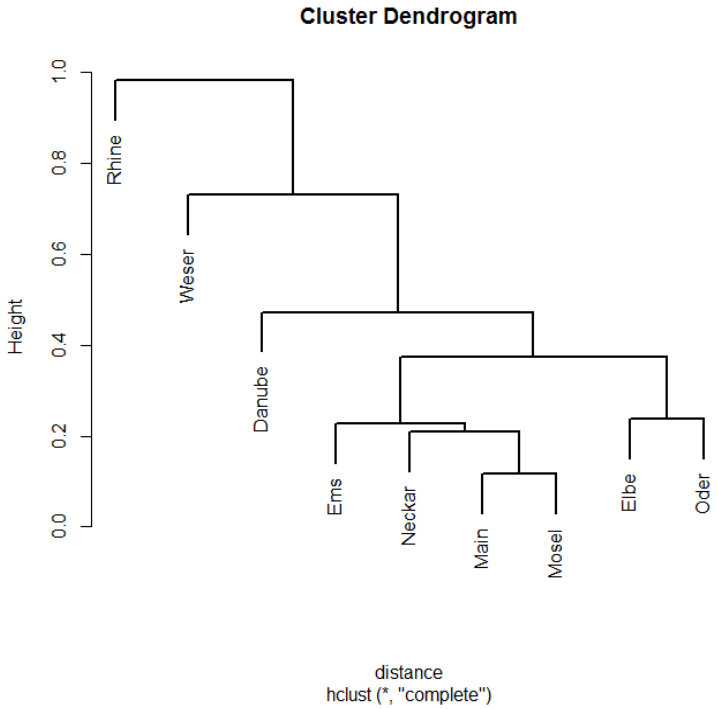

Figure 17: Dendrogram showing similarities between $\delta^{18}O$ time series (original) of the sampling sites. Pearson's r was used as distance measure. Correlation coefficients were calculated for the period from 2002 to 2013.

4.6.2 Smoothed and normalised time series

Since seasonal variations are still contained in original time series, analyses in the previous section mainly identified similarities in seasonality. Similarities in the long-term trends of $\delta^{18}O$ can also be investigated as the isotopic time series cover more than one decade. For that, correlation and cluster analysis were conducted with the smoothed and normalised time series. The results are shown in Table 9. In most cases, isotopic trends only correlate to the ones of adjacent catchments. Such can be observed e.g. for the Main and the Mosel, the Elbe and the

Oder, or the Danube and the Rhine. The Weser as an exception does not positively correlate with any of the other rivers, but it correlates negatively with the Neckar, the Danube, the Rhine and the Ems.

Table 9: Correlation matrix showing similarities between smoothed $\delta^{18}O$ time series of the sampling sites. Pearson's r were calculated for the period from 2002 to 2013. Red colours stand for high correlation coefficients close to 1 and green colours for low or negative correlation coefficients close to 0.

	Danube	Elbe	Ems	Main	Mosel	Neckar	Oder	Rhine	Weser
Danube	-								
Elbe	0.43*	-							
Ems	0.73*	0.34*	-						
Main	0.22	0.42*	0.09	-					
Mosel	0.09	0.36*	-0.05	0.59*	-				
Neckar	0.33*	0.76*	0.48*	0.57*	0.27*	-			
Oder	0.71*	0.79*	0.49*	0.16	0.40*	0.55*	-		
Rhine	0.62*	0.04	0.37*	0.34*	-0.20	0.09	0.05	-	
Weser	-0.39*	0.05	-0.73*	-0.20	0.21	-0.34*	0.03	-0.48*	-

*significant on a significance level of 0.01

Cluster analysis

The dendrogram in Figure 18 shows the result of the cluster analysis with smoothed $\delta^{18}O$ time series. There are two main groups with moderate similarities: the first group involves the Danube, the Ems and the Rhine and the second group contains the Main, the Mosel, the Neckar, the Elbe and the Oder. The adjacent catchments Main and Mosel, as well as Elbe and Oder are formed to groups with high similarities. Interestingly, the Danube and the Ems also have high similarities even though their catchments are located in completely different parts of Germany. The isotopic trends of the Neckar are similar to the ones of the Elbe and the Oder. The long-term trends of the Weser show no similarities to any of the other rivers. The grouping cannot be clearly linked to the geographic location nor to the topography of the catchments. Some adjacent catchments show high similarities but also catchments with completely different locations have similar long-term trends. The same applies to the topography of the catchments.

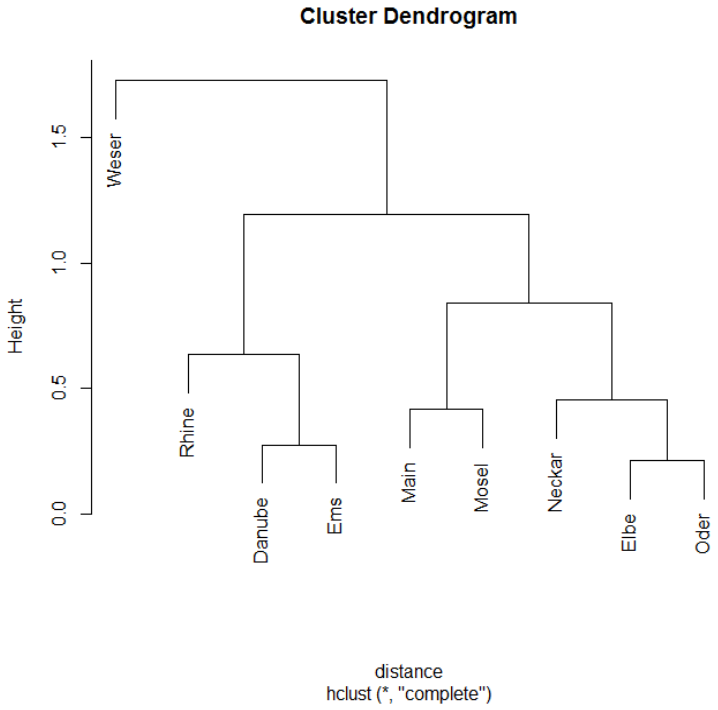

Figure 18: Dendrogram showing similarities between smoothed $\delta^{18}O$ time series of the sampling sites. Pearson's r was used as distance measure. Correlation coefficients were calculated for the period from 2002 to 2013.

4.7 Mean transit time modelling

The mean transit times of fast runoff components were estimated using the original $\delta^{18}O$ time series of the catchment precipitation and the river water. The average $\delta^{18}O$ concentration in the catchment precipitation was calculated for each catchment as input concentration. The model outputs are fitted to the observed $\delta^{18}O$ concentrations in the river water. In lumped parameter models, temporal variations in precipitation and river water data are utilised. As mentioned, the exponential model was chosen as the model type.

In Table 10, the parameter values of the two (three) best-fit models for each river are listed. In general, exponential models provide satisfactory simulations to isotopic observations. However, parameter values for the Rhine could not be identified. The best agreements between model results and observations could be achieved for mean transit times of 1 to 5 months and groundwater contributions of 60 to 80 %. The shortest mean transit time between 1 and 2 months was estimated for the Ems catchment, which is the smallest of the eight catchments. Apart from that, estimated transit times are not related to the catchment sizes. The highest transit times of 4 to 5 months were predicted for the Danube catchment, which has a catchment area that amounts to less than a half of the catchment area of the Elbe or the Oder.

Model predictions in comparison to observation data are shown in Figure 19. The seasonal variations of $\delta^{18}O$ in river water are well reproduced by all models. They are particularly accurate regarding the occurrence and the shape of minima and maxima. However, modelled curves are flatter than the ones of observations. The heights of the maxima are predominantly underestimated and only rarely overestimated. Especially, high maxima are not well reproduced, whereas the heights of the minima are simulated more accurately. Overall, the values for the Danube are predicted to be too low in the time between 2009 and 2013. Apart from that, the predictions fit well to the observations. The same can be observed for the Weser during the period from 2002 to 2005.

Goodness of fit and model performance

In order to assess the quality of the models, the goodness of fit and the model performance was determined. The goodness of fit is quantified by the RMSE and the model performance by the NSE. The model performance and the goodness of fit are not directly related, i.e. a good model fit does not automatically imply a good model performance and vice versa. The values of the RMSE range from 0.23 to 0.58 and the NSE values range from -0.02 to 0.72. Calibrated models for the Elbe, the Ems, the Main, the Neckar and the Oder show good model performances (NSE >0.5). Those of the Danube and the Mosel are moderate. For observations of the Weser, no better models than the two listed ones, which have a model performance around 0, were found.

In the model validation, the model performance and goodness of fit decline just slightly for most models. Thus, the model predictions do not only fit the observations to which the model was calibrated but also fit new data. Just in case of the Danube, the predictions of the two models do not fit well to new observations. The model performances decrease from ca. 0.4 to 0.1. Interestingly, the models of the Weser better fit the observations when applied to the entire time period.

Table 10: Model parameters and measures of model quality for best-fit models.

Catchment	Model no.	β	t_t (months)	$RMSE_{cal}$	NSE_{cal}	$RMSE_{val}$	NSE_{val}
Danube	1	0.8	5	0.25	0.40	0.33	0.12
	2	0.8	4	0.25	0.37	0.34	0.08
Elbe	1	0.7	3	0.35	0.52	0.36	0.54
	2	0.6	4	0.35	0.51	0.37	0.51
Ems	1	0.8	1	0.23	0.62	0.30	0.53
	2	0.7	2	0.23	0.63	0.30	0.51
Main	1	0.6	3	0.28	0.71	0.34	0.66
	2	0.7	3	0.27	0.72	0.33	0.67
Mosel	1	0.7	2	0.46	0.38	0.45	0.46
	2	0.6	3	0.58	0.02	0.47	0.42
Neckar	1	0.8	2	0.28	0.66	0.33	0.64
	2	0.7	2	0.29	0.65	0.34	0.61
Oder	1	0.8	2	0.32	0.60	0.39	0.51
	2	0.7	3	0.31	0.63	0.39	0.50
	3	0.6	5	0.32	0.60	0.42	0.43
Weser	1	0.8	2	0.43	0.07	0.40	0.24
	2	0.7	3	0.45	-0.02	0.42	0.17

cal – calibration period; val – validation period

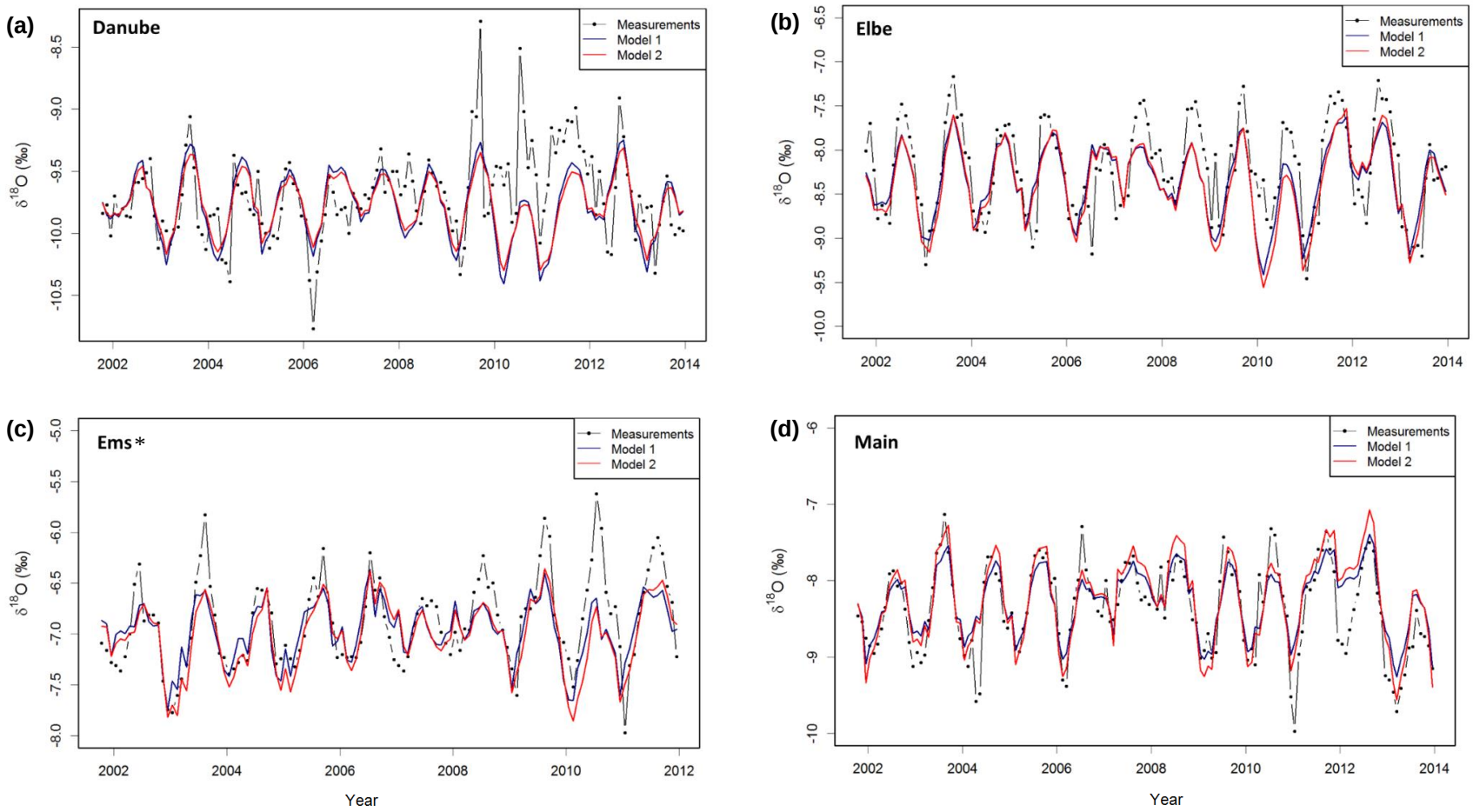

Figure 19: Model predictions and observations of $\delta^{18}O$ in river water.

***Input data (precipitation) was only available until 2012**

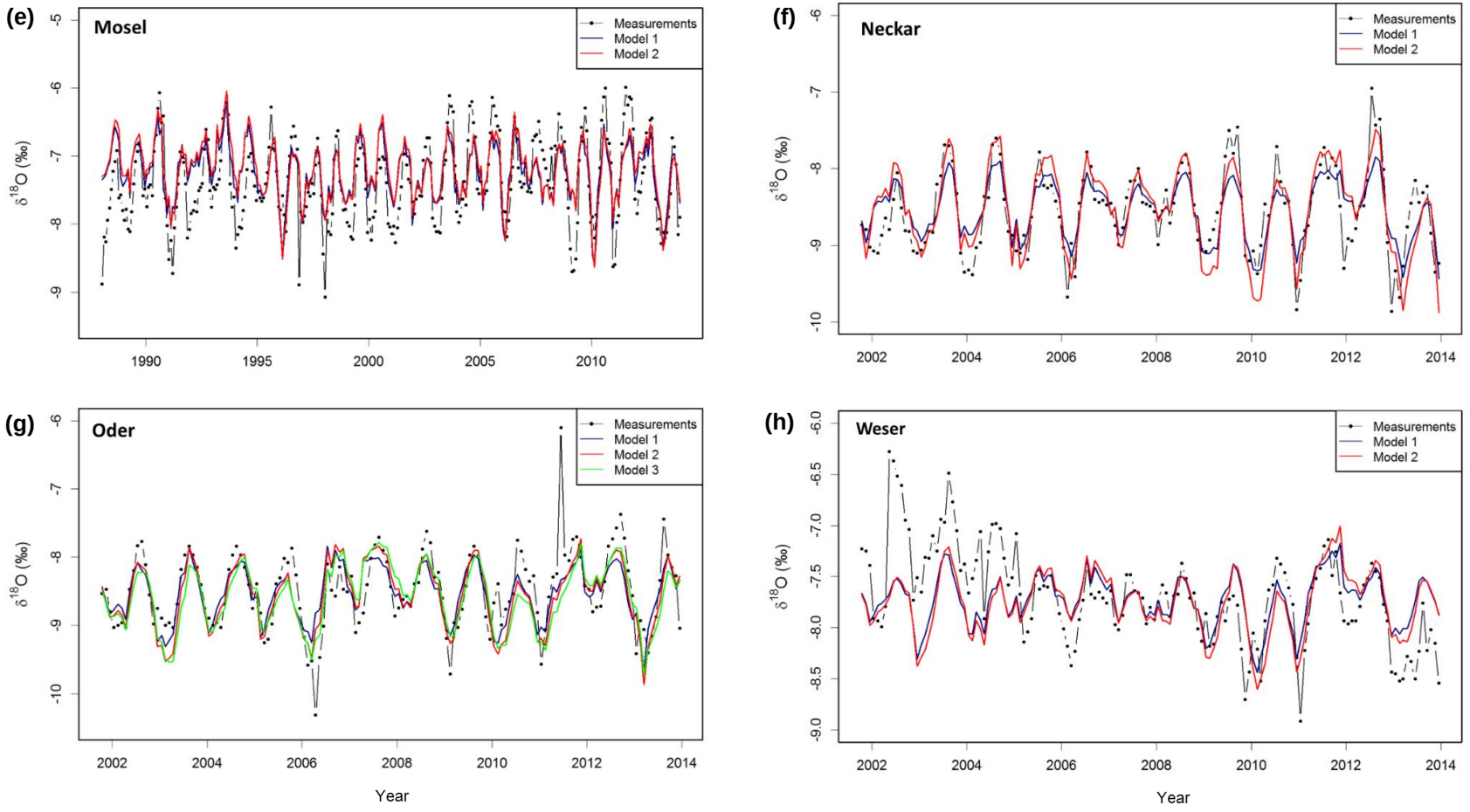

Figure 19: Continued.

4.8 The Rhine in its course

As long-term data from further stations within the Rhine catchment exist, I decided to have a closer look at the Rhine catchment. Moreover, this is also by far the most complex catchment for which, as has been shown in the previous sections, further considerations are required. In Figure 20, the $\delta^{18}O$ long-term trend observed in the Rhine water at Koblenz is shown in comparison to long-term trends observed at river water stations in the upper catchment (see Figure A 2, appendix). Up to 2008, the temporal development of $\delta^{18}O$ is similar at all stations, showing a positive trend, overall. In 2008, the $\delta^{18}O$ values start to decrease again. Interestingly, Koblenz is the only station which shows an onward enrichment from 2008 to 2011. Only in 2011, hence three years later, the $\delta^{18}O$ values rapidly decrease. In the trend curve of the precipitation sampled in Bern, this enrichment cannot be observed, either. As this anomalous enrichment is only apparent at the station in Koblenz, it can be concluded that processes in the middle catchment (between the stations Weil and Koblenz) must cause this extraordinary behaviour.

Trends in the discharge at Koblenz and the air temperature in the Rhine catchment are shown in Figure 21. Both underlie periodic variations. Around the year 2008, discharge is slightly lower than the long-term average and the air temperature is higher in 2007 but decreases rapidly afterwards. In the following years, the air temperature is also lower than the long-term average. As the discharge regime of the Rhine is rather indistinct, it is hard to say whether discharge was different in this time period. The annual discharge variations between the years 2002 and 2011 are plotted in the appendix (see Figure A 5 and A 6). The highest discharges tend to occur in spring as a result of snow melt in the catchment. Yet, the patterns are anything but clear and strongly vary over the years. As shown in section 4.5.2, the d-excess in the Rhine water decreases in the time around 2008, while it increases in the other rivers. Although the low d-excess values indicate a higher influence of evaporation there is no evidence for a higher influence of evaporation, neither increased temperatures nor low water conditions.

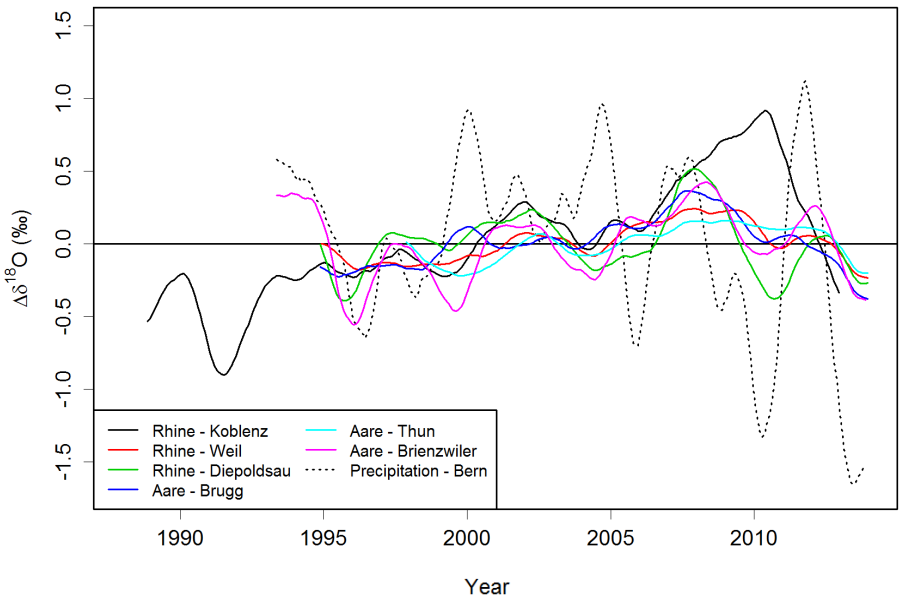

Figure 20: Long-term trends of $\delta^{18}O$ observed in river water and precipitation at several stations along the Rhine and its tributaries.

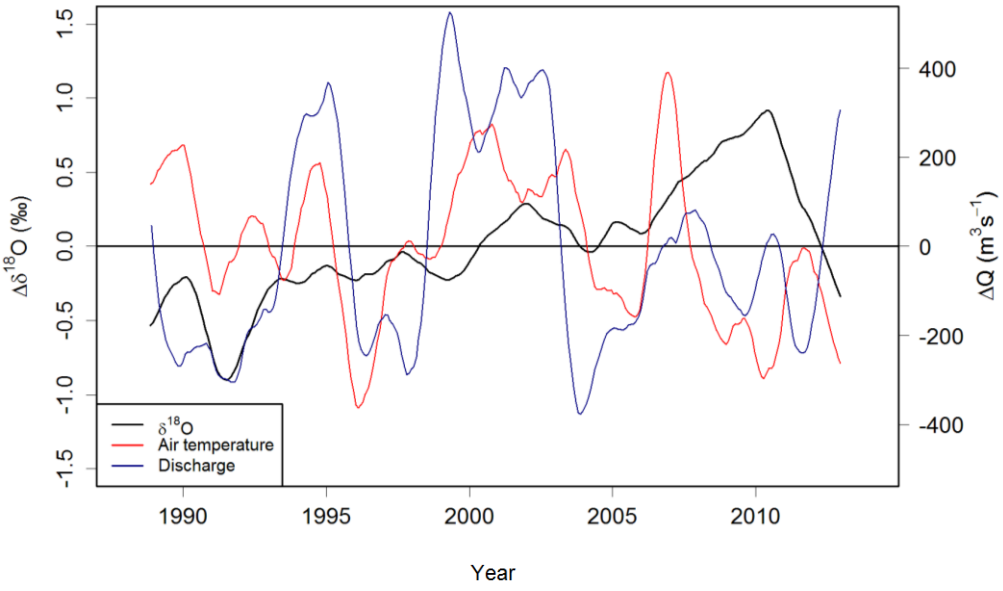

Figure 21: Long-term trend of $\delta^{18}O$ in the Rhine at Koblenz in comparison to long-term trends of discharge (measured at Koblenz) and average air temperature in the Rhine catchment.

5 Discussion

5.1 Spatial distribution

The long-term averages of $\delta^{18}O$ and $\delta^{2}H$ in the German rivers clearly show a northwest-southeast gradient (see Table 6), just as it has been observed for precipitation in Germany (Stumpp et al., 2014). For $\delta^{18}O$, it could be shown that long-term averages in the rivers are closely related to the long-term averages of local precipitation (see Figure A 4.a, appendix). It is assumed that the same applies to $\delta^{2}H$, as $\delta^{2}H$ is, in turn, linearly related to $\delta^{18}O$ (see Table 7). These findings agree with previous studies, which have shown that the spatial patterns observed for isotopic composition in precipitation are reflected in river water (e.g. Diefendorf and Patterson, 2005; Dutton et al., 2005; Katsuyama et al., 2015; Kendall and Coplen, 2001; Mizota and Kusakabe, 1994). In contrast, the long-term averages of d-excess in the nine rivers do not match the d-excess averages in local precipitation (see Figure A 4.b, appendix) and they do not reveal spatial patterns, either.

The slopes of the RWLs estimated for the German rivers are slightly lower (5.4 to 6.7) than the slope of the LMWL of Germany (7.7) (Stumpp et al., 2014) (see Table 7). These lower slopes result from evaporation within the catchment. Evaporation effects have been widely observed in water lines of surface water samples from diverse climate zones (e.g. Darling et al., 2003 *(Great Britian)*; Diefendorf and Patterson *(Ireland)*, 2005; Hogan et al., 2012 *(USA)*; Hughes et al., 2012 *(Australia)*; Kattan, 2012 *(Syria)*). Thus, the isotopic composition in surface water is obviously affected by evaporation not only in arid climate. However, slopes are even lower in arid climate zone. Slopes of 4 to 5 have been reported for the Rio Grande (USA) and the Bowen-Darling Rivers (Australia) (Hogan et al., 2012; Hughes et al., 2012).

5.2 Environmental and geographical controls

The $\delta^{18}O$ in river water shows a negative correlation with the catchment altitude (see Figure 4). The estimated altitude effect for the rivers (0.36‰/100m) is lower than the one in precipitation (0.47‰/100m) (Stumpp et al., 2014). This contradicts previous studies which have reported that altitude effects for river water are typically higher than for local precipitation (Wen et al., 2012; Winston and Criss, 2003). Winston and Criss (2003) explain this intensification of the altitude effect by the downstream transport of discharge within the catchments. However, it must be noted that their investigations have only been done on a regional and catchment scale. In addition, their approach is somewhat different as their calculations are based on the altitude of the sampling stations and not on the mean catchment altitude. I suggest that using the mean catchment altitude is more appropriate as river water is an accumulation of water from regions with different altitudes. Although the estimation might not be representative as it is based on

nine sites only, it indicates that the altitude effect is damped in river water. The isotopic composition in the rivers also tends to be depleted in catchments which are further in the South as a result of the latitude effect in precipitation (see Figure 4). It must be assumed that the continentality of the catchments also plays a role. Yet, this was not statistically tested. The relation between altitude and $\delta^{18}O$ appears to be more distinct than the latitude effect. The terrain in Southern Germany is in general of higher elevations than in Northern Germany. Hence, it is difficult to distinguish between the latitude effect and the altitude effect as both effects add up and the individual effects may be of lower magnitudes. Although the $\delta^{18}O$ long-term averages suggest a northwest-southeast gradient, longitude is not a significant factor. However, the northwest-southeast gradient can also be ascribed to the continentality effect since Germany is dominated by air masses coming from the West.

It could be shown that the d-excess decreases with increasing flow length and catchment area (see Figure 4). However, the parameters flow length and catchment area are not independent from each other as catchment area rises with increasing flow length. Such decreases of d-excess with increasing flow length have already been reported in previous studies (e.g. Kattan, 2012; Yuan and Miyamoto, 2008) and indicate that in-stream evaporation is a relevant process changing the isotopic composition in the rivers. Then, it can also be expected that the river water is enriched in ^{18}O with increasing flow length, but a significant association between $\delta^{18}O$ long-term averages and flow length could not be identified. I suppose that the downstream evaporation effect in $\delta^{18}O$ is hidden by the altitude and latitude effect which have a higher influence.

It was considered to estimate the individual effects of the parameters with a multiple linear regression model. However, the outcomes of the multiple linear regression analyses were not reasonable (see Table A 4, appendix), which may be a result of multicollinearity. As the independent variables latitude and altitude, as well as flow length and catchment area are correlated with each other (referred to as multicollinearity), the standard statistical method of multiple linear regression analysis is not appropriate to quantify the individual effect of the parameters. It has been shown in several studies that multicollinearity leads to biased estimations of multiple linear regression analysis (Chatterjee and Hadi, 2006; Graham, 2003). Therefore, more sophisticated methods and further considerations are required for a proper isolation of the individual effects.

Discharge

Analyses showed that $\delta^{18}O$ values in the rivers tend to be depleted with increasing discharge amount (see Figure 5). Furthermore, a tendency could be observed that the d-excess values are higher at high flows and lower at low flows (see Figure 6). In general, the linear relations are

poor, in particular between discharge and d-excess. They seem to be not linear but rather exponential. It can be assumed, that dependencies could be better described by exponential regression models than by linear regression models. However, direct causalities may not exist since observed relations must be rather ascribed to the discharge regimes of the rivers in Germany, which are characterised by higher discharges in winter and spring. As precipitation in winter formed at low temperatures is characterized by low $\delta^{18}O$ and high d-excess values (see Figure 10 and 12), winter and spring high flows are typically depleted in ^{18}O and have high d-excess values. Therefore, the causalities between discharge amount and $\delta^{18}O$ or d-excess, respectively, are most likely not direct. The observed relations are not analogous to the amount effect in precipitation since the low $\delta^{18}O$ values in high flows are not induced by discharge amounts, but by low winter temperatures. The same has been found by Yi et al. (2010) for the Mackenzie River in Canada featuring a similar discharge regime. They also concluded that correlations are attributed to higher discharge amounts in winter. It would be interesting to see how isotopic values are related to discharge amounts in catchments with different discharge regimes, e.g. in tropical regions.

5.3 Seasonality

Oxygen-18

Most of the rivers show a clear $\delta^{18}O$ seasonality with maximum values in late summer (see Figure 9). These patterns reflect the $\delta^{18}O$ seasonality of the precipitation in the catchments, but with a certain time shift and damping (see Figure 10) just as it has been observed in a number of earlier studies (e.g. Dutton et al., 2005; Katsuyama et al., 2015; Ogrinc et al., 2011; Rodgers et al., 2005; Speed et al., 2011). The time shifts amount to 1 to 2 months, while dampings are diverse (see Table A 2, appendix). This is at least true for catchments with predominantly pluvial discharge regimes. In contrast, the Rhine reveals minimum $\delta^{18}O$ values in summer. The low $\delta^{18}O$ values in summer are a result of the delayed release of precipitation in the form of snow and glacier melt water since the isotopically light melt water contributes greatly to discharge in summer. Such melt water influences have already been observed in previous studies (e.g. Dutton et al., 2005; Yi et al., 2010). The generally indistinct seasonal signal is attributed to the complex discharge regime of the Rhine. The Rhine water at Koblenz is a mixture of tributaries with diverse discharge regimes. Thus, the different seasonal signals overlap to an indistinct signal. Furthermore, the Rhine is dammed at several points in its course (Lake Constance and several watergates in the Upper Rhine Rift). These influences lead to modifications of the $\delta^{18}O$ seasonality. In a comprehensive study about isotope observations in precipitation, surface water and groundwater in Switzerland, it has been shown that the $\delta^{18}O$ seasonality in the Rhine is considerably altered in its course (Schürch et al., 2003). By the comparison of the seasonalities observed at stations along the Rhine and its tributaries, the

authors have shown that the confluence of tributaries from different environments (alpine and lowland) and the damming in the Lake Constance result in a seasonal signal in the Rhine which clearly deviates from the precipitation input signal.

It can be stated that the $\delta^{18}O$ seasonalities of the rivers are strongly dependent on the discharge regimes. These findings are consistent with the study of Halder et al. (2015) in which the $\delta^{18}O$ seasonality of more than 200 GNIR and 500 GNIP stations all over the world has been analysed. The seasonal signals observed in the German rivers correspond to seasonalities typically found in catchments located above a latitude of 30° N (termed as group A) (see Figure 22). The authors have further defined two subgroups: group A.1 are rivers with predominantly pluvial discharge regimes, which are also influenced by snow melt water in spring and group A.2 are rivers whose catchments are either located in alpine or arctic regions. Unsurprisingly, most of the investigated rivers in Germany correspond to subgroup A.1, whereby the seasonal signal of the Rhine looks slightly similar to subgroup A.2 having $\delta^{18}O$ minimum in summer (May/June).

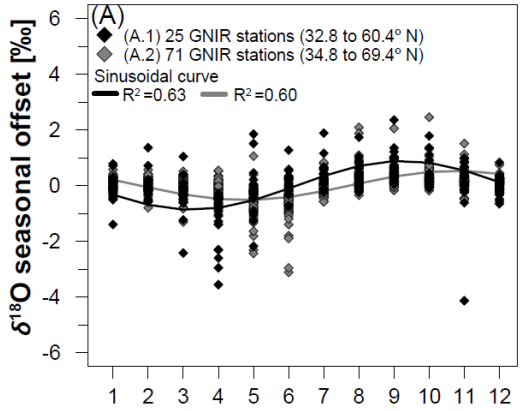

Figure 22: Oxygen-18 seasonality observed in river water at GNIR stations located >30°N (from Halder et al., 2015).

The seasonal signals of $\delta^{18}O$ in the rivers are damped to different extents, i.e. the amplitudes are diverse (see Table A 2). The Danube, the Weser and the Rhine have the smallest amplitudes indicating either high contributions of groundwater or an overlap of different $\delta^{18}O$ signals. The discharge regime of the Weser is relatively simple. Hence, the strong damping is most likely due to high groundwater contributions. In case of the Rhine, the latter is more likely (see discussion in previous paragraphs). The Danube is also influenced by tributaries from different environments but groundwater contributions are estimated to be relatively high, too. Thus, it may be a combination of both which causes the strong signal damping.

Findings of previous studies indicate that amplitudes of seasonal variations of $\delta^{18}O$ in precipitation are related to latitude (Dutton et al., 2005; Feng et al., 2009; Halder et al., 2015). The seasonal variations in precipitation at higher latitudes tend to be more pronounced than at

lower latitudes. However, such relation has not been observed for river water (Halder et al., 2015). Halder et al. (2015) have pointed out that the amplitude of the $\delta^{18}O$ seasonality in river water is rather controlled by processes on the catchment scale and reservoirs within the catchment than by global factors. This agrees with my findings, which also suggest that the damping of the seasonal signal is determined by the amount of groundwater contributing to discharge and the complexity of the flow system. Thus, it can be a meaningful indicator for catchment processes.

D-excess

The d-excess seasonality observed in the majority of the German rivers is characterised by high d-excess values in winter and low d-excess values in summer (see Figure 11). These seasonal signals appear to be distinct in rivers with simple pluvial discharge regimes, similar to what was found for the seasonality of $\delta^{18}O$. The seasonal signals in the river water correspond to the patterns which have been typically observed in precipitation in the Northern Hemisphere (Fröhlich et al., 2002; Pfahl and Sodemann, 2014) (see Figure 23). The d-excess in precipitation is negatively correlated with temperature and relative humidity in the atmosphere. As temperature and relative humidity is generally higher in summer, d-excess values are lower. The d-excess seasonality in precipitation in Germany looks a bit different from what is typical for the Northern Hemisphere only showing higher values from September to December, but not in late winter and spring (see Figure 12). This anomaly may be a result of the hysteresis effect discussed in Jouzel et al. (1997). At some locations, it has been observed that the d-excess in precipitation is higher in autumn than in spring although the values for temperature and relative humidity are comparable. However, this goes beyond the scope of this thesis and should be investigated individually. In rivers, the d-excess can be modified as a result of evaporation. When water evaporates, the d-excess in runoff water decreases. The d-excess seasonality in the rivers considerably deviates from seasonality in precipitation. This suggests that evaporation within the catchment (from soil or water surface) substantially modifies the d-excess in the rivers. However, the seasonal signals of the d-excess in the rivers are not only damped, lower in absolute values and time shifted as one would expect. The relations between the d-excess in river water and in precipitation rather appear to be more complex. In contrast to $\delta^{18}O$, the seasonality of d-excess in river water has been rarely investigated, yet. Katsuyama et al. (2015) just recently published a study in which they have presented seasonal patterns of d-excess observed in rivers in Japan. Therein, they have recognised a strong damping only in the seasonal signals of d-excess. Further investigations are required in order to identify factors determining the d-excess seasonality in the rivers.

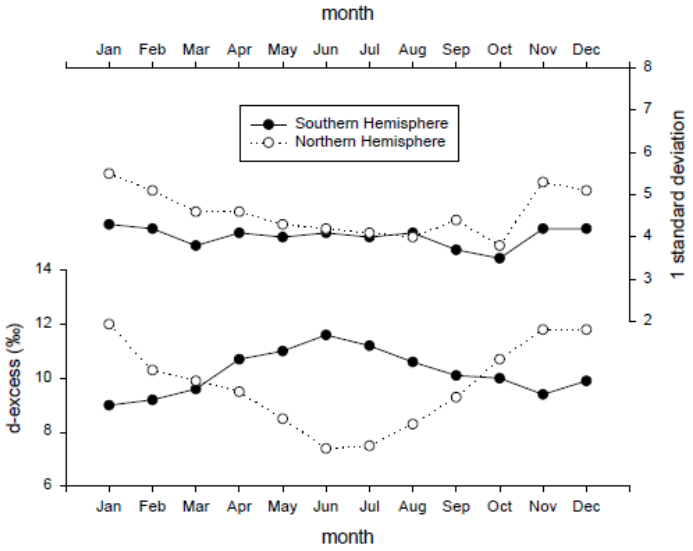

Figure 23: Typical d-excess seasonality in precipitation for Northern and Southern Hemisphere (from Fröhlich et al., 2002).

5.4 Long-term trends

Oxygen-18

In the Elbe, the Main, the Neckar and the Oder the long-terms trends of $\delta^{18}O$ clearly reflect the long-term trends observed in precipitation (see Figure 13). They are, however, less varying and time shifted, which is a result of groundwater confluence and a buffering effect of the catchment. This suggests that further catchment processes modifying the isotopic input from precipitation play a minor role in these catchments. Strong discrepancies between the $\delta^{18}O$ trends in river water and in precipitation are observed in the remaining rivers indicating dominant processes which alter the isotopic composition such as evaporation, damming or storage. In the Danube, the Rhine and the Weser, deviations from precipitation input are merely apparent for certain time periods, which suggests only temporary influences. A general discrepancy between isotopic composition in precipitation and river water can be observed in the Mosel and the Ems. In the Ems, groundwater highly contributes to river discharge (70 to 80 % estimated). Thus, long-term variations in the Ems are nearly averaged out, which makes it hard to identify similarities with the precipitation input. The processes causing deviations from long-term trends in precipitation in the Mosel are not as obvious. Having in mind, that such large catchments are highly heterogeneous, this is not surprising.

Comparable studies analysing such long time series of isotopic composition in river water are rare. As far as is known, analyses of time series of similar length have only been conducted for the Danube catchment, yet (Rank and Papesch, 2010; Rank et al., 1998). Rank et al. (1998) have compared the $\delta^{18}O$ long-term trends (12-month moving averages) of precipitation and the Danube River water in Vienna. They have found that the trend curve of the Danube mostly agrees with precipitation, but they have also observed temporary deviations (1980-1983 and

1993-1995). In the years 1980 to 1983, the Danube shows a depletion in ^{18}O compared to precipitation. The authors explain this depletion by unusual high winter precipitations in regions of higher altitudes during this time. The precipitation from high altitudes was further more depleted than the observed long-term average. However, they could not find reasons for the deviations between 1993 and 1995. In a subsequent and more extended study, Rank and Papesch (2010) have analysed the long-term trends of $\delta^{18}O$ (ten-year moving averages) in several Austrian rivers and in precipitation from sites located across Austria. They have pointed out that decadal variations are more pronounced in precipitation and rivers of higher altitudes, than of lower altitudes. However, this cannot be observed in the rivers in Germany. The trend curves of the rivers Ems (lowland catchment) and Danube (mountainous headwater) are most damped with the result that they hardly show any variations. Therefore, the damping of long-term variations does not seem to be controlled by the catchment altitude but rather by factors on the catchment scale. I could imagine that transit times of groundwater are important. In order to identify the influencing factors, the river catchments need to be investigated in more detail.

Trend test

Statistically significant trends in the $\delta^{18}O$ observations were identified in two rivers whereby the $\delta^{18}O$ shows a positive trend in the Rhine and a negative trend in the Weser (see Figure 14). Long-term trends in isotopic time series have only been examined for precipitation in Europe, yet (Klaus et al., 2015; Lykoudis and Argiriou, 2011; Rozanski et al., 1992; Stumpp et al., 2014). In these studies, significant trends, positive as well as negative ones, have been identified at single stations. So far, they could neither identify consistent spatial patterns nor the factors controlling these trends. In addition, Klaus et al. (2015) have addressed uncertainties of the Mann-Kendall trend test resulting from higher order autocorrelations in the time series. The commonly used approach of TFPW by Yue et al. (2002) only accounts for first order autocorrelations. Therefore, the authors proposed a new method using autoregressive integrate moving average models (ARIMA) for removing autocorrelations from the time series. They could show that trend test results are different when higher order autocorrelations are removed from the time series with ARIMA, in contrast to the TFPW approach. This means that there is evidence that higher order autocorrelations also bias trend test results. In my analyses, it turned out that some of the time series still reveal autocorrelations of higher order after the TFPW adjustment (see Figure A 8, appendix). Thus, the validity of the trend test results must be seen critical. So far, the findings of Klaus et al. (2015) are only indications which need to be further investigated in order to make methods for trend detection in autocorrelated time series more reliable.

D-excess

The d-excess long-term trends are consistent in all rivers except for the Rhine (see Figure 15 and 16). The rivers clearly reflect the average d-excess trend observed in precipitation in Germany. This might suggest that rivers are mainly determined by precipitation input and evaporation processes within the catchments are negligible. However, it is also possible that the d-excess in precipitation and river water is subject to the same controls, i.e. that both, the d-excess in precipitation and in the rivers, are affected by temperature resulting in similar long-term trends. In previous sections, it was shown that evaporation does have an influence on the d-excess in the river water. Hence, the latter explanation appears to be more likely. In contrast, in the Rhine, further processes occurred which led to a remarkable decrease in the d-excess. Compared to the precipitation, the d-excess in the Rhine appears to be lower during the time from 2007 to 2010. This implies that evaporation within the catchment is enhanced during this time, which can have various reasons. Some of them are discussed in section 5.7.

5.5 Spatiotemporal analysis

Seasonality

Based on the $\delta^{18}O$ seasonality of the rivers, six out of the nine rivers were clustered to one group which was further split into two subgroups (see Figure 17). The rivers Danube, Weser and Rhine reveal different $\delta^{18}O$ seasonalities. As shown in previous sections, their seasonal signals are indistinct or strongly damped. In general, the findings suggest that the grouping is linked to the geographic location and topography of the catchments. Obviously, adjacent catchments and catchments featuring comparable topography are similar in their $\delta^{18}O$ seasonality. Halder et al. (2015) have suggested that $\delta^{18}O$ seasonality is strongly dependent on the river's discharge regime. Apparently, this also applies to the investigated rivers in Germany. All rivers characterised by a pluvial discharge regime were clustered to one group with the only exception of the Weser. In addition, the only two rivers which are influenced by spring high flows from melt water (Danube and Rhine) are also correlated with each other.

Long-term trends

In contrast, no spatial patterns can be identified for $\delta^{18}O$ long-term trends in the rivers. The groups determined in the cluster analysis with smoothed time series are neither linked to geographic location nor to topography (see Figure 18). The clustering is inconclusive to a certain degree. Some adjacent catchments show high similarities. Yet, this also applies to some catchments with completely different geographic locations, e.g. the Danube and the Ems. The two rivers are most likely clustered since in both rivers groundwater highly contributes to discharge with the result that their trend curves show nearly no variations (see Figure 13). In the rivers Neckar, Elbe and Oder, the $\delta^{18}O$ trend in precipitation, which is relatively

homogeneous across the country, is well reflected. Thus, they all show similar trends although they do not lie in the same region of Germany. The concrete factors determining the $\delta^{18}O$ long-term trends in the rivers are not clear but the clustering to several small groups suggests that local factors are important. Further, there is evidence that long-term trends are determined by the precipitation input but also on processes on the catchment scale, such as groundwater contribution, evaporation and melt water influence, which modify the isotopic composition in river water.

5.6 Transit time modelling

For the majority of the catchments, it was possible to develop models which adequately simulate the transport of direct flow components through the catchments (see Figure 19). Mean transit times for fast runoff components of 1 to 5 month were estimated (see Table 10). Using original time series, modelling is mainly based on seasonal variations. It must be noted that these seasonal variations only represent the response of fast runoff components. Hence, the mean transit times of fast runoff components are merely estimated. Concerning the investigated catchments, transit time estimations have been conducted earlier for the Danube and the Weser catchment, but for none of the others (Königer et al., 2009; Rank et al., 1998). Königer et al. (2009) quantified fast and slow runoff components and estimated their transit times for several stations along the Weser. They also used lumped parameter models for tracer simulations. For the station at Intschede (close to Langwedel), they suggest a mean transit time for fast runoff components of 1 to 1.5 months and a groundwater contribution of 60 %. In comparison to their findings, slightly higher transit times of 2 to 3 months and a groundwater contribution of 70 to 80 % were calculated for the Weser. However, their simulations have been based on data from a shorter time period (2003-2007). Regarding the Danube, Rank et al. (1998) have estimated a transit time for fast runoff components of 1 year (up to Vienna). My simulations yield a transit time of 4 to 5 months for the Danube at Vilshofen. Considering that the flow length up to Vienna is nearly twice as long as up to Vilshofen, estimations seem to be plausible. The estimated transit times of fast runoff components are not related to catchment size. That transit time is not dependent on catchment size but rather on topography has already been shown in previous studies (e.g. McGlynn et al., 2003; McGuire et al., 2005). Within the scope of this thesis, a relation to topography could not be assessed as the majority of the examined catchments are located in lowlands. They are therefore not diverse enough in topography.

It should be remarked that the models show some uncertainties. In lumped parameter models, relevant catchment processes are not considered, namely evaporation, damming and storage. As shown in previous sections, such processes have considerable effects on the isotopic composition in the investigated rivers. Consequently, in more complex catchments, the

isotopic composition of river water is not well reproduced by lumped parameter models. This can be seen e.g. in the Weser and the Danube, where the isotopic composition is predicted to be too low continuously for the period from 2002 to 2005 and 2009 to 2013, respectively. This indicates that runoff water got enriched in ^{18}O within the catchment which happened most likely by evaporation. As evaporation enrichment is not included in the models, real values are underestimated by the model. The same applies to the other processes stated above. This explains why it was not possible to identify parameter values with which the highly complex Rhine catchment can be adequately described. More sophisticated and flexible models are required for such complex catchments.

The validity of mean transit time estimations for such large catchments is currently under discussion. Kirchner (2015) has criticised that calculating the transit time in such large catchments, which are highly heterogeneous, is inaccurate. The methods used for transit time estimations simply assume one TTD for the catchment, but large catchments typically consist of several subcatchments with different characteristics and therefore different TTDs. He has argued, that such aggregations are not negligible and may lead to errors, which have not been sufficiently investigated, yet. I am aware of uncertainties due to such large-scale simplifications, however, further research is needed to specify the implications of Kirchner's (2015) claims.

5.7 The Rhine in its course

In most catchments, the variations of $\delta^{18}O$ observed in the catchment precipitation are well reflected in the river water observations. However, the analyses showed that there are also clear discrepancies between $\delta^{18}O$ in precipitation and river water. These are most pronounced in the Rhine catchment. Here, neither the $\delta^{18}O$ long-term trends nor the seasonality observed in precipitation and river water correspond with each other (see Figure 10 and 13). Furthermore, it was not possible to predict the $\delta^{18}O$ observations in the Rhine water from the precipitation input as it was possible for the other catchments. One reason for this is that the discharge regime of the Rhine is complex. The discharge is composed of several water sources: direct rainfall runoff, groundwater, snow and glacial melt water. Moreover, the discharge is dammed in the Lake Constance, located at the border of Germany and Switzerland, and at several watergates which substantially alter the flow regime. Due to this complexity the $\delta^{18}O$ in the Rhine water is not as predictable as for the other rivers. Halder et al. (2015) have also demonstrated by a few examples that reservoirs in river systems lead to considerable alterations of the $\delta^{18}O$ seasonal signal. It has already been observed that reservoirs in the Upper Rhine catchment have an impact on the $\delta^{18}O$ seasonality of the Rhine and its tributaries (Schürch et al., 2003).

However, these complex flow conditions explain why seasonal variations are irregular and do not match variations in precipitation, but they do not explain the deviations between the long-term trends in river water and precipitation. An enrichment in ^{18}O is observed at the station in Koblenz during the period from 2008 to 2011, but at none of the stations in the upper catchment (see Figure 20). Thus, this enrichment must be caused by processes in the Upper Rhine Rift. Several consideration were made in order to find possible explanations for this phenomenon. Strong anomalies can neither be observed in the discharge (amount or occurrence) nor in the air and water temperatures (see Figure 21) (Internationale Kommission zum Schutz des Rheins, 2013). Several power plants and watergates are located along the Rhine. To the best of my knowledge, such anthropogenic influences have not been intensified for the last few years at the Rhine (EDF, n.d.; Internationale Kommission zum Schutz des Rheins, 2014). Interestingly, an enrichment in ^{18}O can also be observed in the Danube from 2008 to 2011, which suggests that regional factors are important. However, it was not possible to identify factors or processes responsible for this anomalous enrichment. Hence, further isotope studies in the Rhine catchment with higher spatial and temporal resolution are definitely worthwhile.

6 Summary and conclusion

In this thesis, long-term data of stable isotopic composition in river water from nine large catchments in Germany were examined and analysed. It could be shown that the spatial and temporal patterns observed in precipitation in Germany are reflected in the majority of the rivers. The isotopic long-term averages of the catchments correlate with altitude and latitude and show therefore a northwest-southeast gradient. Thus, the isotopic composition in German rivers can basically serve as a proxy for the local precipitation. It was also found that long-term averages of d-excess are inversely related to flow length and catchment size, which indicates that evaporation enrichment has an impact on the isotopic composition in catchments with humid climate as well. Moreover, the $\delta^{18}O$ and d-excess values correlate with discharge. These relations are not directly causal but can rather be attributed to isotopically light winter and spring high flows in the catchments.

The $\delta^{18}O$ seasonality and long-term trends of the local precipitation can be clearly recognised in rivers with simple pluvial discharge regimes. In comparison to precipitation, the $\delta^{18}O$ signals in the rivers are only damped and time shifted. The time shifts in the signals provide information about the catchment transit times. The dampings mainly depend on the amount of isotopically stable groundwater contributing to discharge but can also be caused by reservoirs or by an overlap of different signals from tributaries. In contrast, in rivers with more complex discharge regimes, deviations from the isotopic composition in precipitation input can be observed. Such deviations are caused by several catchment processes and factors, e.g. evaporation enrichment, precipitation temporarily stored as snow and ice, and damming by lakes and artificial reservoirs. However, in order to identify the concrete reasons for these deviations, additional considerations and studies with higher spatial and temporary resolution are necessary. Statistically significant long-term trends were identified for the Weser and the Rhine whereby in the Weser the $\delta^{18}O$ values decrease, while they increase in the Rhine. General spatial patterns for the $\delta^{18}O$ seasonality or long-term trends could not be found. The $\delta^{18}O$ seasonality rather seems to be controlled by the discharge regimes of the rivers. Factors which determine the $\delta^{18}O$ long-term trends in the rivers are not clear, as they are also uncertain for precipitation.

The temporal variation of the d-excess in the rivers also seem to be a meaningful indicator for hydrological processes. It could be shown that the d-excess seasonality in German rivers is closely related to the discharge regime, too. However, the d-excess seasonality of the local precipitation appears to be strongly modified in the rivers, most likely by evaporation in the catchment. In contrast, the long-term trends of the d-excess correspond to the precipitation and are consistent for almost all rivers. This suggests that controlling factors are rather global.

Mean transit times of fast runoff components could be estimated using lumped parameter models. The model simulations are based on the variations of the stable isotopic composition observed in the river water and precipitation. With the use of exponential TTD, adequate models could be developed for all catchments with the only exception of the Rhine. Mean transit times of fast runoff components were estimated to be between 1 and 5 months. In the exponential model, several processes such as evaporation, damming or storage are not considered. These processes modify the isotopic composition of runoff water. Therefore, the model results show some uncertainties. In rivers with complex flow systems (particularly in the Rhine), uncertainties are high, which suggests that more flexible and sophisticated models are needed. However, this study demonstrated that stable isotopes can be utilised to estimate mean transit time of fast runoff components in large river catchments. It could also be shown that methods usually applied on small scales can be basically adopted for large scale studies.

References

Bormann, H.: Runoff regime changes in German rivers due to climate change, Erdkunde, 64(3), 257–279, doi:10.3112/erdkunde.2010.03.04, 2010.

Bowen, G., Wassenaar, L. and Hobson, K.: Global application of stable hydrogen and oxygen isotopes to wildlife forensics, Oecologia, 143(3), 337–348, doi:10.1007/s00442-004-1813-y, 2005.

Bronaugh, D. and Werner, A.: Package 'zyp': Zhang + Yue-Pilon trends package, [online] Available from: https://cran.r-project.org/web/packages/zyp/index.html, 2013.

Bundesministerium für Umwelt Naturschutz und Reaktorsicherheit (BMU): Hydrologischer Atlas von Deutschland., 2003.

Burgman, J. O., Calles, B. and Westman, F.: Conclusions from a ten year study of oxygen-18 in precipitation and runoff in Sweden, in Isotope Techniques in Water Resources Development. Proceedings of an International Symposium, March 30-April 3, 1987, pp. 579–590, International Atomic Energy Agency, Vienna., 1987.

Buttle, J. M.: Fundamentals of Small Catchment Hydrology, Elsevier B.V. [online] Available from: http://dx.doi.org/10.1016/B978-0-444-81546-0.50008-2, 1998.

Chatterjee, S. and Hadi, A. S.: Regression analysis by example, John Wiley & Sons Ltd, New Jersey., 2006.

Clark, I. D. and Fritz, P.: Environmental isotopes in hydrogeology, CRC Press, New York., 1997.

Craig, H.: Isotopic Variations in Meteoric Waters., Science, 133(3465), 1702–1703, 1961.

Dansgaard, W.: The O18-abundance in fresh water, Geochim. Cosmochim. Acta, 6(5–6), 241–260, doi:http://dx.doi.org/10.1016/0016-7037(54)90003-4, 1954.

Dansgaard, W.: Stable isotopes in precipitation, Tellus, 16(4), 436–468, doi:10.1111/j.2153-3490.1964.tb00181.x, 1964.

Darling, W. G., Bath, A. H. and Talbot, J. C.: The O and H stable isotope composition of freshwaters in the British Isles. 2. Surface waters and groundwater, Hydrol. Earth Syst. Sci., 7(2), 183–195, doi:10.5194/hess-7-183-2003, 2003.

Diefendorf, A. F. and Patterson, W. P.: Survey of stable isotope values in Irish surface waters, J. Paleolimnol., 34(2), 257–269, 2005.

Dutton, A., Wilkinson, B. H., Welker, J. M., Bowen, G. J. and Lohmann, K. C.: Spatial distribution and seasonal variation in 18 O/ 16 O of modern precipitation and river water across the conterminous USA, Hydrol. Process., 19(20), 4121–4146, doi:10.1002/hyp.5876, 2005.

EDF: Die Wasserkraftanlagen am deutsch-französischen Rhein. [online] Available from: https://web.archive.org/web/20120813160552/http://energie.edf.com/fichiers/fckeditor/Commun/En_Direct_Centrales/Hydraulique/Commun/documents/BrochureD 12p Rhin.pdf, n.d.

European Environment Agency: European river catchments, [online] Available from: http://www.eea.europa.eu/data-and-maps/data/european-river-catchments-1#tab-metadata (Accessed 20 March 2015), 2008.

European Environment Agency: WISE Large rivers and large lakes, [online] Available from: http://www.eea.europa.eu/data-and-maps/figures/wise-large-rivers-and-large-lakes (Accessed 20 March 2015), 2009.

Feng, X., Faiia, A. M. and Posmentier, E. S.: Seasonality of isotopes in precipitation: A global perspective, J. Geophys. Res. Atmos., 114(D8), n/a–n/a, doi:10.1029/2008JD011279, 2009.

Frederickson, G. C. and Criss, R. E.: Isotope hydrology and residence times of the unimpounded Meramec River Basin, Missouri, Chem. Geol., 157(3-4), 303–317, 1999.

Friedman, I.: Deuterium content of natural waters and other substances, Geochim. Cosmochim. Acta, 4(1–2), 89–103, doi:http://dx.doi.org/10.1016/0016-7037(53)90066-0, 1953.

Fröhlich, K., Gibson, J. J. and Aggarwal, P.: Deuterium excess in precipitation and its climatological significance, in Study of environmental change using isotope techniques, pp. 54–66, International Atomic Energy Agency, Vienna, Austria., 2002.

Gibson, J. J., Aggarwal, P., Hogan, J., Kendall, C., Martinelli, L. A., Stichler, W., Rank, D., Goni, I., Choudhry, M., Gat, J., Bhattacharya, S., Sugimoto, A. ., Fekete, B. ., Pietroniro, A. ., Maurer, T. ., Panarello, H., Stone, D., Seyler, P., Maurice-Bourgoin, L. and Herczeg, A.: Isotope Studies in Large River Basins: A New Global Research Focus, Eos (Washington. DC)., 83(52), 613–620, 2002.

Gibson, J. J., Edwards, T. W. D., Birks, S. J., St Amour, N. A., Buhay, W. M., McEachern, P., Wolfe, B. B. and Peters, D. L.: Progress in isotope tracer hydrology in Canada, Hydrol. Process., 19(1), 303–327, 2005.

Graham, M. H.: Confronting multicolinearity in ecological multiple regression, Ecology, 84(11), 2809–2815, doi:10.1890/02-3114, 2003.

Gremillion, P. and Wanielista, M.: Effects of evaporative enrichment on the stable isotope hydrology of a central Florida (USA) river, Hydrol. Process., 14(8), 1465–1484, doi:10.1002/1099-1085(20000615)14:8<1465::AID-HYP987>3.0.CO;2-6, 2000.

Halder, J., Terzer, S., Wassenaar, L. I., Araguás-Araguás, L. J. and Aggarwal, P. K.: The Global Network of Isotopes in Rivers (GNIR): integration of water isotopes in watershed observation and riverine research, Hydrol. Earth Syst. Sci., 19(8), 3419–3431, doi:10.5194/hess-19-3419-2015, 2015.

Helsel, D. R. and Hirsch, R. M.: Statistical Methods in Water Resources Techniques of Water Resources Investigations, in Book 4, p. 522, U.S. Geological Survey., 2002.

Hogan, J., Phillips, F., Eastoe, C., Lacey, H., Mills, S. and Oelsner, G.: Isotopic tracing of hydrological processes and water quality along the Upper Rio Grande, USA, in Monitoring Isotopes in Rivers: Creation of the Global Network of Isotopes in Rivers (GNIR), p. 258, International Atomic Energy Agency., 2012.

Hughes, C. E., Stone, D. J. M., Gibson, J. J., Meredith, K. T., Sadek, M. A., Cendon, D. I., Hankin, S. I., Hollins, S. E. and Morrison, T. N.: Stable water isotope investigation of the Barwon-Darling River system, Australia, in Monitoring Isotopes in Rivers: Creation of the Global Network of Isotopes in Rivers (GNIR), p. 258, International Atomic Energy Agency., 2012.

International Atomic Energy Agency: Monitoring Isotopes in Rivers: Creation of the Global Network of Isotopes in Rivers (GNIR): Results of a Coordinated Research Project 2002–2006, Vienna. [online] Available from: http://www-naweb.iaea.org/napc/ih/documents/TECDOCS/TECDOC 1673 Monitoring Isotopes in Rivers.pdf (Accessed 1 March 2015), 2012.

International Atomic Energy Agency: Application and development of isotope techniques to evaluate human impacts on water balance and nutrient dynamics of large river basins (F33021), [online] Available from: http://cra.iaea.org/cra/stories/2014-01-17-F33021-Water-balance.html (Accessed 20 August 2015), 2014.

International Atomic Energy Agency: Global Network of Isotopes in Precipitation (GNIP), [online] Available from: http://www-naweb.iaea.org/napc/ih/IHS_resources_gnip.html (Accessed 25 February 2015a), n.d.

International Atomic Energy Agency: Global Network of Isotopes in Rivers (GNIR), [online] Available from: http://www-naweb.iaea.org/napc/ih/IHS_resources_gnir.html (Accessed 25 February 2015b), n.d.

Internationale Kommission zum Schutz des Rheins: Darstellung der Entwicklung der Rheinwassertemperaturen auf der Basis validierter Temperaturmessungen von 1978 bis 2011. [online] Available from: https://www.google.de/url?sa=t&rct=j&q=&esrc=s&source=web&cd=1&cad=rja&uact=8&ved=0CCIQFjAAahUKEwiGuua8pPHHAhUL0hoKHW9rA6o&url=http://www.iksr.org/fileadmin/user_upload/Dokumente_de/Berichte/209_d.pdf&usg=AFQjCNGd5aqovDGIVEfHtvrd-DZkO3jMuw, 2013.

Internationale Kommission zum Schutz des Rheins: Entwurf: 2. International koordinierter Bewirtschaftungsplan für die internationale Flussgebietseinheit Rhein. [online] Available from: http://www.iksr.org/fileadmin/user_upload/Dokumente_de/Rhein_Aktuell/2._BWP-Entwurf_d.pdf, 2014.

Jacob, H. and Sonntag, C.: An 8-year record of the seasonal variation of 2H and 18O in atmospheric water vapour and precipitation at Heidelberg, Germany, Tellus, 291–300, 1991.

Jouzel, J., Froehlich, K. and Schotterer, U.: Deuterium and oxygen-18 in present-day precipitation: data and modelling, Hydrol. Sci. J., 42(5), 747–763, 1997.

Kaiser, A., Scheifinger, H., Kralik, M., Papesch, W., Rank, D. and Stichler, W.: Links between meteorological conditions and spatial/temporal variations in long-term isotope records from the Austrian precipitation network, in Study of Environmental Change using Isotope Techniques, pp. 67–76, International Atomic Energy Agency, Vienna., 2002.

Katsuyama, M., Yoshioka, T. and Konohira, E.: Spatial distribution of oxygen-18 and deuterium in stream waters across the Japanese archipelago, Hydrol. Earth Syst. Sci., 19(3), 1577–1588, doi:10.5194/hess-19-1577-2015, 2015.

Kattan, Z.: Chemical and isotopic compositions of the Euphrates River water, Syria, in Monitoring Isotopes in Rivers: Creation of the Global Network of Isotopes in Rivers (GNIR), p. 112, International Atomic Energy Agency, Vienna. [online] Available from: http://www-pub.iaea.org/books/IAEABooks/8693/Monitoring-Isotopes-in-Rivers-Creation-of-the-Global-Network-of-Isotopes-in-Rivers-GNIR, 2012.

Kendall, C. and Coplen, T. B.: Distribution of oxygen-18 and deuterium in river waters across the United States, Hydrol. Process., 15(7), 1363–1393 [online] Available from: http://dx.doi.org/10.1002/hyp.217, 2001.

Kendall, M. G.: Rank Correlation Methods, 4th ed., Charles Griffin, London., 1975.

Kirchner, J. W.: Aggregation in environmental systems: catchment mean transit times and young water fractions under hydrologic nonstationarity, Hydrol. Earth Syst. Sci. Discuss., 12(3), 3105–3167, doi:10.5194/hessd-12-3105-2015, 2015.

Klaus, J., Chun, K. P. and Stumpp, C.: Temporal trends in δ18O composition of precipitation in Germany: insights from time series modelling and trend analysis, Hydrol. Process., 29(12), 2668–2680, doi:10.1002/hyp.10395, 2015.

Königer, P., Leibundgut, C. and Stichler, W.: Spatial and temporal characterisation of stable isotopes in river water as indicators of groundwater contribution and confirmation of modelling results; a study of the Weser river, Germany., Isotopes Environ. Health Stud., 45(4), 289–302, 2009.

Königer, P., Wittmann, S., Leibundgut, C. and Krause, W. J.: Tritium balance modelling in a macroscale catchment, Hydrol. Process., 19(17), 3313–3320, doi:10.1002/hyp.5972, 2005.

Kresic, N. and Stevanovic, Z.: Groundwater hydrology of springs, Elsevier, Oxford., 2009.

Leibundgut, C., Maloszewski, P. and Külls, C.: Tracers in Hydrology, John Wiley & Sons, Ltd., 2009.

Liu, J., Fu, G., Song, X., Charles, S. P., Zhang, Y., Han, D. and Wang, S.: Stable isotopic compositions in Australian precipitation, J. Geophys. Res. Atmos., 115(D23), n/a–n/a, doi:10.1029/2010JD014403, 2010.

Lu, B., Sun, T., Wang, C., Dai, S., Kuang, J. and Wang, J.: Temporal and Spatial Variations of d 18O Along the Main Stem of Yangtze River, China, in Monitoring Isotopes in Rivers: Creation of the Global Network of Isotopes in Rivers (GNIR), pp. 211–219., 2012.

Lykoudis, S. P. and Argiriou, A. A.: Temporal trends in the stable isotope composition of precipitation: a comparison between the eastern Mediterranean and central Europe, Theor. Appl. Climatol., 105(1-2), 199–207, doi:10.1007/s00704-010-0384-6, 2011.

Maloszewski, P., Rauert, W., Trimborn, P., Herrmann, A. and Rau, R.: Isotope hydrological study of mean transit times in an alpine basin (Wimbachtal, Germany), J. Hydrol., 140(1–4), 343–360, doi:http://dx.doi.org/10.1016/0022-1694(92)90247-S, 1992.

Maloszewski, P. and Zuber, A.: Determining the turnover time of groundwater systems with the aid of environmental tracers, J. Hydrol., 57(3-4), 207–231, 1982.

Maloszewski, P. and Zuber, A.: Lumped parameter models for the interpretation of environmental tracer data, in Manual on Mathematical Models in Isotope Hydrogeology, vol. TECDOC-910, pp. 9–58, International Atomic Energy Agency., 1996.

Maloszewski, P. and Zuber, A.: Manual on lumped parameter models used for the interpretation of environmental tracer data in groundwaters, in Use of isotopes for analyses of flow and transport dynamics in groundwater systems. Results of a co-ordinated research project 1996-1999, p. 394, International Atomic Energy Agency. [online] Available from: http://www.iaea.org/inis/collection/NCLCollectionStore/_Public/33/037/33037892.pdf , 2002.

Mann, H. B.: Nonparametric Tests Against Trend, Econometrica, 13(3), 245–259 CR – Copyright © 1945 The Econometri, doi:10.2307/1907187, 1945.

Martinelli, L. A., Gat, J. R., De Camargo, P. B., Lara, L. L. and Ometto, J. P. H. B.: The Piracicaba river basin: isotope hydrology of a tropical river basin under anthropogenic stress, Isotopes Environ. Health Stud., 40(1), 45–56, doi:10.1080/10256010310001652016, 2004.

Martinelli, L. A., Victoria, R. L., Silveira Lobo Sternberg, L., Ribeiro, A. and Zacharias Moreira, M.: Using stable isotopes to determine sources of evaporated water to the atmosphere in the Amazon basin, J. Hydrol., 183(3–4), 191–204, doi:http://dx.doi.org/10.1016/0022-1694(95)02974-5, 1996.

McGlynn, B., McDonnell, J., Stewart, M. and Seibert, J.: On the relationships between catchment scale and streamwater mean residence time, Hydrol. Process., 17(1), 175–181, doi:10.1002/hyp.5085, 2003.

McGuire, K. J. and McDonnell, J. J.: A review and evaluation of catchment residence time modeling, J. Hydrol., doi:10.1016/j.jhydrol.2006.04.020, 2006.

McGuire, K. J., McDonnell, J. J., Weiler, M., Kendall, C., McGlynn, B. L., Welker, J. M. and Seibert, J.: The role of topography on catchment-scale water residence time, Water Resour. Res., 41(5), n/a–n/a, doi:10.1029/2004WR003657, 2005.

Michel, R. L.: Residence times in river basins as determined by analysis of long-term tritium records, J. Hydrol., 130(1-4), 367–378, 1992.

Mizota, C. and Kusakabe, M.: Spatial distribution of d-D-d-18O values of surface and shallow groundwaters from Japan, south Korea and east China., Geochem. J., 28(5), 387–410, doi:10.2343/geochemj.28.387, 1994.

Nash, J. E. and Sutcliffe, J. V: River flow forecasting through conceptual models part I — A discussion of principles, J. Hydrol., 10(3), 282–290, doi:http://dx.doi.org/10.1016/0022-1694(70)90255-6, 1970.

Ogrinc, N., Kanduc, T., Miljevic, N., Golobocanin, D. and Vaupotic, J.: Isotope Tracing of Hydrological Processes in River Basins: The Rivers Danube and Sava, in Monitoring Isotopes in Rivers: Creation of the Global Network of Isotopes in Rivers (GNIR), pp. 187–196., 2011.

Panarello, H. O. and Dapena, C.: Large scale meteorological phenomena, ENSO and ITCZ, define the Paraná River isotope composition, J. Hydrol., 365(1–2), 105–112, doi:http://dx.doi.org/10.1016/j.jhydrol.2008.11.026, 2009.

Peng, H., Mayer, B., Harris, S. and Krouse, H. R.: A 10-year record of stable isotope ratios of hydrogen and oxygen in precipitation at Calgary, Alberta, Canada, Tellus, Ser. B Chem. Phys. Meteorol., 56(2), 147–159, 2004.

Pfahl, S. and Sodemann, H.: What controls deuterium excess in global precipitation?, Clim. Past, 10(2), 771–781, doi:10.5194/cp-10-771-2014, 2014.

R Core Team: R: A language and environment for statistical computing, [online] Available from: http://www.r-project.org/, 2014.

R Core Team and contributors worldwide: The R Stats Package, [online] Available from: https://stat.ethz.ch/R-manual/R-patched/library/stats/html/stats-package.html, 2015.

Rank, D., Adler, A., Araguás Araguás, L., Froehlich, K., Rozanski, K. and Stichler, W.: Hydrological parameters and climatic signals derived from long-term tritium and stable isotope time series of the River Danube, in IAEA, Isotope Techniques in the Study of Environmental Change, pp. 191–205, IAEA-SM-349., 1998.

Rank, D. and Papesch, W.: Mean residence time (MRT) of baseflow water in the Upper Danube Basin derived from decadal climatic signals in long-term isotope records of river water, in 38th IAD Conference, pp. 2–6, Dresden, Germany., 2010.

Rank, D., Papesch, W., Heiss, G. and Tesch, R.: Environmental Isotope Ratios of River Water in the Danube Basin, in Monitoring Isotopes in Rivers: Creation of the Global Network of Isotopes in Rivers (GNIR)., pp. 13–40, International Atomic Energy Agency, Vienna., 2012.

Rank, D., Wyhlidal, S., Schott, K., Jung, M., Heiss, G. and Tudor, M.: A 50 Years' isotope record of the danube river water and its relevance for hydrological, climatological and environmental research, Acta Zool. Bulg., 66(SUPPL. 7), 109–115, 2014.

Rodgers, P., Soulsby, C., Waldron, S. and Tetzlaff, D.: Using stable isotope tracers to assess hydrological flow paths, residence times and landscape influences in a nested mesoscale catchment, Hydrol. Earth Syst. Sci., 9(3), 139–155, doi:10.5194/hess-9-139-2005, 2005.

Rozanski, K., Araguás-Araguás, L. and Gonfiantini, R.: Relation between long-term trends of oxygen-18 isotope composition of precipitation and climate., Science, 258(5084), 981–985, 1992.

Rozanski, K., Araguás-Araguás, L. and Gonfiantini, R.: Isotopic patterns in modern global precipitation, in Climate Change in Continental Isotope Records, vol. 78, pp. 1–36, American Geophysical Union., 1993.

Rozanski, K. and Gonfiantini, R.: Isotopes in climatological studies, Int. At. Energy Agency Bull., 32(4), 9–15, 1990.

Schotterer, U., Schürch, M., Rickli, R. and Stichler, W.: Wasserisotope in der Schweiz: Neue Ergebnisse und Erfahrungen aus dem nationalen Messnetz ISOT, GWA, 90(12), 1073–1081, 2010.

Schürch, M., Kozel, R., Schotterer, U. and Tripet, J.-P.: Observation of isotopes in the water cycle—the Swiss National Network (NISOT), Environ. Geol., 45(1), 1–11, doi:10.1007/s00254-003-0843-9, 2003.

Sen, P. K.: Robustness of Some Nonparametric Procedures in Linear Models, Ann. Math. Stat., 39(6), 1913–1922, doi:10.2307/2239290, 1968.

Simpson, H. J. and Herczeg, A. L.: Stable isotopes as an indicator of evaporation in the River Murray, Australia, Water Resour. Res., 27(8), 1925–1935, 1991.

Speed, M., Tetzlaff, D., Hrachowitz, M. and Soulsby, C.: Evolution of the spatial and temporal characteristics of the isotope hydrology of a montane river basin, Hydrol. Sci. J., 56(3), 426–442, doi:10.1080/02626667.2011.561208, 2011.

Stumpp, C., Klaus, J. and Stichler, W.: Analysis of long-term stable isotopic composition in German precipitation, J. Hydrol., 517, 351–361, doi:http://dx.doi.org/10.1016/j.jhydrol.2014.05.034, 2014.

Terzer, S., Wassenaar, L. I., Araguás-Araguás, L. J. and Aggarwal, P. K.: Global isoscapes for δ18O and δ2H in precipitation: improved prediction using regionalized climatic regression models, Hydrol. Earth Syst. Sci., 17(11), 4713–4728, doi:10.5194/hess-17-4713-2013, 2013.

Uhlenbrook, S., Frey, M., Leibundgut, C. and Maloszewski, P.: Hydrograph separations in a mesoscale mountainous basin at event and seasonal timescales, Water Resour. Res., 38(6), 14–31, doi:10.1029/2001WR000938, 2002.

Vitvar, T., Aggarwal, P. K. and Herczeg, A. L.: Global network is launched to monitor isotopes in rivers, Eos (Washington. DC)., 88(33), 325–326, 2007.

Vitvar, T., Aggarwal, P. K. and McDonnell, J. J.: A Review of Isotope Applications in Catchment Hydrology, in Isotopes in the Water Cycle, pp. 151–169., 2005.

Wen, R., Tian, L., Weng, Y., Liu, Z. and Zhao, Z.: The altitude effect of δ 18O in precipitation and river water in the Southern Himalayas, Chinese Sci. Bull., 57(14), 1693–1698, doi:10.1007/s11434-012-4992-7, 2012.

Winston, W. and Criss, R.: Oxygen isotope and geochemical variations in the Missouri River, Environ. Geol., 43(5), 546–556 [online] Available from: http://dx.doi.org/10.1007/s00254-002-0679-8, 2003.

Yi, Y., Gibson, J. J., Hélie, J.-F. and Dick, T. A.: Synoptic and time-series stable isotope surveys of the Mackenzie River from Great Slave Lake to the Arctic Ocean, 2003 to 2006, J. Hydrol., 383(3–4), 223–232, doi:http://dx.doi.org/10.1016/j.jhydrol.2009.12.038, 2010.

Yuan, F. and Miyamoto, S.: Characteristics of oxygen-18 and deuterium composition in waters from the Pecos River in American Southwest, Chem. Geol., 255(1–2), 220–230, doi:http://dx.doi.org/10.1016/j.chemgeo.2008.06.045, 2008.

Yue, S., Pilon, P., Phinney, B. and Cavadias, G.: The influence of autocorrelation on the ability to detect trend in hydrological series, Hydrol. Process., 16(9), 1807–1829, doi:10.1002/hyp.1095, 2002.

Yurtsever, Y.: An overview of conceptual model formulations for evaluation of isotope data in hydrological systems, in Tracer Technologies for Hydrological Systems ms (Proceedings of a Boulder Symposium), pp. 3–12, IAHS Publ. no. 229., 1995.

Zwiers, F. W. and von Storch, H.: Taking Serial Correlation into Account in Tests of the Mean, J. Clim., 8(2), 336–351, doi:10.1175/1520-0442(1995)008<0336:TSCIAI>2.0.CO;2, 1995.

Appendix

Abbreviations

ARIMA	Autoregressive integrate moving average models
BfG	German Federal Institute of Hydrology
BMU	Bundesministerium für Umwelt, Naturschutz und Reaktorsicherheit
DWD	Germany's National Meteorological Service
FOEN	Swiss Federal Office for the Environment
GIS	Geographic information system
GMWL	Global meteoric water line
GNIP	Global Network for Isotopes in Precipitation
GNIR	Global Network for Isotopes in Rivers
IAEA	International Atomic Energy Agency
LMWL	Local meteoric water line
NISOT	Swiss National Network for the Observation of Isotopes in the Water Cycle
NSE	Nash-Sutcliffe efficiency
RMSE	Root Mean Square Error
RWL	River water line
TFPW	Trend-free pre-whitening
TTD	Transit time distribution
VSMOW	Vienna Standard Mean Ocean Water

List of symbols

β	Constant flow component
C_β	Tracer concentration of the constant flow component
C_{in}	Input tracer concentration
C_{out}	Output tracer concentration
δ	Delta notation
Da	Danube
E	Mean
El	Elbe
Em	Ems
g(t)	Transit time distribution
H_0	Null hypothesis
H_1	Alternative hypothesis
Ma	Main
$MA(x_t)$	Moving average
Mo	Mosel
n	Number of data points
Ne	Neckar
O	Observations
Od	Oder
P	Model predictions
R	Isotope ratio
r	Correlation coefficient
Rh	Rhine
s	Standard deviation
S	Mann-Kendall statistic
t	Time
t’	Transit time
t_r	Pearson’s r test statistic
t_t	Transit time of the tracer
V	Variance
W	Weight
We	Weser
x,y	Data points
Z	Standardised Mann-Kendall test statistic

Maps

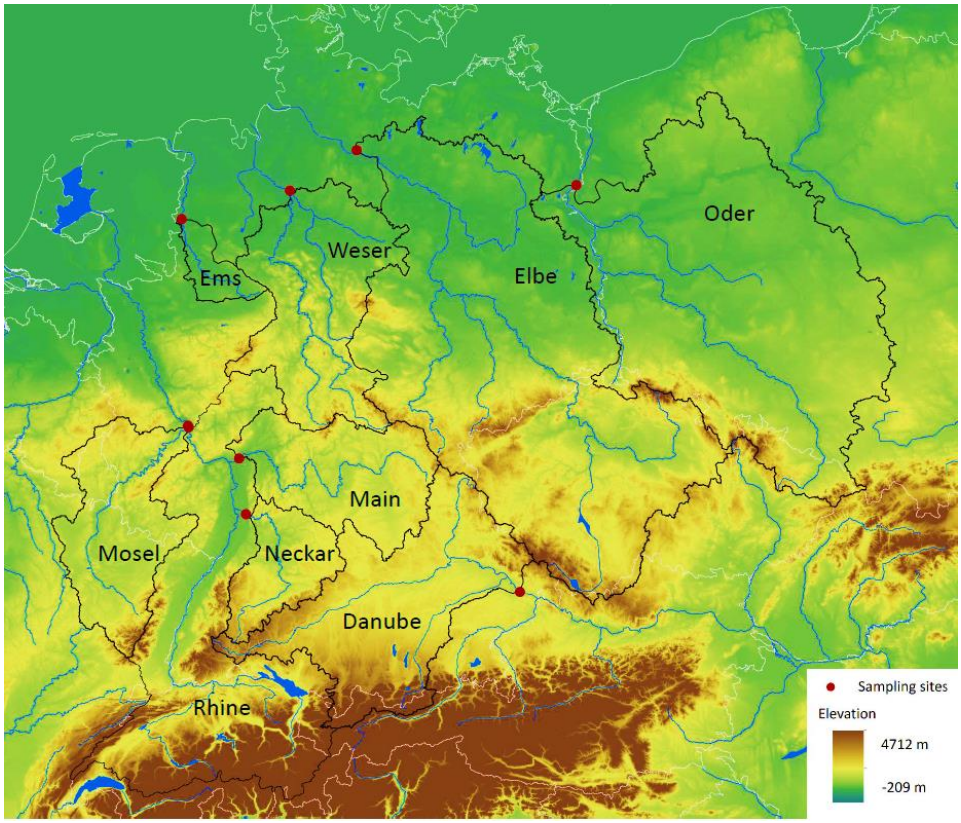

Figure A 1: Topographical map of the study areas.

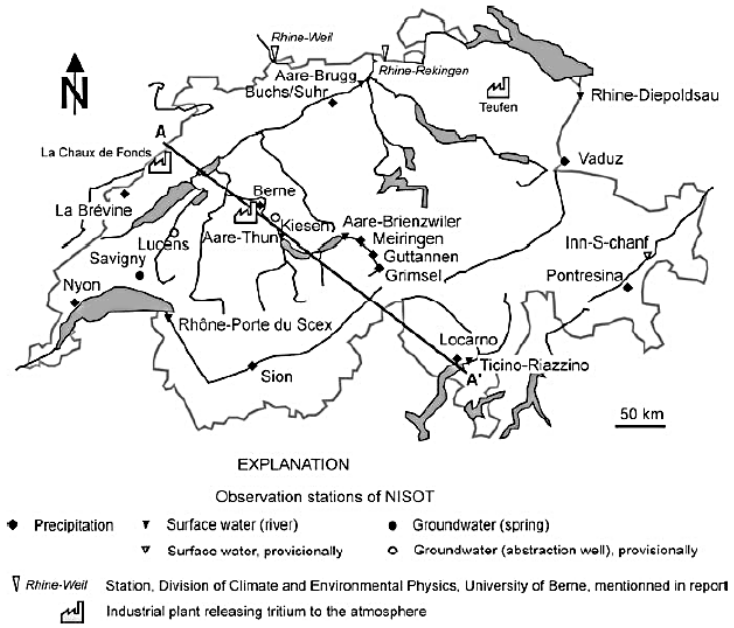

Figure A 2: Map of the NISOT sampling stations at the Rhine and its tributaries in Switzerland. From Schürch et al. (2003).

Discharge regimes

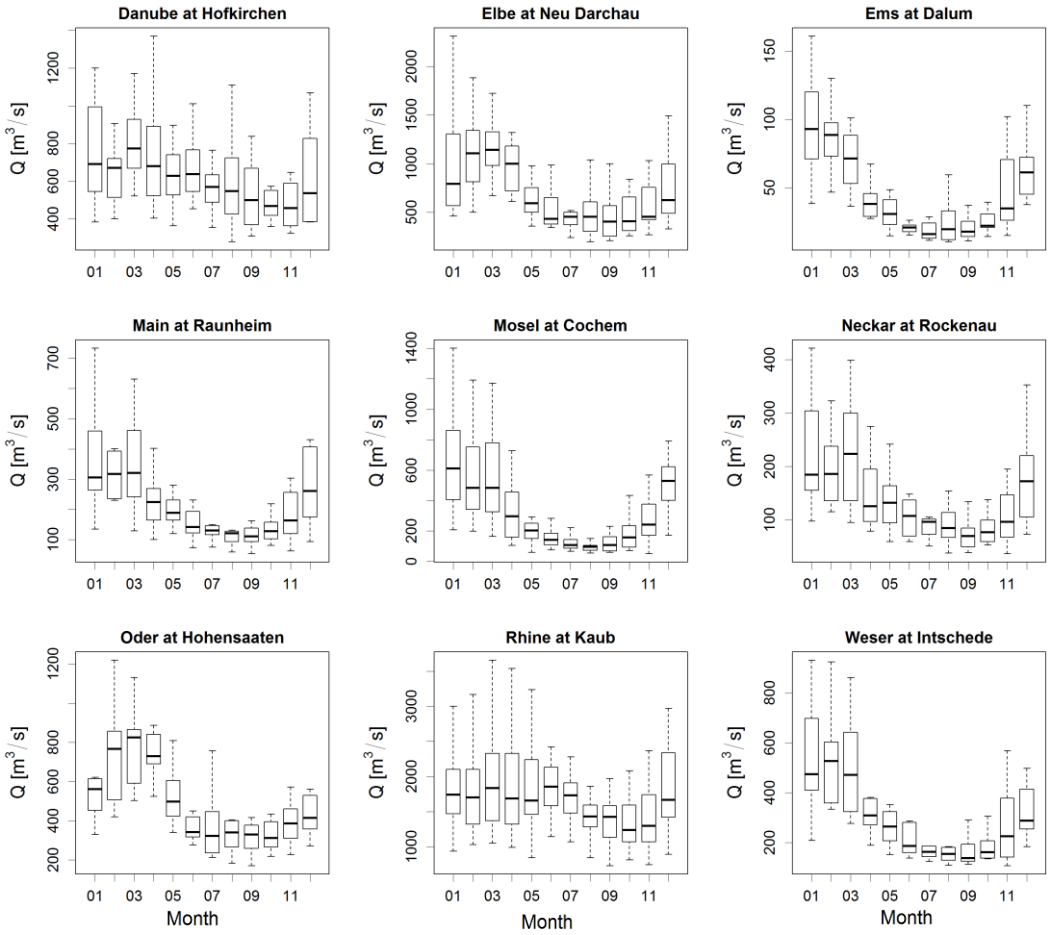

Figure A 3: Discharge regimes of the rivers with variations. The medians of the values are displayed as bold lines. The rectangles extent from the lower to the upper quartiles and the whiskers show the minimum and maximum values. Calculations are based on data from 2002 to 2013; except for the Mosel and the Rhine, where data from 1988 to 2013 were used. Calendar year is used.

Long-term averages

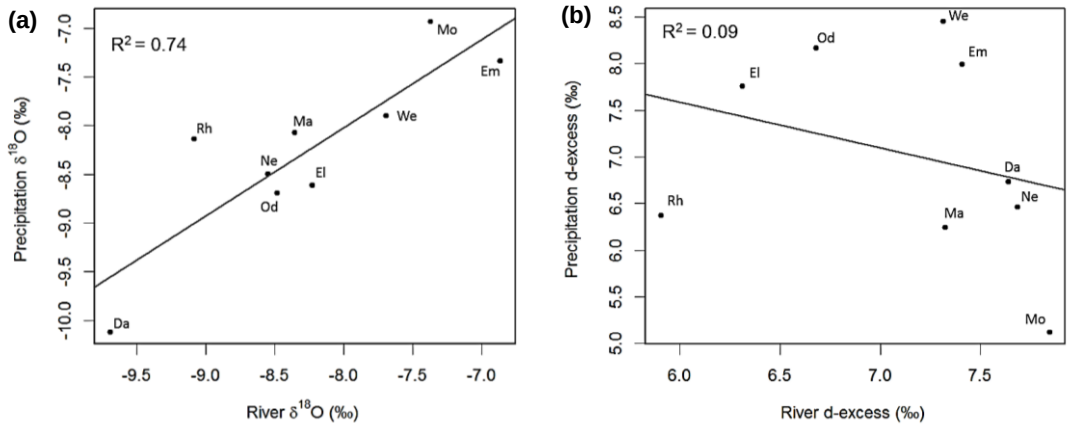

Figure A 4: River water long-term averages versus precipitation long-term averages of (a) $\delta^{18}O$ and (b) d-excess.

Table A 1: Long-term averages of $\delta^{18}O$ and d-excess in river water and precipitation.

	Long-term average $\delta^{18}O$ (‰)		Long-term average D-excess (‰)	
	Precipitation	**River**	**Precipitation**	**River**
Danube[a]	-10.11	-9.69	6.74	7.64
Elbe[a]	-8.61	-8.23	7.76	6.31
Ems[a]	-7.34	-6.87	7.99	7.41
Main[a]	-8.07	-8.35	6.24	7.32
Mosel[b]	-6.93	-7.37	5.12	7.84
Neckar[a]	-8.50	-8.55	6.46	7.68
Oder[a]	-8.69	-8.48	8.17	6.68
Rhine[b]	-8.13	-9.08	6.38	5.90
Weser[a]	-7.90	-7.69	8.46	7.31

[a] Records from 01/2002 to 12/2013; [b] Records from 01/1988 to 12/2013

Discharge Rhine

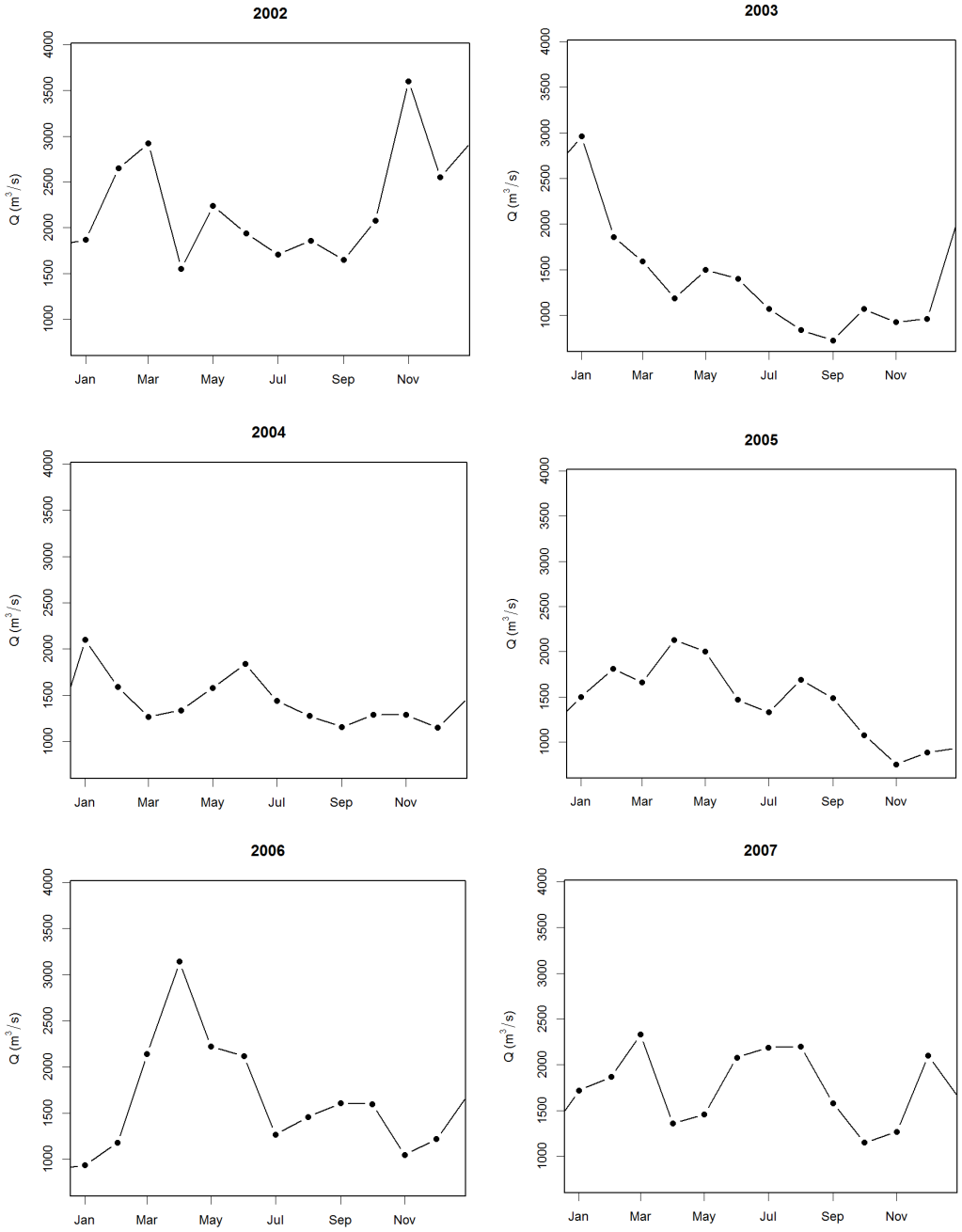

Figure A 5: Mean monthly discharge of the Rhine at Koblenz from 2002 to 2011.

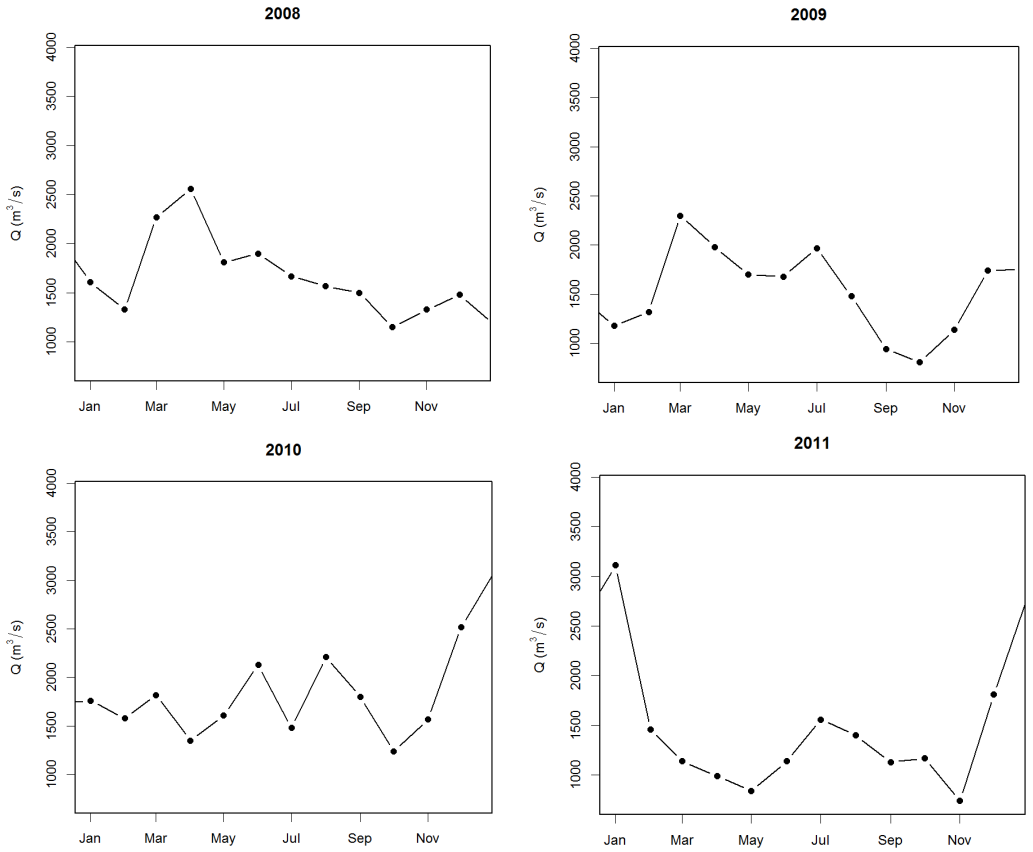

Figure A 5: Continued.

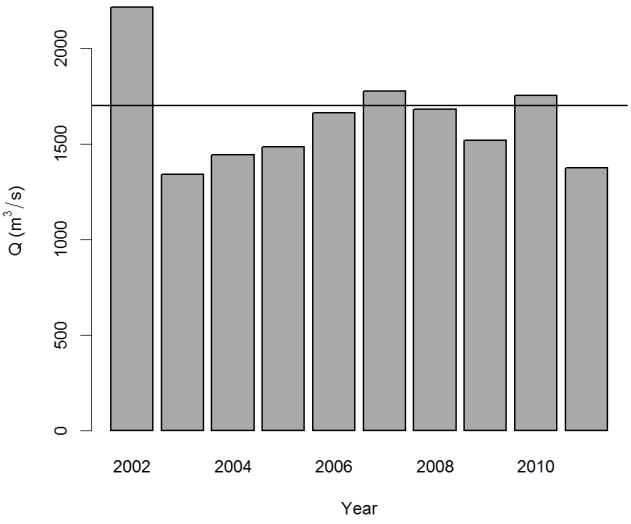

Figure A 6: Mean annual discharge of the Rhine at Koblenz from 2002 to 2011. The black line shows the long-term mean discharge.

Seasonality oxygen-18

Table A 2: Amplitudes of $\delta^{18}O$ seasonal signals of river water and average catchment precipitation. Based on mean monthly values.

	Amplitude (‰)	
	River water	Catchment precipitation
Danube[a]	0.63	7.8
Elbe[a]	1.21	6.16
Ems[a]	1.07	3.75
Main[a]	1.26	6.08
Mosel[b]	1.36	4.69
Neckar[a]	1.33	6.29
Oder[a]	1.19	6.57
Rhine[b]	0.72	5.47
Weser[a]	0.66	4.05

[a] Records from 01/2002 to 12/2013; [b] Records from 01/1988 to 12/2013

Trend analysis

Table A 3: Calculated Sen-slopes and results from Mann-Kendall trend tests.

	Sen-slope over the whole period (‰)	Sen-slope per year (‰/yr)	Mann-Kendall tau	Mann-Kendall p-value
Danube	0.26	0.02	0.10	0.09
Elbe	0.01	0.00	0.01	0.91
Ems	0.35	0.03	0.05	0.35
Main	-0.07	-0.01	-0.02	0.68
Mosel	0.34	0.01	0.01	0.81
Neckar	0.12	0.01	0.03	0.60
Oder	0.27	0.02	0.04	0.51
Rhine	1.00	0.04	0.16	<0.01
Weser	-0.83	-0.07	-0.17	<0.01

Correlograms of original $\delta^{18}O$ time series

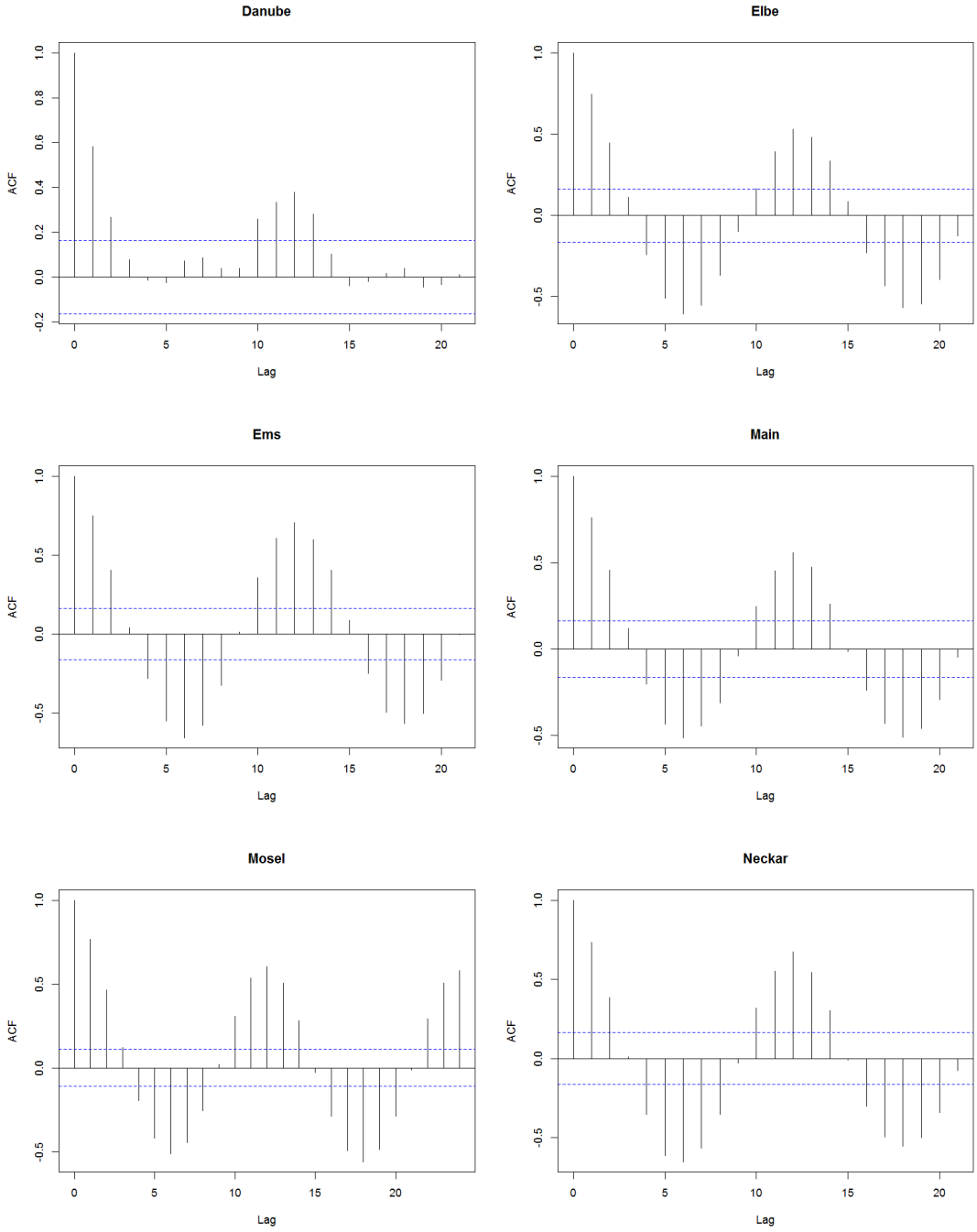

Figure A 7: Correlograms of original $\delta^{18}O$ time series. Blue dotted lines show the confidence intervals. Bars larger than confidence intervals indicate significant correlation with the specific lags.

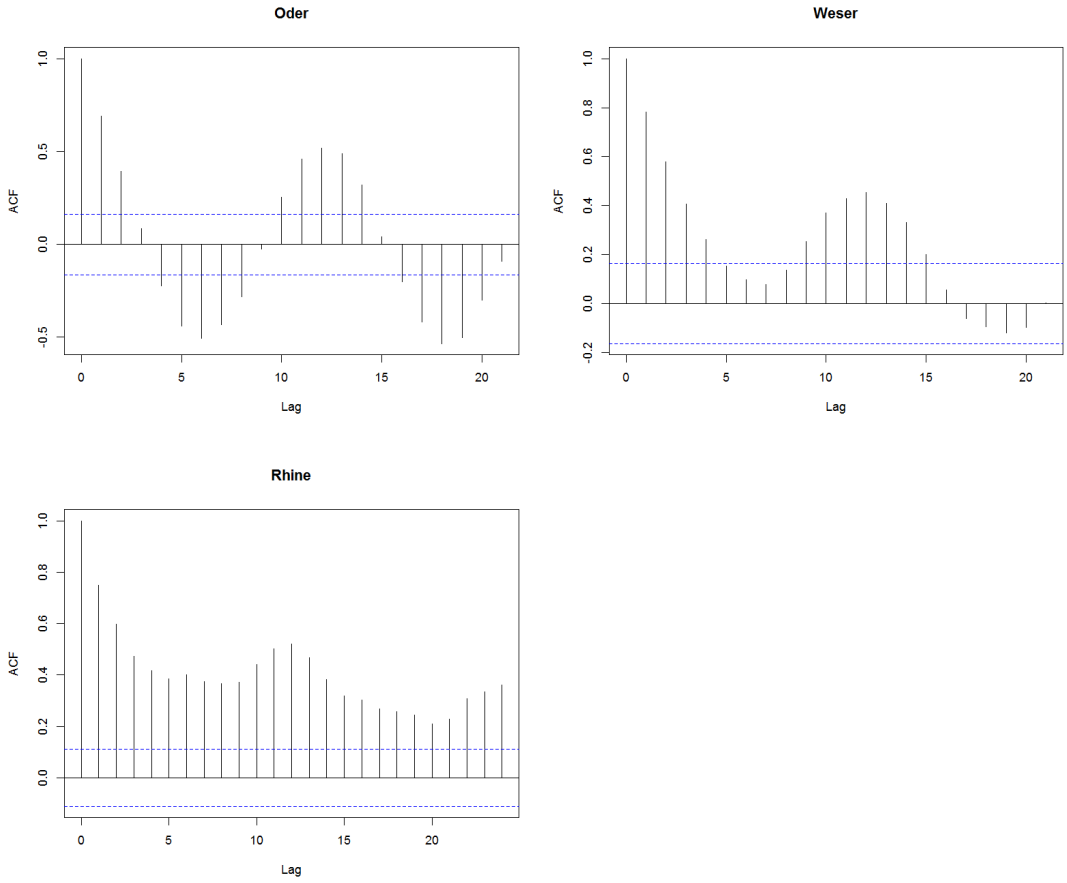

Figure A 7: Continued.

Correlograms of $\delta^{18}O$ time series after removing first order autocorrelation

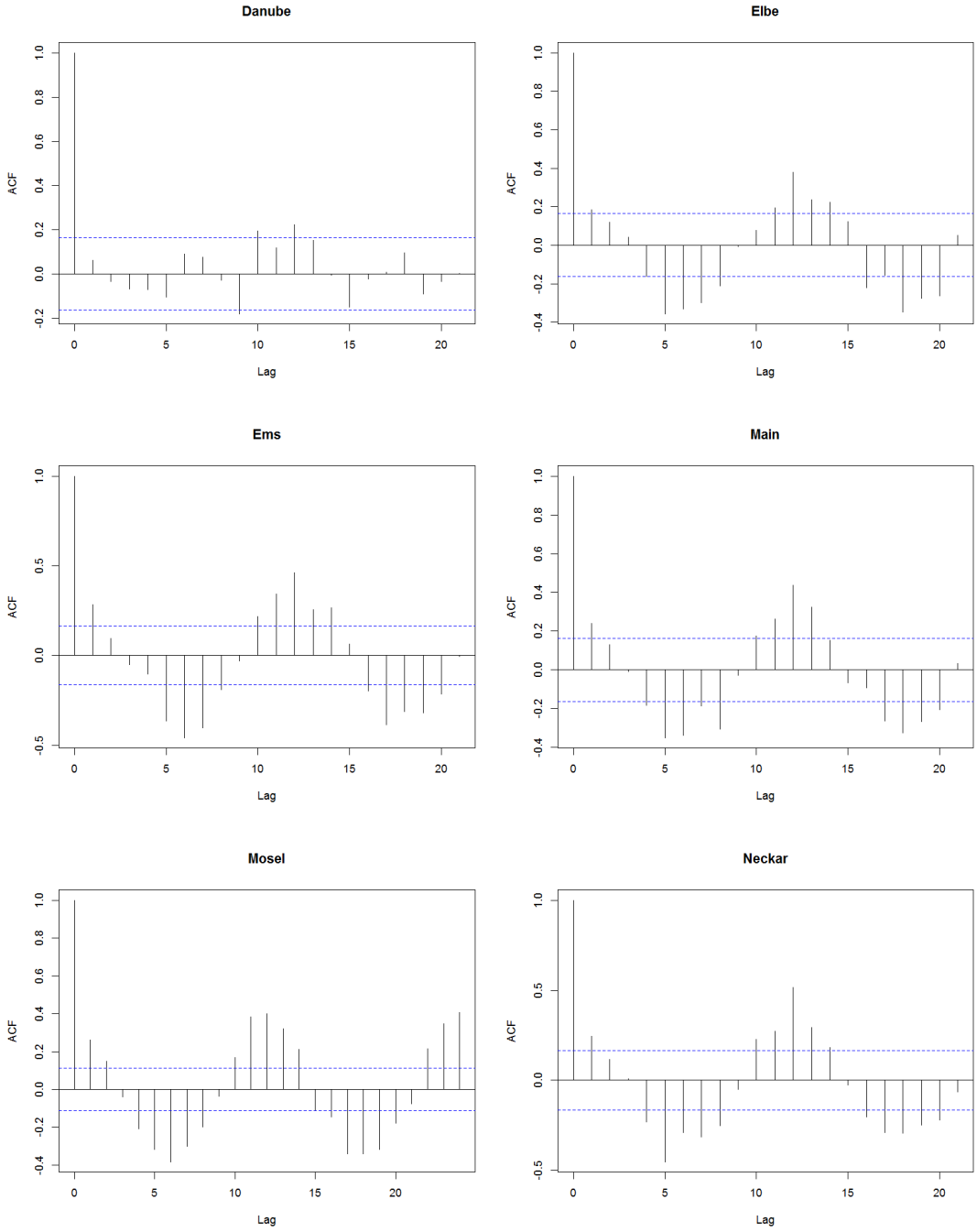

Figure A 8: Correlograms of $\delta^{18}O$ time series after removing first order autocorrelation. Blue dotted lines show the confidence intervals. Bars larger than confidence intervals indicate significant correlation with the specific lags.

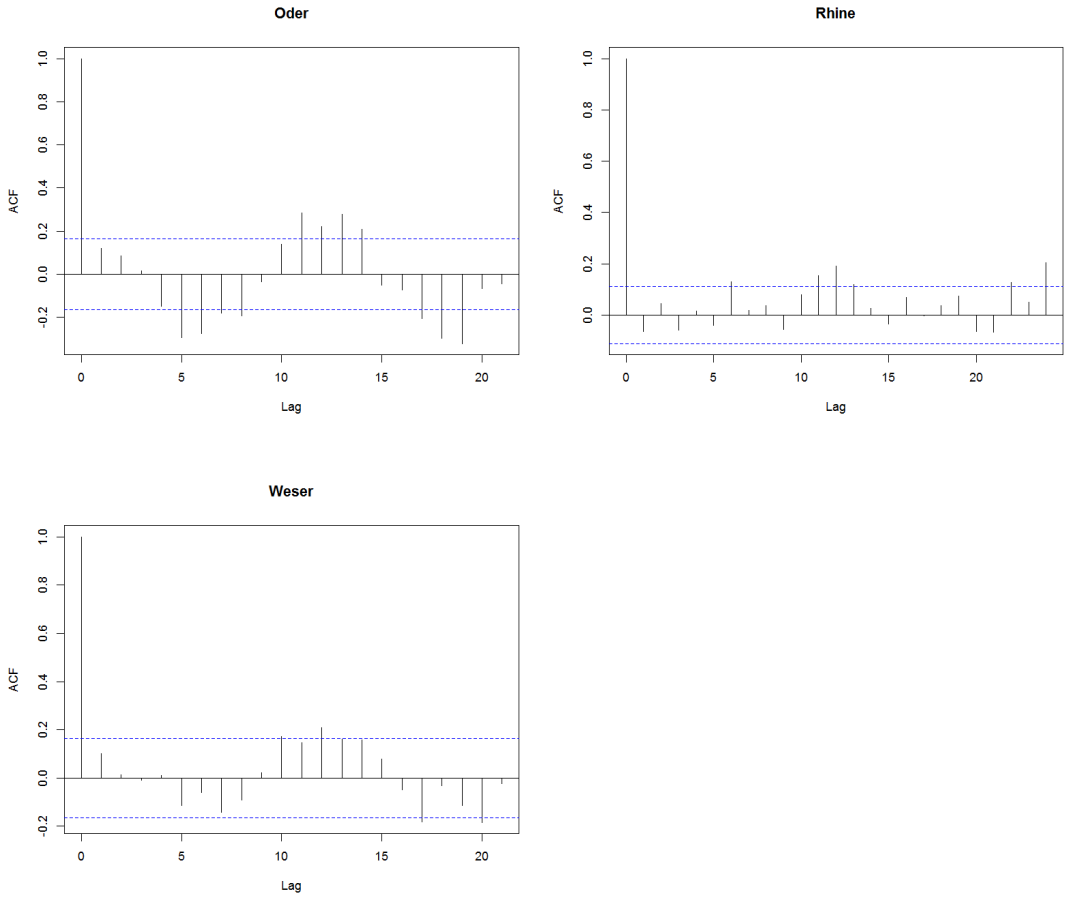

Figure A 8: Continued.

Table A 4: Results of multiple linear regression analysis for $\delta^{18}O$ versus latitude and altitude and d-excess versus catchment area and flow length.

	Estimate	p-value
	$\delta^{18}O$	
Latitude	-0.39	0.24
Altitude	-0.01	0.04
	D-excess	
Catchment area	-2.06E-06	0.82
Flow length	-8.38E-04	0.21

Ehrenwörtliche Erklärung

Hiermit erkläre ich, dass die Arbeit selbständig und nur unter Verwendung der angegebenen Hilfsmittel angefertigt wurde.

Ort, Datum Unterschrift